UNIVERSITY OF TRENTO - Italy

International Ph.D. Program in Biomolecular Sciences
Centre for Integrative Biology

29th Cycle

Twist of messenger Fate: novel mechanisms for TDP43 in modulating mRNA decay and alternative polyadenylation

TUTOR

Prof. **ALESSANDRO QUATTRONE**

CIBIO – University of Trento

ADVISOR

Dr. **DANIELE PERONI**

CIBIO – University of Trento

Ph.D. Thesis of

VALENTINA POTRICH

CIBIO – University of Trento

Academic Year 2015-2016

“What we see depends mainly on what we look for”
- John Lubbock -

Original authorship

Declaration:

I, Valentina Potrich, confirm that this is my own work and the use of all material from other sources has been properly and fully acknowledged.

TABLE OF CONTENTS

ABSTRACT

TDP43 is an ubiquitously expressed RNA-binding protein implicated in several aspects of RNA metabolism. It can shuttle between the nucleus and the cytoplasm; however, when it is mutated in some familial Amyotrophic Lateral Sclerosis (ALS) cases, it undergoes nuclear clearance and cytoplasmic accumulation, driving neuronal degeneration. The same phenotype is present in patients bearing ALS-inducing mutations in other genes and ALS sporadic patients, defining TDP43 proteinopathy as a common feature in this pathology. Why does it cause specific motor neuron death?

Our quantitative proteomics analysis of the TDP43 interactome revealed the interaction with components of the mRNA surveillance pathway, suggesting a still undiscovered function in nonsense-mediated decay. We demonstrated that TDP43 acts translation- and SMG1-dependently as a mRNA decay enhancer of specific transcripts by binding their 3'UTR. In particular, it leads to the down-regulation of transcripts with a long 3'UTR.

From our sequencing data of spinal cords from TDP43^{Q331K} transgenic mouse model and of motor neuron-like NSC-34 cells silenced for TDP43 emerged that TDP43 plays another striking role in the 3'UTR, modulating mRNA alternative polyadenylation and promoting the generation of shorter transcripts. This finding is supported by the direct interaction of TDP43 with the cleavage stimulation factor, a core component of the polyadenylation machinery.

These results broaden our knowledge of the role of TDP43 in the post-transcriptional gene expression regulation. The impairment of these two biological processes by TDP43 proteinopathy could have implications in ALS pathogenesis, representing possible new targets for therapeutic approaches.

ABBREVIATIONS

ALS	Amyotrophic Lateral Sclerosis
APA	Alternative PolyAdenylation
BP	Biological Process
CC	Cellular Compartment
CDS	coding sequence
cEJC	canonical Exon Junction Complex
CRISPR	clustered regularly interspaced short palindromic repeats
DEG	Differentially Expressed Gene
DPG	Differentially Polyadenylated Gene
DSMA	Distal Spinal Muscular Atrophy
EJC	Exon Junction Complex
DIST	Distal
DSE	Downstream Sequence Element
fALS	familial Amyotrophic Lateral Sclerosis
GO	Gene Ontology
GWAS	Genome Wide Association Studies
hnRNP	heterogeneous nuclear RiboNucleoProtein
IB	Inclusion Body
KD	Knockdown
KO	Knockout
MF	Molecular Function
MND	Motor Neuron Disease
MS	Mass Spectrometry
ncEJC	non canonical Exon Junction Complex
NB	Northern Blot
NES	Nuclear Export Signal
NLS	Nuclear Localization Signal
NMD	Nonsense-Mediated Decay
OE	Overexpressed
ORF	Open Reading Frame
pAu	polyAdenylation site usage
PPI	Protein-Protein Interaction
PROX	Proximal
PTC	Premature Termination Codon
RBP	RNA Binding Protein
RNP	RiboNucleoProtein
SILAC	Stable Isotope Labeling with Amino acids in Cell culture
sALS	sporadic Amyotrophic Lateral Sclerosis
SMA	Spinal Muscular Atrophy
TARDBP	TransActivation Response Element DNA-Binding protein
USE	Upstream Sequence Element
UTR	UnTranslated Region
WB	Western Blot
WES	Whole-Exome Sequencing

1. INTRODUCTION

1.1 AMYOTROPHIC LATERAL SCLEROSIS

Amyotrophic lateral sclerosis (ALS) is a progressive and lethal neurodegenerative disease that affects upper and lower motor neurons (**Figure 1.1**), leading to weakness and paralysis of voluntary muscles and death from respiratory failure within 3-5 years after diagnosis. The onset of the disease occurs at a mean age of 55 years, in 1-2 individuals per 100000 each year and the risk increases with age. More than 1 in 500 deaths in adults is caused by ALS (Taylor et al., 2016).

The neurologist Jean-Martin Charcot diagnosed and described the first cases of ALS at the end of the 19th century (Kumar et al., 2011). The name of this condition reflects the muscle wasting ("a" for without, "myo" for muscle, "trophic" for nourishment) and the degeneration of motor neurons ("lateral" for the side of the spinal cord, "sclerosis" for hardening or scarring). In the United States, it is also referred to as Lou Gehrig's disease.

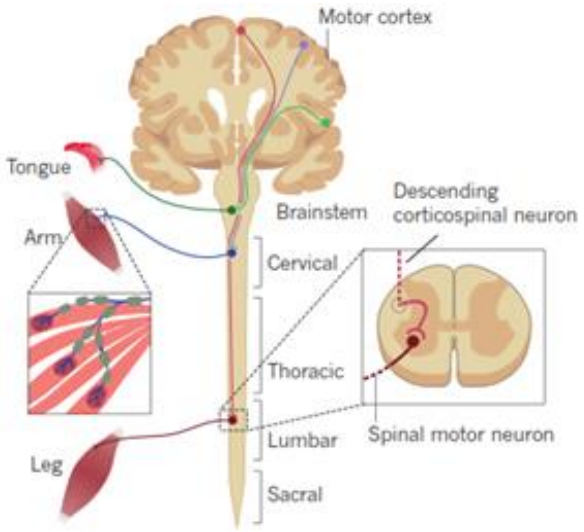

Figure 1.1 Components of the nervous system targeted by ALS. The upper motor neurons project from the motor cortex into the brainstem and spinal cord; the lower motor neurons innervate skeletal muscles and trigger their contraction (Taylor et al., 2016).

1.1.1 THE GENETICS BEHIND ALS

ALS is dominantly inherited in 10% of the cases (fALS), with a high penetrance. The

remaining 90% are sporadic cases (sALS) without a family history, even if they can have a genetic cause. In 1993 the first ALS-linked mutation affecting the *SOD1* gene was reported, and in the next years, more than 50 putative ALS genes have been proposed. The gene identification strategies evolved along the years: linkage analysis, genome wide association studies (GWAS), whole-exome sequencing (WES) and genome sequencing (Bettencourt and Houlden, 2015). The confirmed causative genes of ALS are listed in **Table 1.1**; they are involved in RNA metabolism, protein quality control, dynamics of cytoskeleton, autophagy and axonal transport. ALS has a complex genetic architecture, and several risk genetic factors have been reported to contribute to its susceptibility; recent examples are *Nek1* (Kenna et al., 2016) and *C21orf2* (van Rheenen et al., 2016).

Table 1.1 ALS-causative genes

Gene	Protein	Protein function	Mutations	ALS		Year of discovery
				Familial	Sporadic	
Sod1	Cu-Zn superoxide dismutase	Superoxide dismutase	>150	20%	2%	1993
Dctn1	Dynactin subunit 1	Component of dynein motor complex	10	1%	<1%	2003
Ang	Angiogenin	Ribonuclease/ RNA-binding protein	>10	<1%	<1%	2006
Tardbp	TDP43	RNA-binding protein	>40	5%	<1%	2008
Fus	FUS	RNA-binding protein	>40	5%	<1%	2009
Optn	Optineurin	Autophagy adaptor	1	4%	<1%	2010
Vcp	Transitional endoplasmic reticulum ATPase	Ubiquitin segregase	5	1-2%	<1%	2010
Ubqln2	Ubiquilin2	Autophagy adaptor	5	<1%	<1%	2011
C9orf72	C9orf72	Possible guanine nucleotide exchange factor	Intronic GGGGCC repeat	34%	6%	2011
Sqstm1	Sequestosome 1	Autophagy adaptor	10	<1%	?	2011
Pfn1	Profilin-1	Actin-binding protein	5	<1%	<1%	2012
Hnrnpa1	hnRNPA1	RNA-binding protein	3	<1%	<1%	2013
Tuba4a	Tubulin α-4A chain	Microtubule subunit	7	<1%	<1%	2014
Chchd10	Coiled-coil-helix-coiled-coil-helix domain-containing protein 10	Mitochondrial protein of unknown function	2	<1%	<1%	2014
Matr3	Matrin 3	RNA-binding protein	4	<1%	<1%	2014
Tbk1	Serine/threonine-protein kinase TBK1	Autophagy and inflammation regulator	10	?	?	2015

Note: adapted from (Taylor et al., 2016)

A common feature of ALS-affected neurons is the presence of cytoplasmic and

nuclear inclusion bodies (IBs) containing protein aggregates. In 2006, Virginia Lee and colleagues identified TDP43 as a component of the cytoplasmic ubiquitin-positive, tau- and alpha-synuclein-negative inclusions present in sALS-affected neurons using a “brute force” monoclonal antibody approach coupled with bi-dimensional electrophoresis and mass spectrometry analysis (Arai et al., 2006; Neumann et al., 2006). The importance of TDP43 in ALS pathogenesis increased in 2008 by the identification of more than 40 ALS-linked missense mutations in the *TARDBP* gene (**Figure 1.2b**) (Pesiridis et al., 2009).

1.2 TDP43

The transactivation response element DNA-binding protein (*TARDBP*) gene on chromosome 1 codifies for TDP43, a DNA/RNA binding protein of 414 amino acids and 43 kDa, member of the heterogeneous nuclear ribonucleoprotein (hnRNP) family. It is ubiquitously expressed and highly conserved among mammals and invertebrates (**Figure 1.2a**) (Ayala et al., 2005).

The protein structure, depicted in **Figure 1.2a**, presents an N-terminal domain, two RNA/DNA recognition motives (RRM1 and RRM2), which mediate the binding with single-stranded UG- or TG- repeats, but also with non-UG sequences (Buratti and Baralle, 2001; Tollervey et al., 2011; Bhardwaj et al., 2013; Lukavsky et al., 2013) and a glycine-rich C-terminal domain, which regulates interactions with other RNA-binding proteins (Buratti et al., 2005) and TDP43 itself via a prion-like region (Polymenidou and Cleveland, 2011; Budini et al., 2012). The protein is located mostly in the nucleus in punctuated structures, designated as T-bodies (Wang et al., 2002), due to the presence of a nuclear localization signal (NLS). The nuclear export signal (NES) instead allows it to shuttle to the cytoplasm, where it forms RNA granules, dendritic processing bodies (P-bodies) and stress granules (Wang et al., 2007; Colombrita et al., 2009; Liu-Yesucevitz et al., 2010).

TDP43 RNA interactome includes more than 6000 RNA species, and the TDP43 binding is preferentially localized in introns, 3′ untranslated regions (3’UTRs) and non-coding RNAs (Polymenidou et al., 2011; Van Nostrand et al., 2016).

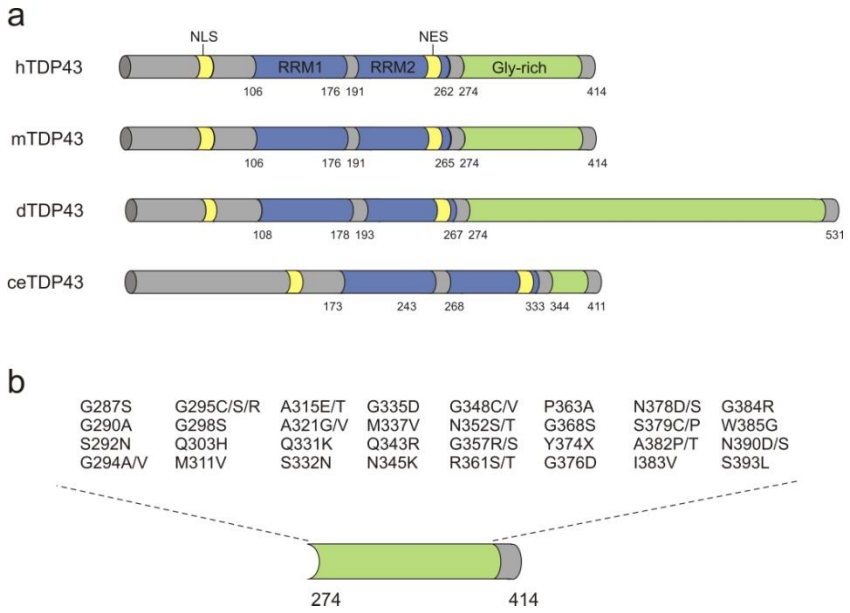

Figure 1.2 TDP43 in different species and in ALS. (**a**) Schematic representation of TDP43; the comparison with the orthologous genes (h, human; m, murine; d, Drosophila, ce, C.elegans) highlights its conservation among species (adapted from Vanden Broeck et al., 2014). (**b**) ALS-linked mutations are predominantly in the C-terminal domain (adapted from Pesiridis et al., 2009).

1.2.1 TDP43 LOSS-OF-FUNCTION and/or GAIN-OF-FUNCTION IN ALS?

TDP43 controls RNA metabolism at every stage of the RNA life cycle. It is involved in regulation of transcription (Ou et al., 1995; Lalmansingh et al., 2011) and multiple aspects of RNA processing and functioning. It plays a role in splicing of pre-mRNA, mRNA stability, transport from nucleus to cytoplasm and neurites, translation and microRNA processing (Buratti et al., 2001; Fiesel et al., 2009; Freibaum et al., 2010; Tollervey et al., 2011; Polymenidou et al., 2011; Ling et al., 2015) (**Figure 1.3**).

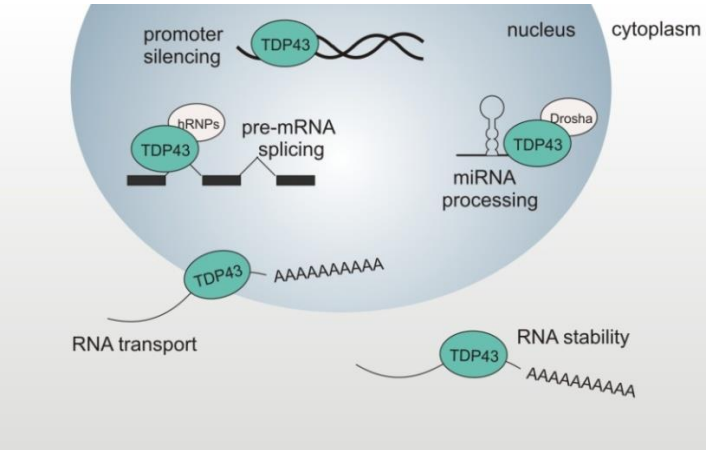

Figure 1.3 Biological functions of TDP43 (adapted from Lee et al., 2012).

To understand how the ALS-linked mutations can affect the TDP43 functions and mediate the neurotoxicity, several models of gain- and loss-of-function have been established in different species (Feiguin et al., 2009; Lu et al., 2009; Sephton et al., 2009;Wegorzewska et al., 2009; Kabashi et al., 2010; Xu et al., 2010; Li et al., 2010; Kraemer et al., 2010; Wu et al., 2010; Zhou et al., 2010; Stallings et al., 2010; Wils et al., 2010; Estes et al., 2011; Wang et al., 2011; Igaz et al., 2011; Xu et al., 2011).

Box 1. Use of transgenic animals as an assay for the investigation of disease mechanism

In the **gain-of-function** models, the overexpression of the mutated gene causes the disease, whereas the absence of the gene does not. If the overexpression of the wild type is also pathological, the effect is due to an increase of a normal function. Otherwise, it means that the mutation induces a novel toxic function.

The mutation generates a **loss-of-function** when its presence decreases or abolishes the protein activity; in this case, the gene knockout in homozygosis or also in heterozygosis or the gene knockdown leads to the disease, which is not induced by the overexpression of the mutant or the wild type protein.

A third disease model is a **dominant-negative** condition, where the allele with the mutation inhibits the function of the wild-type. Overexpression of the mutant gene and knockdown/knockout reproduce the pathological phenotype. Overexpression of the wild type is pathological only in some cases, as when it forms multi-protein complexes.

Table 1.2 Transgenic animals as disease models

Transgene expression	Disease model		
	Gain-of-function	Loss-of-function	Dominant negative
mutant OE	+	-	+
wild type OE	-/+	-	-/+
KO or KD	-	+	+

Notes: positive (+) or negative (-) for disease phenotype; overexpression (OE); knockout (KO); knockdown (KD); adapted from Xu, 2012.

Based on the phenotype of transgenic animal models (Drosophila, zebrafish, rodents), high levels of both mutated and wild type TDP43 cause neurodegeneration. According to the gain-of-function model, the phenomenon can be explained by the increase of a regular function, which becomes toxic.
However, a loss-of-function cannot be excluded, since neurological and neurodegenerative phenotypes are also shown in the absence of TDP43.
These observations could be consistent with a dominant-negative model: TDP43 is part of ribonucleoprotein complexes, and when it is up- or down-regulated it alters their stoichiometry, rendering them dysfunctional.
In the ALS-patients TDP43 is cleared from the nucleus, hyperphosphorylated, polyubiquitinated and cleaved (Neumann et al., 2006; Igaz et al., 2008). The produced 25 kDa fragment corresponds to the C-terminal part, has a high propensity for aggregation and sequesters the full-length TDP43 in cytoplasmic aggregates, which may induce a gain-of-cytotoxicity, but also a dysfunction of TDP43 and its complexes. In most of the ALS-cases, TDP43 is not mutated and may aggregate as a result of proteostasis impairment, causing the TDP43 pathology. Aggregation represents an hallmark of several neurodegenerative diseases (Kumar et al., 2016), even if the link between them, as well as the cause and effect relationship are still unclear.

1.2.2 TDP43 AUTO-REGULATION

TDP43 protein level is tightly controlled by a negative feedback loop, which depends on the interplay between splicing, 3’ end processing, and mRNA stability.
TDP43 binds to its 3′ untranslated region and promotes RNA instability in an exosome-dependent way (Ayala et al., 2010). It also mediates the splicing in the 3’UTR of its pre-mRNA, leading to introns removal. The presence of an exon junction complex (EJC) after the stop codon induces Tdp43 mRNA degradation by nonsense-mediated decay (NMD) pathway (Polymenidou et al., 2011; Koyama et al., 2016). The mRNA decay can also occur through a NMD-independent mechanism, which involves spliceosomal assembly and/or intron 7 processing and produces a not fully processed pre-mRNA, retained in the nucleus and degraded (Bembich et al., 2014).

Moreover, TDP43 overexpression blocks its canonical polyadenylation site (PAS) recognition and activates a cryptic PAS, promoting a nuclear mRNA retention mechanism (Avendaño-Vázquez et al., 2012; Koyama et al., 2016).
These auto-regulatory mechanisms maintain the TDP43 homeostatic concentration, preventing its toxic up-regulation. It has been demonstrated *in vivo* and *in vitro*, that wild type and mutated TDP43 overexpression reduces the endogenous mRNA and protein level, whereas a lower expression of one allele is compensated by the up-regulation of the other one (Xu et al., 2010; Ayala et al., 2011; Igaz et al., 2011; Polymenidou et al., 2011).

1.3 NONSENSE-MEDIATED DECAY (NMD)

Nonsense-mediated mRNA decay (NMD) is a translation-dependent pathway involved in mRNA surveillance and post-transcriptional gene expression regulation. NMD acts as a quality control mechanism, degrading abnormal transcripts with a premature termination codon (PTC) and preventing the synthesis of potentially toxic truncated protein isoforms (Losson and Lacroute 1979; Maquat et al., 1981). Transcriptional errors and genetic mutations are sources of defective mRNAs targeted by NMD. Alternative splicing is also able to introduce a PTC by translational frameshift alteration. Moreover, the removal of an intron in the 3'UTR generates an exon-exon junction after the canonical stop codon, causing the transcript degradation (Nagy and Maquat 1998). Also, NMD plays a physiological role, since it controls the abundance of several endogenous mRNAs, leading to their down-regulation under specific cellular conditions. Examples of NMD-sensitive transcripts are mRNAs with upstream open reading frames (uORFs) or with abnormal extensions of their 3′ untranslated regions (3′UTRs) (Yepiskoposyan et al., 2011).
In mammalian cells, NMD can be activated by two different mechanisms, which depend or not on the involvement of the exon junction complex (EJC), when a premature translation termination or a functionally equivalent improper termination event takes place.

1.3.1 EJC-DEPENDENT NMD

The EJC is a dynamic protein complex (**Figure 1.4**) deposited 20-24 nucleotides upstream of exon-exon junctions in a sequence independent manner during pre-mRNA splicing (Le Hir et al., 2000; Singh et al., 2012). It is assembled in the nucleus, remains associated with the mRNA during the nucleus-cytoplasm translocation and is removed during the "pioneer" round of translation by the ribosome machinery (Dostie and Dreyfuss, 2002; Sato and Maquat, 2009; Gehring et al., 2009). This round occurs at a distance of ~430 nm outside the nucleus, within 5 – 56 seconds after the entrance into the cytoplasm (Trcek et al., 2013) and displaces all EJCs located in the 5'UTR and the coding sequence.

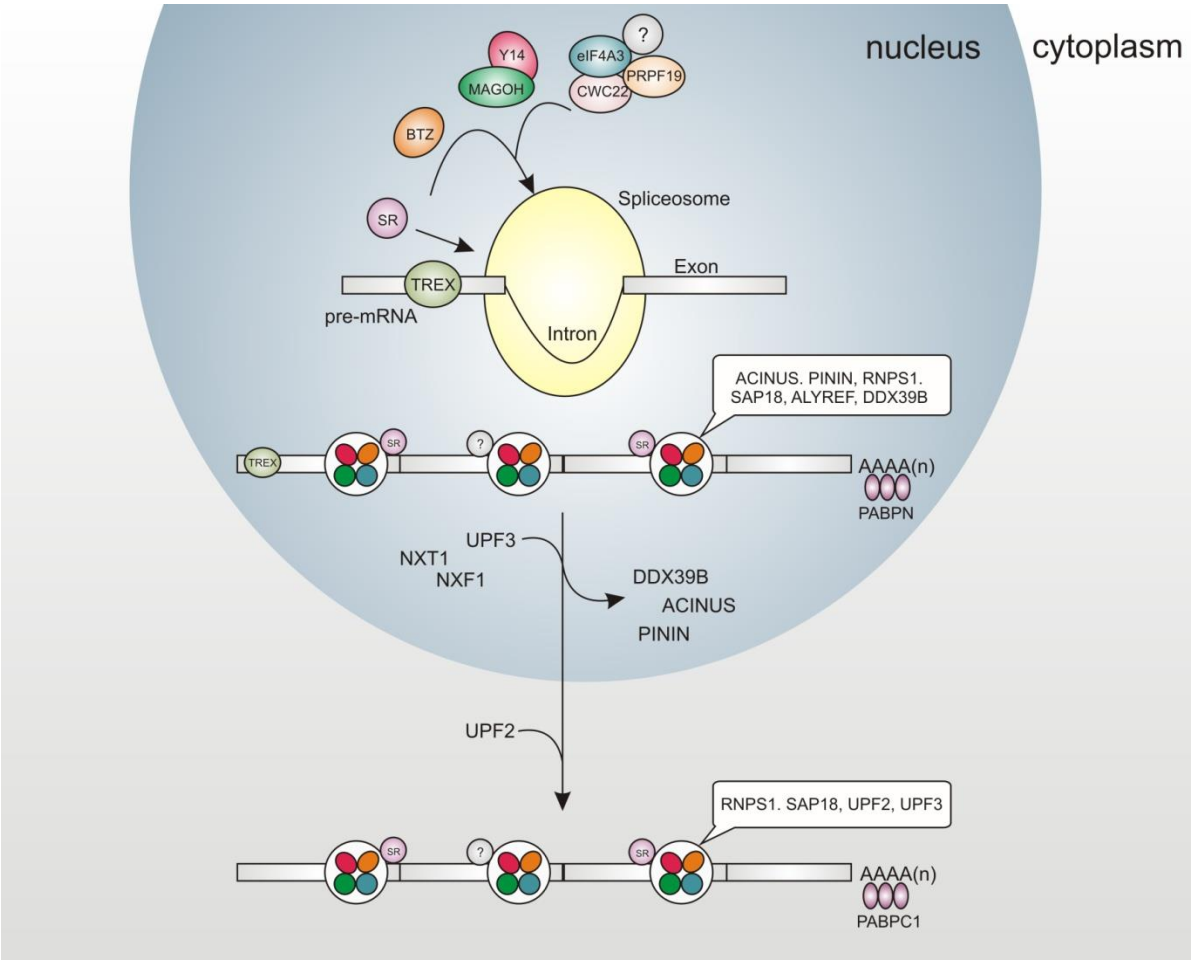

Figure 1.4 The Exon Junction Complex composition in the nucleus and cytoplasm. The EJC is a dynamic structure which tags the splice junction. It consists of a core complex, composed by eukaryotic translation initiation factor 4A3 (EIF4A3), cancer susceptibility candidate 3 (CASC3 or BARENTSZ, BTZ or MLN51), RNA-binding motif protein 8A (RBM8A or Y14) and mago-nashi homolog (MAGOH). It is also formed by splicing factors (RNPS1, DDX39B or UAP56, SAP18, ACINUS, PININ) and exporting factors (DDX39B, ALYREF, NXF1-NXT1). Some undefined RNA-

binding proteins (?), as well as SR proteins, promote the EJC recruitment and deposition and remain associated with the mRNA during its transport (Adapted from Le Hir et al., 2016).

The EJC-dependent NMD (**Figure 1.5**) is based on the “50-55 nucleotides rule”. In the presence of an EJC located more than 50-55 nucleotides downstream of the first stop codon of the open reading frame, the ribosome stalls at this premature termination codon (Nagy and Maquat, 1998) allowing the recruitment of UPF1 (Up-frameshift protein 1), SMG1 (Suppressor with Morphogenic effect on Genitalia 1), SMG8, SMG9, eRF1 and eRF3 (eukaryotic Release Factors 1 and 3) and the assembly of the Surveillance complex (SURF) (Kashima et al., 2006; Ivanov et al., 2008; Singh et al., 2008; Yamashita et al., 2009). The interaction of this complex with UPF2, UPF3b and the EJC forms the decay-inducing complex (DECID). SMG1 phosphorylates and activates the NMD effector UPF1 (Czaplinski et al., 1995; Bhattacharya et al., 2000; Yamashita et al., 2001), leading to ribosome release and degradation factors recruitment. UPF1 is a RNA-dependent ATPase and ATP-dependent RNA helicase which unwinds the RNA and removes the proteins from the NMD target. Following phosphorylation and possibly induced by ATP hydrolysis, UPF1 undergoes a conformational change that increases its affinity for RNA (Bhattacharya et al., 2000; Yamashita et al., 2001; Kashima et al., 2006; Chamieh et al., 2008; Franks et al., 2010; Shigeoka et al., 2012; Okada-Katsuhata et al., 2012; Fiorini et al., 2013;). At this point, the target mRNA is irreversibly committed to decay. SMG5, SMG6, SMG7, PNRC2 (proline-rich nuclear receptor coregulatory protein 2) and the protein phosphatase 2A (PP2A) are recruited. The endonuclease SMG6 cleaves the mRNA near the PTC (Huntzinger et al., 2008; Eberle et al., 2009); SMG5 and SMG7 promote mRNA deadenylation followed by decapping and exonucleolytic decay (Unterholzner and Izaurralde 2004); PNRC2 interacts with the decapping enzyme DCP1a; PP2A dephosphorylates UPF1 to make it accessible for the next round of NMD. The NMD target, without the 5′ cap and the 3′ poly(A) tail, is unstable and is degraded from both ends (Anders et al., 2003; Boehm et al., 2014; Chiu et al., 2003; Kurosaki et al., 2014; Lee et al., 2015; Ohnishi et al., 2003; Schmidt et al., 2015).

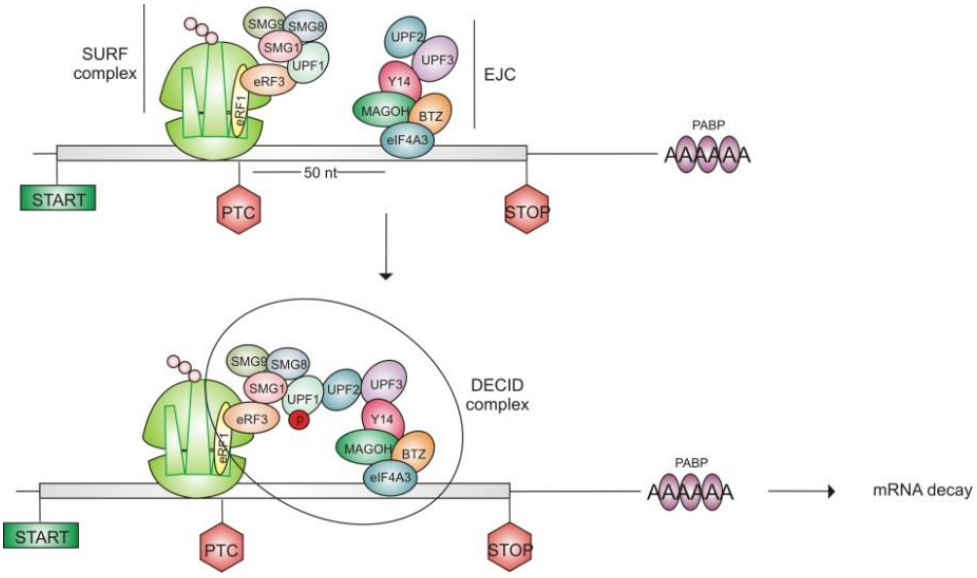

Figure 1.5 EJC-dependent NMD (Adapted from Kervestin and Jacobson, 2012).

The EJC-dependent model does not fit with all the experimental data. For example, in some cases, NMD can be triggered by an EJC located less than 50 nucleotides upstream of the stop codon. Otherwise, in other cases, NMD can be insensitive to the presence of a PTC. Moreover, transcriptome-wide analysis of EJC deposition revealed that EJCs are not present upstream of all exon-exon junctions (Saulière et al., 2012, Mühlemann 2012); half of all EJCs are present at non-canonical positions (**Figure 1.6**), and it is still unknown if alterations of EJC deposition can affect the efficiency of the EJC-dependent NMD.

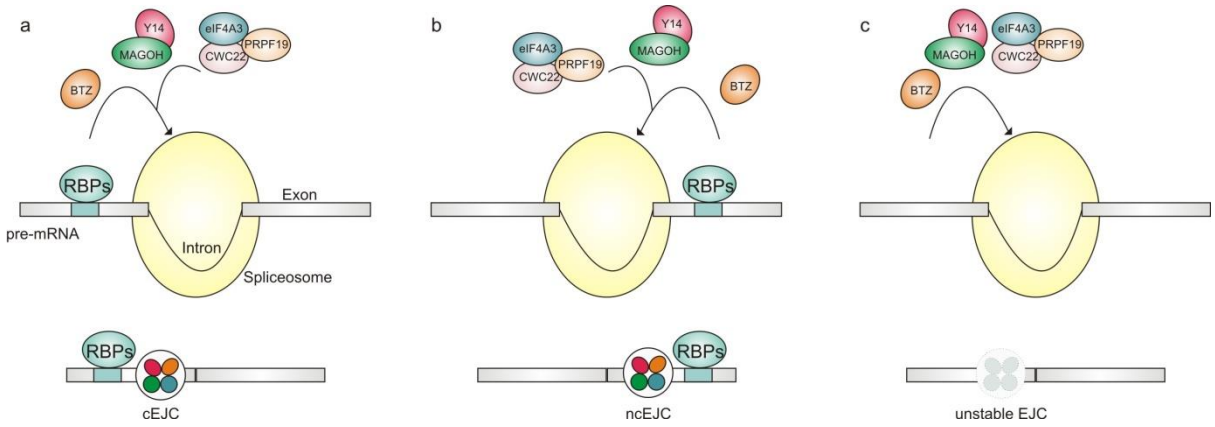

Figure 1.6 Involvement of RNA binding proteins (RBPs) in EJC deposition. (**a**) The canonical EJC (cEJC) is assembled 20-24 nucleotides upstream the exon-exon junction. RBPs may be involved in the recruitment and the stabilization of the EJC core complex. (**b**) RBPs may influence the loading of EJC in non-canonical regions (ncEJC). (**c**) The absence of specific RBPs may affect negatively the stabilization of the EJC, which is disassembled (adapted from Le Hir et al., 2016).

1.3.2 EJC-INDEPENDENT NMD

The NMD activation in eukaryotic cells can also be influenced by the distance between the stop codon and the cytoplasmic poly(A)-binding protein 1 (PABPC1) in an EJC-independent manner.

During translation termination, PABPC1 interacts with eRF3 enhancing the release of the ribosome stalled at the stop codon and its recycling to the 5' end of the same transcript (**Figure 1.7a**) (Hoshino et al., 1998; Amrani et al., 2004; Behm-Ansmant et al., 2007). However, some studies observed that the effect of PABPC1 on efficient termination is weaker in transcripts with a long 3'UTR. UPF1 binds promiscuously the cytoplasmic mRNA and is displaced by the translating ribosomes in the 5'UTR and in the coding region (Gregersen et al., 2014; Hogg and Goff, 2010; Hurt et al., 2013; Kurosaki and Maquat, 2013; Kurosaki et al., 2014; Lee et al., 2015; Zünd et al., 2013); it accumulates in the 3'UTR, where it can compete with PABPC1 for the interaction to eRF3 eliciting NMD (**Figure 1.7b**) (Singh et al., 2008). This model leads to degradation of PTC-harbouring mRNA but is also involved in the regulation of endogenous transcripts. In general, the NMD targets are characterized by a termination codon that is not in a favorable environment for efficient translation termination (Amrani et al., 2006; Nicholson et al., 2010).

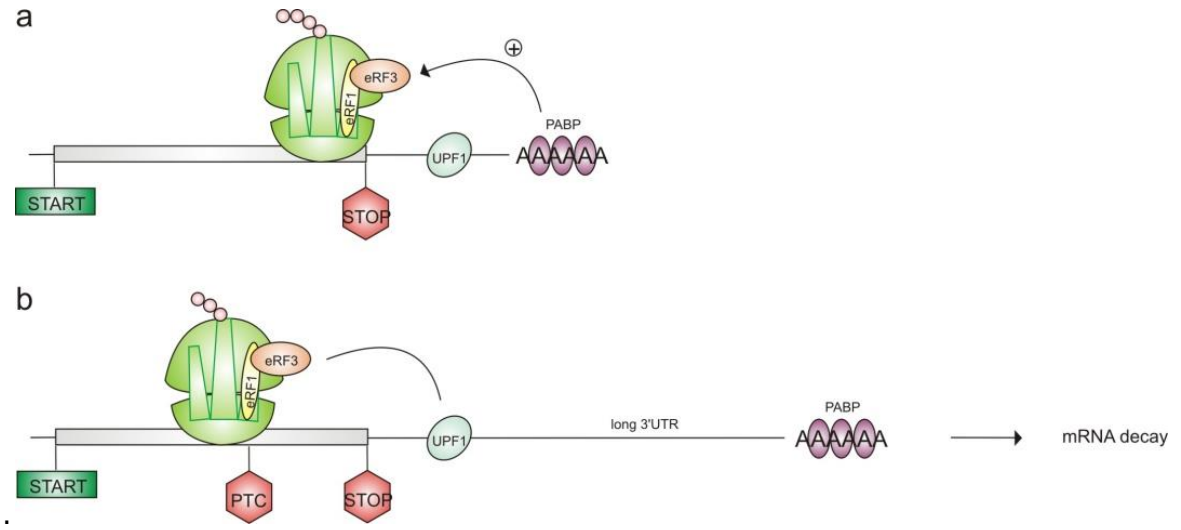

Figure 1.7 EJC-independent NMD. (**a**) Schematic representation of a normal translation termination and (**b**) how a long 3'UTR triggers EJC-independent NMD (Adapted from Kervestin and Jacobson, 2012).

Box 2. Which are the physiological NMD targets and how can they be studied?

The NMD program was described for the first time in a patient affected by beta-thalassemia (Chang and Kan, 1979). Since then the human *beta-globin* gene has been used to develop RNA reporter systems to investigate deeper the mechanism (Maquat et al., 1981; Thermann et al., 1998). In particular, the tethering reporter assay was used to demonstrate the involvement of UPF1, Y14, RNPS1, PYM, and Barentsz in this pathway (Lykke-Andersen et al., 2000; Lykke-Andersen et al., 2001; Gehring et al., 2003; Bono et al., 2004; Palacios et al., 2004). Among the mRNA surveillance pathways, the nonsense-mediated decay is the most studied, and in the last years, the knowledge of this process is increased. However, the identification of NMD targets using high-throughput data remains challenging. Transcriptomic analysis revealed the up regulation of transcripts-lacking NMD features after UPF1 depletion, whereas many predicted NMD-targets remained unchanged in its absence. The hypothesis is that the presence of a PTC is a strong NMD-eliciting feature, but for what concern the physiological mRNA targets, their susceptibility to NMD may depend on more than one factor (Mendell et al., 2004; Wittmann et al., 2006).

1.3.3 STAUFEN1-MEDIATED DECAY (SMD)

In mammalian cells, another mRNA degradation process has been reported in 2005 (Kim et al., 2005), the STAUFEN1-mediated mRNA decay (SMD). STAUFEN1 binds STAUFEN1-binding sites (SBS) in the 3'UTR of target mRNAs. SBS are dsRNA structures formed by either intra-molecular (**Figure 1.8a**) or inter-molecular (**Figure 1.8b**) base-pairing (Gong and Maquat 2011). During the first round of translation, when the ribosome reaches a stop codon sufficiently upstream of an SBS, the bound STAUFEN1 is not removed, recruits the NMD effector UPF1 and enhances its helicase activity (Park et al., 2013), eliciting a splicing-independent mRNA decay.

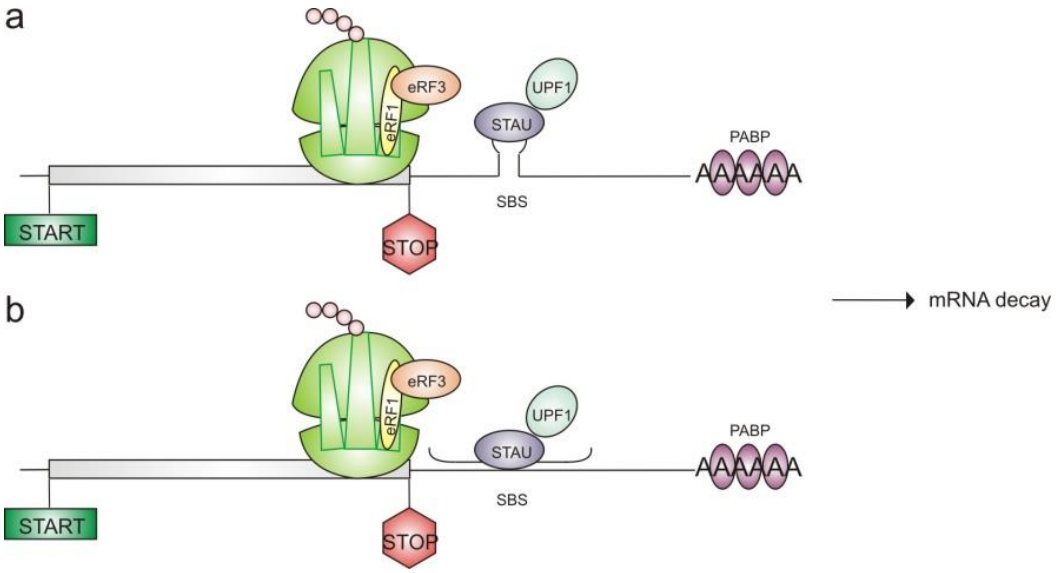

Figure 1.8 STAUFEN1 mediated decay (SMD). STAUFEN1 binds the 3'UTR of its targets, through the recognition of STAUFEN1-binding sites (SBS), which can be (**a**) intra-molecular or inter-molecular (**b**) dsRNA structures (adapted from Park and Maquat, 2013).

1.4 ALTERNATIVE POLYADENYLATION (APA)

Polyadenylation is a cotranscriptional maturation process by which premature messenger RNAs (pre-mRNAs) are cleaved and acquire a poly(A) tail at their 3' end. This process involves almost all eukaryotic mRNA and other products of polymerase II, especially long non-coding RNAs (lncRNAs). In mammalian genome ~70% of genes and about half of the genes in flies, worms, and zebrafish present more than one polyadenylation site, leading to the formation of several transcripts with different 3' termini (Tian et al., 2005; Jan et al., 2011; Hoque et al., 2012; Derti et al., 2012; Smibert et al., 2012; Ulitsky et al., 2012). Alternative polyadenylation (APA) allows the differential usage of these sites, representing a post-transcriptional gene regulation mechanism spread across all eukaryotic species.

1.4.1 MECHANISM OF POLYADENYLATION

The 3' end maturation is a two-step process, which involves specific endonucleolytic cleavage of the nascent RNA, followed by adenosine tail synthesis on the 3´ terminus of the cleaved product by poly(A) polymerase (PAP). The 3' end cleavage

and polyadenylation site selection in mammalian pre-mRNAs is controlled by *cis*-acting RNA elements and *trans*-acting factors (**Figure 1.9**) (reviewed in Elkon et al., 2013, Gruber et al., 2014; Tian and Manley, 2017). The polyadenylation signal (PAS) represents the leading *cis*-element; its canonical sequence is the hexanucleotide AAUAAA, even if more than ten weaker close variants are known (Derti et al., 2012), and it is mostly located 10–35 nucleotides upstream of the cleavage site. Other RNA elements upstream (UGUA elements, U-rich elements) and downstream (GU-rich or U-rich sequences) of the PAS, typically more than 40 nucleotides away, can enhance polyadenylation efficiency. The proteomic and structural characterization of the 3' end processing machinery identified the core processing factors and revealed the presence of other 50 proteins typically involved in other cellular processes (Shi et al., 2009). The polyadenylation machinery is composed of four complexes: Cleavage and Polyadenylation Specificity Factor (CPSF), Cleavage Stimulation Factor (CSTF), Cleavage Factor I and II (CFI, and CFII). Single auxiliary proteins are also involved: symplekin, poly(A) polymerase (PAP), poly(A)binding protein (PABP), retinoblastoma-binding protein 6 (RBBP6) and the C-terminal domain (CTD) of RNA polymerase II (RNApol II) largest subunit. CPSF recognizes the AAUAAA sequence, and CSTF binds to the downstream sequence element (DSE), cooperatively interacting one with each other and promoting the cleavage between their binding sites. CFI interact with the upstream sequence element (USE) and CFII cleaves the RNA, generating a CA 3' end for poly(A) tail extension (~200 residue length), which is catalyzed by PAP with the help of PABP.

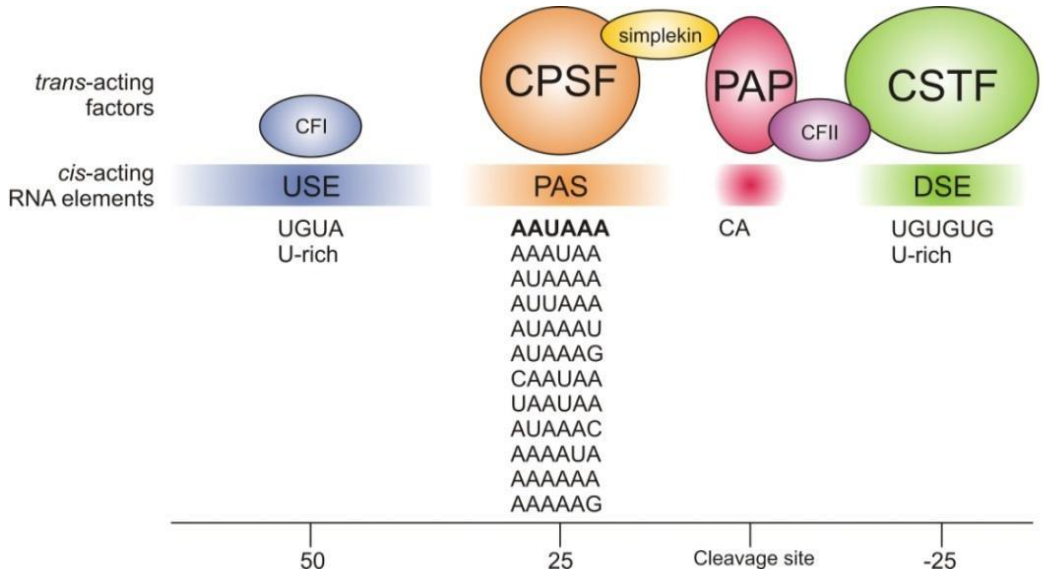

Figure 1.9 Factors involved in cleavage and polyadenylation during the 3'end maturation.

Trans-acting factors and their corresponding *cis*-acting RNA elements are colored similarly. Cleavage and Polyadenylation Specificity Factor (CPSF) contains CPSF1 (or CPSF160), CPSF 2 (or CPSF100), CPSF3 (or CPSF73), CPSF4 (or CPSF30), WDR33 and Fip1 (factor interacting with PAP) and specifically recognizes the polyadenylation signal (PAS) through CPSF1. The canonical 6-mer PAS and its variants are listed (Gruber et al., 2014). Cleavage Stimulation Factor (CSTF) is an hexamer composed by CSTF1 (or CSTF50), CSTF2 (or CSTF64, or its paralogue, τCSTF64), CSTF3 (CSTF77) and its interaction with the downstream U-/GU-rich sequence element (DSE) is mediated by CSTF2. Cleavage factor I (CFI) is a tetramer which includes CFI25 and either CFI68 or CFI59 and binds the upstream U-rich/ UGUA sequence element (USE). Cleavage factor II (CFII) contains PCF11 and CLP1 and assists the termination of the RNA Pol II-mediated transcription (adapted from Tian et al., 2013; Elkon et al., 2013; Gruber et al., 2014).

1.4.2 CLASSIFICATION OF ALTERNATIVE POLYADENYLATION

Polyadenylation events can be categorized into two classes, according to the splicing involvement (**Figure 1.10a**) (reviewed in Lutz and Moreira, 2011; Di Giammartino et al., 2011; Tian et al., 2013; An et al., 2013; Elkon et al., 2013). In the first class, multiple PASs are present within the last exon; the resulting mRNAs encode the same polypeptide chain, even if the protein amount can be affected. When the distal alternative polyadenylation signal is chosen, the 3'UTR length increases, introducing binding sites for regulatory elements, as RNA binding proteins, miRNAs, and lncRNAs, that can influence the mRNA stability, translation efficiency and cellular localization (**Figure 1.10b**). The second class combines alternative splicing with alternative polyadenylation; it involves PASs located in upstream introns or exons, generating mRNAs with different coding sequences. Both tandem and splicing dependent alternative polyadenylation generate transcripts with different 3' ends, however, the downstream effects of these two processes at the protein level are not the same.

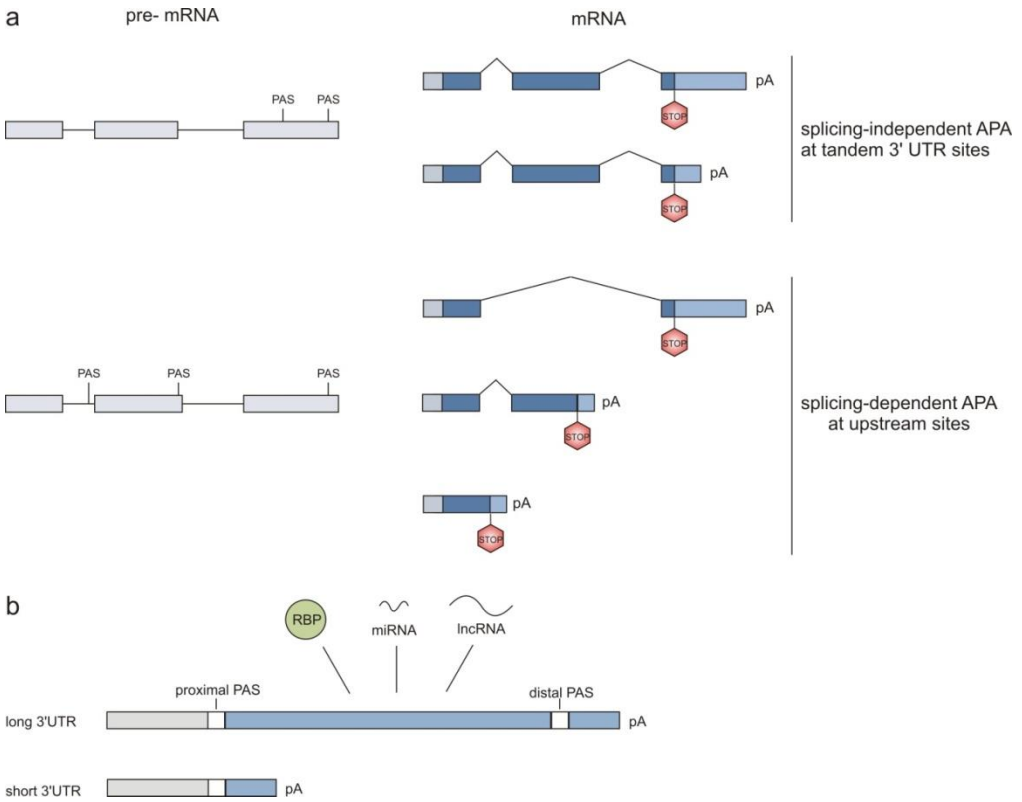

Figure 1.10 Classification of alternative polyadenylation. (**a**) Alternative polyadenylation events are divided into two classes. Discrimination of splicing dependent and independent mechanism is indicated. Schematic of the pre-mRNA with one or more alternative polyadenylation signal (left) and the relative mRNAs (right). Light gray boxes, exons; lines, introns; light blue boxes, untranslated regions; dark blue boxes, coding regions. (**b**) Splicing independent alternative polyadenylation generates mRNA products with different 3' UTR length. A long 3'UTR can potentially contain more *cis*-regulatory sequences targeted by RNA binding proteins (RBPs), microRNAs (miRNAs), and long noncoding RNAs (lncRNA) (adapted from Lutz and Moreira, 2011; Di Giammartino et al., 2011; Tian et al., 2013; An et al., 2013; Elkon et al., 2013; Gruber et al., 2014; Tian and Manley, 2017).

Box 3. Methods for polyadenylation sites mapping

The genome-wide mapping of polyadenylation sites and the quantitative analysis of APA changes can be achieved by several sequencing methods. Standard RNA-seq can be adopteded for this kind of analysis (Wang et al., 2008; Masamha et al., 2014; Prucendio et al., 2015). The identification of the 3′ ends can be performed by using reads with untemplated A-stretches. APA isoforms are quantified by comparing the density of the reads mapped only in the longer transcript with that of the reads in the common region. However, the presence of more than two APA isoforms may complicate the analysis. Moreover, RNA-seq needs a great sequencing depth since it is characterized by a low coverage at the extremities of the transcript (**Figure 1.11**). Other approaches (cDNA/EST-seq, PAS-seq, PASAS and PolyA-seq) rely on oligo(dT)-based cDNA synthesis for library preparation. Since they can be affected by oligo(dT) priming at internal A-rich sequences, different computational approaches have been implemented to reduce the false discovery rate (Mangone et al., 2010; Fox-Walsh et al. 2011; Shepard et al., 2011; Fu et al., 2011; Derti et al., 2012). In 3P-seq and 3′ READS, 3′ end fragments are captured by RNA ligation, avoiding the internal priming issue, but the protocol requires more enzymatic steps, and the RNA ligation bias can affect quantitative performance (Jan et al., 2010; Hafner et al. 2011; Hoque et al., 2012). During direct RNA sequencing (DRS), the poly(A) RNAs are captured on oligo(dT) coated slides and directly sequenced on Helicos single-molecule sequencing platform. The internal priming could still be a problem, even if the number of false positives reported in the literature is very low. In comparison with the Illumina system, the reads count is lower and the average read length is shorter. However, this technique is more quantitative, since individual RNAs are sequenced without possible biases introduced during library production, as RT- PCR or other enzymatic reactions (Ozsolak et al., 2010; Ozsolak and Milos 2011; Sherstnev et al., 2012).

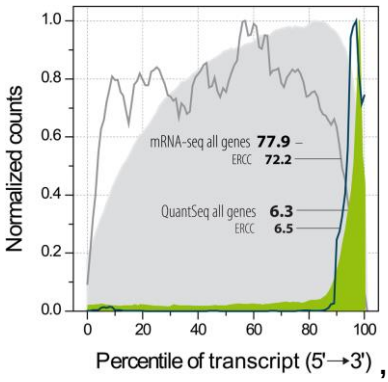

Figure 1.11 RNA-seq *versus* 3'end-seq. Coverage is plotted for all transcripts; mRNA-seq gray area; 3'end-seq green area, spike-in control mix lines (from Mol et al., 2014).

1.4.3 ROLE OF RNA BINDING PROTEINS IN APA REGULATION

The alternative polyadenylation mechanism is finely tuned; variations in the core factors expression level can cause differential PAS selection, unbalancing the relative ratio of the produced transcripts. For example, CFIm25 is a repressor of proximal poly(A) site usage and its knockdown leads to the production of shorter transcripts (Masamha et al., 2014). The up regulation of CSTF components promotes the usage of the proximal PAS and their silencing, in particular, the CSTF2 depletion, results in an opposite phenomenon (Takagaki et al., 1996).

The 3' end processing can also be modulated by other RNA binding proteins, which compete and/or cooperate with the polyadenylation machinery, according to their binding site (**Table 1.3**) (Erson-Bensan, 2016). As previously explained, alternative polyadenylation and alternative splicing are interconnected processes. Therefore they can share RNA binding proteins which are involved in the regulation of both mechanisms.

Table 1.3 RBPs involved in APA

RNAbp	Binding site	Effect	Reference
hnRNP H	proximal PAS	Enhancer	*Katz et al., 2010*
CPEB1	USE of the proximal PAS	Enhancer	*Bava et al., 2013*
PTB	DSE	Inhibitor	*Castelo-Branco et al., 2004*
Hu proteins	DSE	Inhibitor	*Zhu et al., 2007; Dai et al., 2012; Mansfield and Keene, 2012*
ESRP1/2	DSE	Inhibitor	*Dittmar et al., 2012*
PABPN1	USE of the proximal PAS	Inhibitor	*Jenal et al., 2012*
dSXL	DSE	Inhibitor	*Gawande et al., 2006*
dELAV	proximal PAS	Inhibitor	*Hilgers et al., 2012*
MBNL	USE of the PAS	Enhancer	*Batra et al., 2014*
	PAS	Inhibitor	
NOVA2	PAS	Inhibitor	*Licatalosi et al., 2008*
FUS	DSE of the PAS	Enhancer	*Masuda et al., 2015*
	USE of the PAS	Inhibitor	
TDP43	USE or close to the proximal PAS	Inhibitor	*Rot et al., 2017*
	DSE of the proximal PAS	Enhancer	

Note: d = Drosophila; DSE = downstream sequence element; USE = upstream sequence element

1.4.4 MODELS OF REGULATORY MECHANISMS FOR PAS SELECTION

The PAS selection is regulated by multiple mechanisms, acting in combination (reviewed in Shi, 2012). According to the *survival of the fittest model* (**Figure 1.12a**), the alternative polyadenylation outcome depends on the intrinsic affinity of the PAS with the polyadenylation machinery and the abundance of the core 3' processing factors. The distal PAS is typically the strongest, presumably to ensure proper transcription termination; on the other hand, proximal PAS is transcribed earlier and has more time to be chosen. Elevated protein levels of the core processing factors promote the usage of the proximal PAS. When the factors are limited, the distal PAS is preferred. A concrete example of this model is the alternative polyadenylation of IgM mRNA. During B-cell activation, high level of CSTF2 results in shorter transcripts; however in resting B-cells the distal PAS is preferentially chosen, due to a limited presence of CSTF2 (Takagaki et al., 1996). The PAS selection can be enhanced or inhibited by regulatory factors, as explained by the *agonist/antagonist model* (**Figure 1.12b**); several examples are listed in **Table 1.3**. Moreover, alternative polyadenylation depends on the RNA polymerase II (RNApol II) processing (**Figure 1.12c**). High transcription activity is correlated with proximal PAS choice, while high transcription elongation rate promotes the usage of distal PAS.

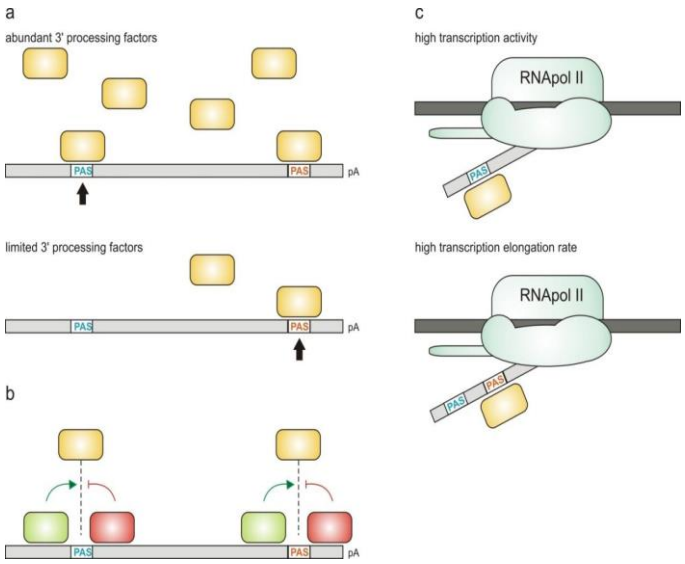

Figure 1.12 Mechanisms of regulation in PAS selection. The strong PAS is highlighted in red, the weak PAS in blue; yellow box, 3' processing factor; green box, agonist factor; red box, antagonist factor; RNA is in light gray, DNA in dark gray (adapted from Shi, 2012).

2. AIM

Motor neuron diseases (MNDs) are a group of untreatable and lethal disorders characterized by progressive degeneration of upper and lower motor neurons in the central nervous system and gradual weakness of bulbar, limb, thoracic, and abdominal muscles. In most cases, these pathological conditions lead to paralysis of the voluntary muscles and a poor prognosis.

The etiology is largely unknown; environmental, toxic, viral or genetic factors may be implicated in sporadic MNDs. Even if in some hereditary forms different mutations in ubiquitously expressed genes have been identified to be responsible for the selective death of motor neurons, it is still unclear which are the converging mechanisms underlying the phenomenon.

Alterations in RNA metabolism are a common signature in different neurodegenerative pathologies. The RNA binding proteins represent critical players in the RNA-processing events and, when their functionality is compromised, deleterious consequences can arise for the cell. Many genes mutated in familial forms of MND are involved in RNA splicing, transport, stability, and translation. Among them, we mainly focused our attention on TDP43. The major objective of this study is to find out novel possible roles of TDP43, potentially impaired in ALS, and to analyze the molecular mechanisms through which TDP43 exploits its functions *in vivo* and *in vitro*, making use of high- and low-throughput proteomic and transcriptomic approaches, molecular assays and already published data.

Another aim of the project is the generation of a panel of MND cell models, in which tagged wild type and mutated RNA binding proteins involved in Amyotrophic Lateral Sclerosis (ALS), Spinal Muscular Atrophy (SMA), and Distal Spinal Muscular Atrophy type 1 (DSMA1) can be induced. The engineered motorneuron-like cells are suitable for *in vitro* studies, protein and RNA interactome analysis.

3. RESULTS: TDP43 AND NONSENSE-MEDIATED DECAY

3.1 TDP43 INTERACTS WITH mRNA SURVEILLANCE PATHWAY COMPONENTS

We quantitatively assessed the TDP43 protein interactome in the NSC-34 motor neuron-like cell line (**Table 3.1** and **Figure 3.1b**) through SILAC-based proteomics (**Figure 3.1a**). We obtained an enrichment in components of the spliceosome (KEGG mmu03040, 34 interacting proteins, Fold Enrichment: 17.7, Enrichment p value 1.97e-34), the ribosome (KEGG mmu03010, 35 interacting proteins, Fold Enrichment: 16.8, Enrichment p value 1.64e-34) and the mRNA surveillance pathway (KEGG mmu03015, 12 interacting proteins, Fold Enrichment: 12.07, Enrichment p value 5.84e-15). We identified members of the exon-junction complex (EJC), two transient EJC interacting factors, and ten SR proteins. We also found the principal nonsense-mediated mRNA decay (NMD) effector UPF1, the phosphatase PPP2R1A, which dephosphorylates UPF1 for the next round of NMD, and the central NMD suppressor PABPC1. Referring to the study published by Singh and colleagues in 2012, our list of proteins bound by TDP43 is also enriched in components of EJC interactome (EJC-ome, fold enrichment: 15.5, p value = 1.38e-27). Among the other interactors, we found proteins involved in RNA processing, post-transcriptional gene expression regulation, and epigenetic gene silencing (**Table 3.1**).

We validated the binding with the core EJC components Y14, EIF4A3, BTZ and with UPF1 and PABPC1 by immunoprecipitation and Western blot analysis (**Figure 3.1c**). Since the interactions that we tested are RNA-dependent (except for PABPC1), we wanted to understand if the enrichment in components of the mRNA surveillance pathway is specific for the TDP43 interactome or whether these proteins can be also present among the binders of other RNA binding proteins.

We compared the immunoprecipitation of TDP43 with the pulldown of the FET family members FUS, EWSR1, and TAF15 (**Figure 3.1d**). The Western blot analysis revealed that the interaction of TDP43 with elements of the mRNA surveillance pathway, as UPF1 and EIF4A3, is a specific feature and it does not depends on its

intrinsic nature of RBP (**Figure 3.1e**).

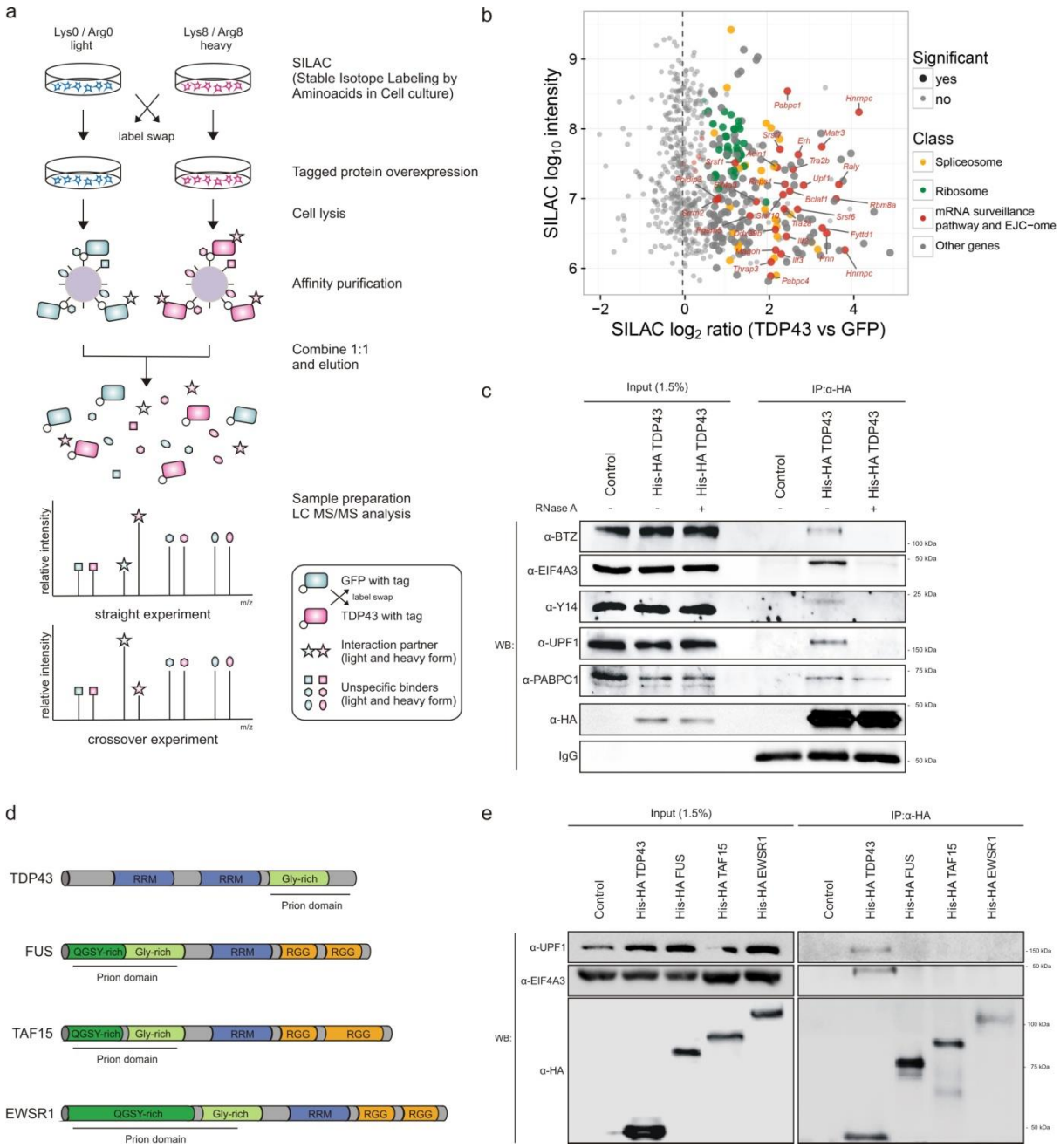

Figure 3.1 TDP43 interacts with the mRNA surveillance pathway. (**a**) Workflow of protein-protein interaction analysis by SILAC based q-AP-MS, Stable Isotope Labeling with Amino acids in cell culture based quantitative Affinity Purification coupled with high-resolution Mass Spectrometry (figure adapted from Paul et al., 2011). His-HA hTDP43 and His-HA GFP were overexpressed for 48 h in NSC-34 cell line cultured in heavy (Lys8/Arg8) or light (Lys0/Arg0) medium, respectively. After the pull-down, beads were mixed 1:1 and captured bait/prey complexes were eluted and analyzed by LC-MS/MS. We performed in parallel a crossover experiment by label swap. Specific interaction partners have a heavy-to-light ratio >1 in the straight experiment and heavy-to-light ratio <1 in the crossover experiment, whereas unspecific binders have 1:1 heavy-to-light ratio in both experimental conditions.

We performed the SILAC based q-AP-MS analysis in quadruplicate to identify TDP43 protein interactors (2 straight and 2 crossover experiments). This analysis was carried out in the absence of RNase to identify the composition of TDP43 mRNPs. (**b**) Scatter plot of SILAC results. For each quantified protein, the SILAC intensity (y axis) and the fold change between TDP43 pull-down and GFP pull-down (used as negative control, x-axis) are represented. We identified 176 high-confidence interacting proteins (highlighted in bigger dots), with the fold-change > 1.5 and the t-test p value < 0.1. TDP43 interacting proteins belonging to the spliceosome (KEGG mmu03040), the ribosome (KEGG mmu03010), the mRNA surveillance pathway (KEGG mmu03015) and the EJC-ome (Singh et al., 2012; 24 interacting proteins, Fold Enrichment: 15.5, Enrichment p value 1.38e-27) are highlighted in colours. No specific GFP-interactors were found. (**c**) The TDP43 interaction with the mRNA surveillance pathway components (UPF1, PABPC1, EIF4A3, and Y14) was validated by Western blot in combination with RNase A treatment. BTZ was not present in the MS-list of TDP43 interactors but emerged from this analysis. All interactions, except the one with PABPC1, show RNA-dependence. Antibody anti-HA tag was used as a control for the efficiency and specificity of TDP43 pull-down. 1.5% of input was loaded for each condition; the control represents NSC-34 without tagged TDP43 expression. (**d**) Schematic representation of TDP43 and the members of the FET family (FUS, EWSR1 and TAF15). (**e**) The specificity of the interaction of the NMD components (UPF1, EIF4A3) with TDP43 in NSC-34 cell line was validated by Western blot comparing the pull-down of TDP43, FUS, TAF15, and EWSR1.

Table 3.1 TDP43 protein interactors

Spliceosome (KEGG mmu03040)	**U1**	Snrnp70, Snrpa
	U2	Phf5a, Sf3a3, Sf3b2
	U4/U6	Nhp2l1
	U5	Prpf8, Snrnp200
	Sm	Snrpb, Snrpd2, Snrpd3, Snrpg
	Prpl9 complex	Prpf19, Hspa8, Plrg1, Cdc5l
	Prpl9 related	Snw1
	EJC-TREX	Acin1, Magoh, Y14, Eif4a3, Ddx39b
	hnRNPs	Hnrnpa1, Hnrnpa3, Hnrnpc, Hnrnpk, Hnrnpm, Hnrnpu, Rbmxl1
	SR family	Srsf1, Srsf5, Srsf6, Srsf7, Srsf10, Tra2a, Tra2b
Ribosome (KEGG mmu03010)	**Small subunit**	Rps2, Rps3, Rps5, Rps8, Rps10, Rps12, Rps15a, Rps16, Rps19, Rps20, Rps21, Rps27, Rps27l, Rps28, Rps29, Rpsa
	Large subunit	Rpl3, Rpl4, Rpl5, Rpl6, Rpl7, Rpl9, Rpl10a, Rpl12, Rpl13, Rpl13a, Rpl14, Rpl15, Rpl18, Rpl18a, Rpl19, Rpl35a, Rpl36, Rplp0, Rplp1, Rplp2
mRNA surveillance pathway (KEGG mmu03015)	**EJC**	Acin1, Magoh, Y14, Pnn, Rnps1, Eif4a3
	Transiently interacting factors	Nxf7, Ddx39b
	NMD	Pabpc1, Pabpc4, Ppp2r1a, Upf1
Exon junction complex-ome (Singh et al., 2012)	**EJC core**	Magoh, Y14, Eif4a3
	Peripheral EJC	Acin1, Pnn, Poldip3, Rnps1
	TREX	Fyttd1, Ddx39b
	hnRNPs	Hnrnpc, Raly
	SR family	Srrm2, Srsf1, Srsf10, Srsf6, Srsf7, Tra2a, Tra2b, Thrap3
	other mRNP	Bclaf1, Erh, Ilf2, Ilf3, Matr3, Pabpc1, Pgam5

Others	**RNA processing** (Biological Process, p value 1.082e-25)	Chtop, Ddx1, Ddx21, Dhx9, Dkc1, Elavl1, Elavl2, Elavl4, Fbl, Gar1, Hnrnpa2b1, Hnrnpd, Hnrnpf, Hnrnph1, Hnrnpl, Hnrnpr, Khdrbs1, Mocs3, Mov10, Ncl, Nhp2, Nop10, Nop56, Nop58, Ptbp1, Rbfox2, Rpf2, Rpsa, Safb, Sf3a1, Snrnp40, Snrpb2, Snrpd1, Ssb, Tardbp, Ybx1
	Post-transcriptional gene expression regulation (Biological Process, p value 2.388e-16)	Caprin1, Ddx1, Dhx9, Dkc1, Elavl1, Elavl4, Fxr1, Hnrnpa2b1, Hnrnpd, Hnrnpl, Hnrnpr, Igf2bp2, Igf2bp3, Khdrbs1, Mov10, Ptbp1, Pura, Serbp1, Tardbp, Ybx1, Ybx3
	Chromosome organization (Biological Process, p value 4.814e-8)	Chtop, Ddx1, Dhx9, Dkc1, Fbl, Gar1, H2afv, H2afx, H2afy, Hist1h2al, Hist1h2bc, Hist1h3b, Hist1h4a, Hnrnpa2b1, Nhp2, Nop10, Pura, Safb, Smarca5, Top2a
	RNA binding (Molecular Function, p value 4.314e-36)	Canx, Caprin1, Chtop, Ddx1, Ddx21, Dhx9, Dkc1, Elavl1, Elavl2, Elavl3, Elavl4, Fbl, Fxr1, G3bp2, Gar1, Hist1h4a, Hnrnpa2b1, Hnrnpd, Hnrnpf, Hnrnph1, Hnrnpl, Hnrnpr, Hnrnpul2, Igf2bp2, Igf2bp3, Khdrbs1, Mov10, Myef2, Ncl, Nhp2, Nop10, Nop56, Nop58, Prrc2c, Ptbp1, Pura, Rbfox2, Rpf2, Rpsa, Safb, Sec23ip, Serbp1, Sf3a1, Snrnp40, Snrpb2, Snrpd1, Ssb, Tardbp, Top2a, Txn, Ybx1, Ybx3
	Bag3, Banf1, Chchd3, Cisd1, Coil, Colgalt1, Cse1l, D10Wsu52e, Dpysl3, Gm17669, Gnb2l1, Hist3h2ba, Hsph1, Lmna, Map1b, Ott, Prdx2, Prdx4, S100a6, Sf3b14, Slc25a1, Tecr, Tmpo, Vdac3, Ywhaq	

3.2 TDP43 ENHANCES mRNA DEGRADATION BY A TRANSLATION-DEPENDENT MECHANISM THAT REQUIRES SMG1 ACTIVITY

Based on our finding that TDP43 binds to several components of the mRNA surveillance pathway, in particular, the nonsense-mediated mRNA decay, we investigated whether TDP43 could have a role in this process using a tethering assay performed in HeLa cells. The protein of interest fused to the bacteriophage MS2 coat protein is co-expressed with a mRNA reporter containing tandem RNA stem-loop MS2 binding sites in the 3'UTR, more than 50 nucleotides downstream of the normal termination codon. The protein function on the stability of the reporter can, therefore, be analyzed by directing it to a position functionally effective for NMD, potentially leading to a decrease of the reporter mRNA level (**Figure 3.2a**). Glutathione S-transferase (GST), a NMD-unrelated protein, is used as a negative control of the experiment. Y14, a component of the EJC, serves as a positive control since its presence downstream of the stop codon induces the assembly or the recruitment of the EJC and triggers NMD. As shown by Northern blot analysis, TDP43 tethering to the 3'UTR of the β-globin reporter reduces its mRNA abundance at the steady-state level (**Figure 3.2b**). This result is consistent with the hypothesis that TDP43 could be involved in the NMD pathway. To obtain a confirmation of this effect and a characterization of the mechanism, we combined the tethering assay with cycloheximide treatment obtaining a stabilization of the reporter, which demonstrates that the observed effect upon TDP43 tethering is translation-dependent (**Figure 3.2c**). Furthermore, both the silencing of SMG1, the kinase

necessary for UPF1 phosphorylation to trigger NMD, and its pharmacological inhibition through caffeine counteracted TDP43-mediated decrease of the reporter mRNA (**Figure 3.2d** and **e**). We can observe that the drug treatments have a stronger effect on the NMD pathway inhibition than gene silencing. However, the knockdown approach allows identifying the involvement of specific proteins in the mechanism, avoiding secondary spurious effects of the drugs. Our results suggest that TDP43 promotes the reduction of the β-globin mRNA by a translation- and SMG1-dependent process.

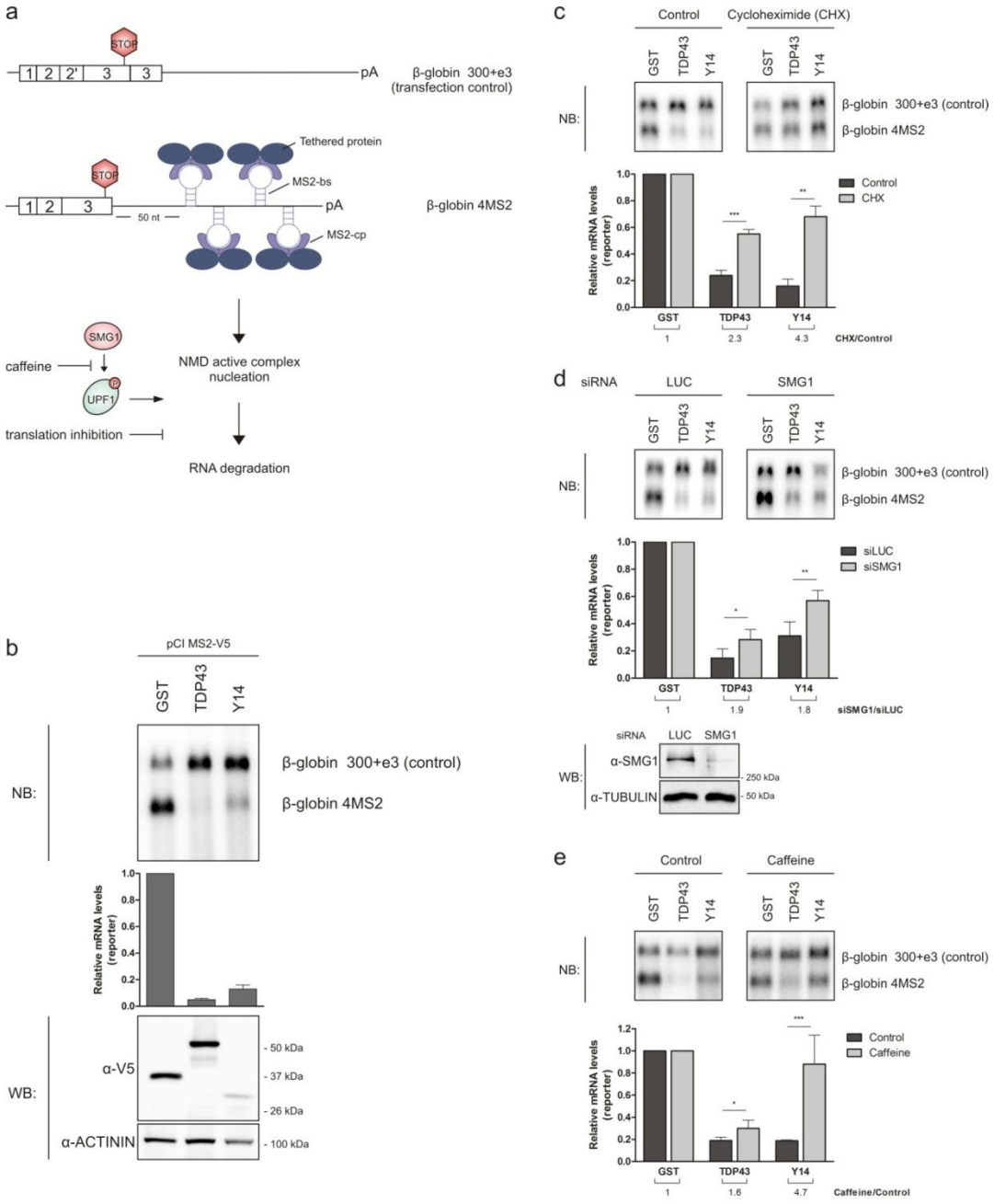

Figure 3.2 Tethered TDP43 in the 3'UTR reduces mRNA abundance by a translation-dependent mechanism involving SMG1 activity. (**a**) Schematic representation of the tethering assay performed

in HeLa cells. The protein of interest fused to the MS2 bacteriophage coat protein (MS2-cp) is brought to the 3'UTR of β-globin derived reporter mRNA harboring four MS2 binding sites (MS2-bs). An elongated human β-globin gene (wt+300+e3) without the MS2 binding sites serves as a control of the transfection efficiency. If the tethered protein nucleates the formation of an active NMD complex, the reporter is degraded. NMD is a translation-dependent mechanism, and UPF1 phosphorylation is necessary for its activation. NMD inhibition can be achieved by cycloheximide treatment or blocking SMG1 activity. (**b**) Northern blot (NB, upper panel) of MS2-V5 TDP43 tethering to the MS2 binding sites in the β-globin 3'UTR. MS2-V5 GST and MS2-V5 Y14 tethering were used as negative and positive controls, respectively. Western Blot analysis (WB, bottom panel) evidences the expression of the fusion proteins with the expected sizes, using the antibody anti-V5 tag. ACTININ served as protein loading control. Northern blots of the tethering assays in combination with (**c**) cycloheximide treatment, (**d**, upper panel) SMG1 knockdown and (**e**) caffeine treatment. Western blot confirmed the SMG1 silencing efficiency; TUBULIN served as protein loading control (**d**, bottom panel). Mean values of relative mRNA level with standard deviations from three independent replicates are indicated. Fold change of treatment/ control is indicated. Paired t-test was performed (* = p value < 0.05; ** = p value < 0.01; *** = p value < 0.001).

3.3 TDP43 IS A TRANSCRIPT SPECIFIC NMD ENHANCER

These results drove us to examine whether TDP43 is a universal player in NMD pathway, irrespective of its localization on target mRNAs. We employed a well-characterized NMD reporter system composed of the β-globin pre-mRNA and a mutant form of it. In the mutant reporter, a nonsense mutation in the second exon generates a premature termination codon (PTC) after splicing (**Figure 3.3a**). The PTC-containing β-globin mRNA has been verified to be a *bona fide* mRNA target for NMD (Zhang et al., 1998). Moreover, in the 3'UTR of the wild type and the mutant reporter, XRN1-resistant RNA structures (xrRNA) were inserted to monitor the 5'-3' mRNA degradation by the exoribonuclease XRN1, which occurs during NMD (Boehm et al., 2016). The presence of xrRNA protects the downstream sequence from degradation and produces a XRN1-resistant decay RNA fragment (xrFrag), which is used as a readout for 5'-3' reporter degradation (**Figure 3.3b**). The expression of stably integrated wild type (WT) or mutant (PTC) β-globin reporters was induced in HeLa cells after TDP43 down-regulation by siRNA. Silencing of SMG1 and luciferase were used as a positive and negative control, respectively (**Figure 3.3c**). As expected, the presence of the PTC results in a strong reduction of the steady state mRNA level and an accumulation of xrFrag. The depletion of SMG1,

the kinase involved in UPF1 phosphorylation and NMD activation, leads to the stabilization of the full-length β-globin PTC reporter and a decrease in the level of the decay fragment. On the contrary, TDP43 is not required for the degradation of a general nonsense-containing mRNA through NMD, since its knockdown does not alter the ratio between the xrFrag and the full-length reporter mRNA.

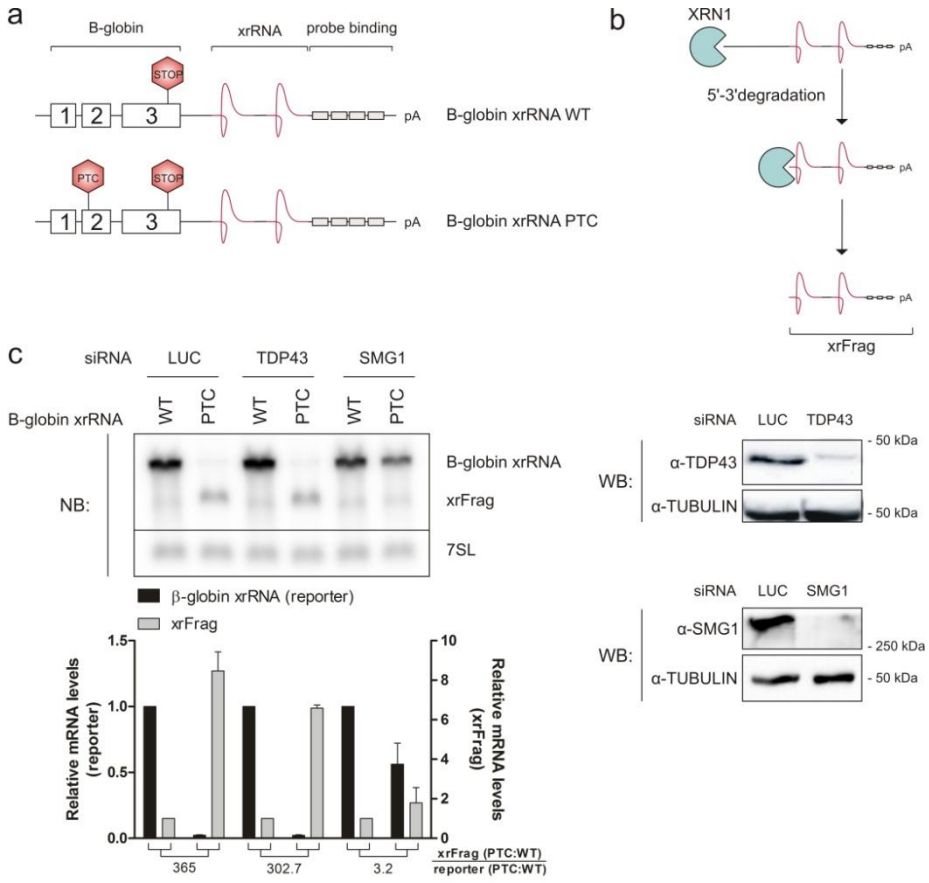

Figure 3.3 TDP43 silencing does not affect NMD. (**a**) Schematic representation of the β-globin xrRNA reporters. The *β-globin* gene contains three exons, represented as white boxes. The positions of the normal stop codon (STOP) and the premature termination codon (PTC) are shown. Radioactive probe binding sites in the 3'UTR are depicted as light gray boxes, and xrRNA structures are shown in red. (**b**) 5'-3' mRNA degradation by XRN1 is prevented from further progression by XRN1-resistant RNA structure (xrRNA). The remaining RNA fragment (xrFrag) is protected from degradation and still contains the probe binding sites for Northern blot detection. (**c**) HeLa Flp-In T-REx cells were transfected with the indicated siRNA 48h before induction of the β-globin reporter expression with 1 µg/mL doxycycline for 24h. Total RNA was extracted and analyzed by Northern blot (NB; left panel). The slower-migrating band corresponds to the full-length reporter, whereas the faster-migrating band is due to the xrFrag. 7SL RNA was used as endogenous control RNA. Mean values of reporter and xrFrag signals from three independent replicates were quantified and normalized to the WT control; standard deviations are shown. The ratio of xrFrag to reporter mRNA level is indicated below the graph. The siRNA knockdown efficiency of TDP43 and SMG1 was analyzed by Western Blot (WB; right panels). TUBULIN served as protein loading control.

3.4 TDP43 DEPLETION UP-REGULATES TARGETED mRNAs WITH LONG 3'UTR

Taken together, the previous observations highlight that TDP43 enhances mRNA decay when tethered in the 3'UTR of a reporter mRNA through a translation- and SMG1-dependent mechanism, but it is not required for general NMD activity. This suggests a target-specific function for the NMD promoting activity of TDP43. We, therefore, focused on the identification of mRNAs controlled by TDP43 through this novel biological function, which could also be deregulated in TDP43-related pathogenesis. Since we propose TDP43 as a positive NMD regulator, the mRNA level of the TDP43 targets should increase upon TDP43 knockdown. We silenced TDP43 in the NSC-34 cell line and performed a high-throughput RNA-seq analysis. In the TDP43 knocked-down cells 378 up-regulated and 404 down-regulated transcripts were identified (**Figure 3.4a**).

We compared our dataset of up regulated genes with other available sequencing data and a functional annotation enrichment analysis (**Figure 3.4b**) pointed out the presence of genes involved in neuron apoptosis and autophagy regulation. Moreover, some of them were found to be increased in ALS-induced pluripotent stem cells-derived neurons, in ALS samples, and in other TDP43 knockdown experiments, confirming the reliability of our experiment.

Sequence analysis of differentially expressed RNAs upon siTDP43 revealed a significant increase in the average 3'UTR size for up-regulated transcripts (more than two-fold) compared to transcripts with unaffected expression levels (**Figure 3.4c**). The overlap with a published catalog of TDP43 binding sites in the mouse brain by HITS-CLIP (Polymenidou et al., 2011) revealed a specific enrichment of TDP43 binding sites located in the 3'UTR region of the up-regulated transcripts (**Figure 3.4d**). Prompted by this evidence, we selected a subset of up-regulated transcripts reported to be bound by TDP43 in their 3'UTR, and we confirmed the TDP43 binding by RNA immunoprecipitation (RIP), demonstrating that the CLIP data from mouse brain were validated in our cell model (**Figure 3.4e**).

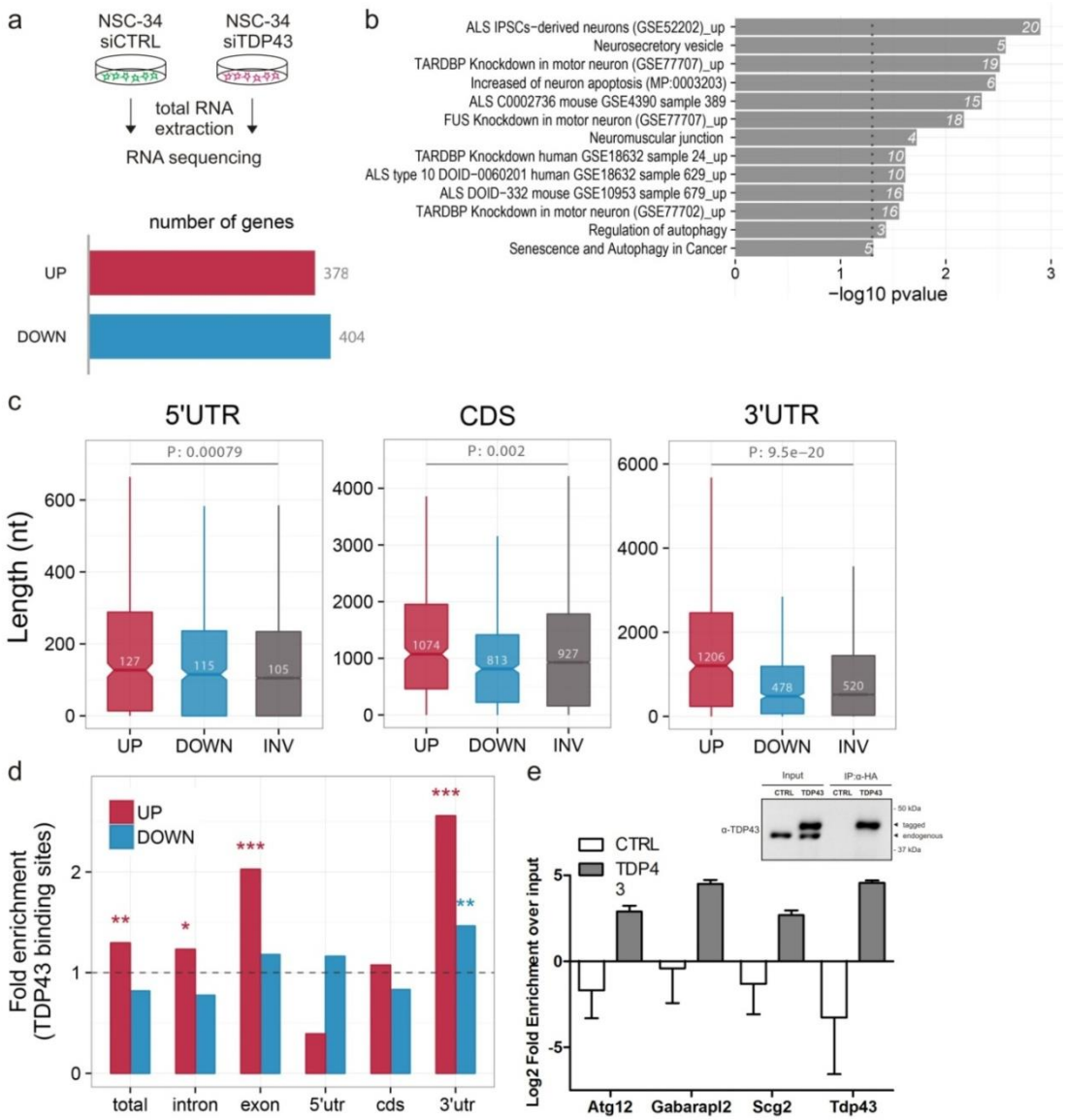

Figure 3.4 Analysis and characterization of transcripts altered upon TDP43 silencing. (**a**) Number of differentially expressed genes obtained upon TDP43 silencing in NSC-34 cell line. (**b**) Functional annotation enrichment analysis of up-regulated genes performed with the clusterProfiler Bioconductor package and the enrichR web server (10.1093/nar/gkw377, http://amp.pharm.mssm.edu/Enrichr/). (**c**) Sequence length analysis of 5'UTR, coding sequence (CDS) and 3'UTR of up-regulated transcripts (UP), down-regulated transcripts (DOWN) and transcripts without a change in their expression level (INV). Differences in 5'UTR/CDS/3'UTR length distributions were tested with the Wilcoxon Rank Sum Test. (**d**) Custom enrichment analysis of experimental TDP43 binfing sites in the three populations of transcripts was performed with Fisher test, using a published catologue of TDP43 binding sites in the mouse brain by HITS-CLIP (Polymenidou et al., 2011). (**e**) RNA immunoprecipitation analysis (RIP) of His-HA TDP43 in NSC-34. A subset of transcripts already published as TDP43 mRNA targets was significantly enriched in TDP43 immunoprecipitation compared with the control (NSC-34 without tagged TDP43 expression). The mRNA level was measured by RT-qPCR and normalized to Rpl10a. Fold enrichment was calculated versus the 5% input in three replicates. The binding of Tdp43 transcript was used as a

positive control of the experiment. Western blot (top panel) was used to validate the efficiency and specificity of TDP43 pull-down.

We finally focused on Atg12, whose mRNA has been already reported as a conserved NMD target, in both mouse embryonic stem cells (Hurt et al., 2013) and yeast (Mendell et al., 2004). Atg12 mRNA is bound by TDP43 in our motor neuron-like cells (**Figure 3.5a**). To confirm that Atg12 is an NMD target in our cell model, UPF1 silencing, as well as treatment with cycloheximide and caffeine, was performed. Interestingly, TDP43 down-regulation resulted in a similar increase of the Atg12 mRNA to that obtained by siRNA-mediated inactivation of NMD, considering the different knockdown efficiency of the two genes. As previously observed, the caffeine and cycloheximide treatment resulted in a more pronounced up regulation of the transcript level, showing how the pharmacological treatment determines a stronger inhibition of NMD, compared to the silencing approach (**Figure 3.5b**). Therefore, this evidence prompts us to conclude that Atg12 is targeted by NMD in NSC-34 cells, and TDP43 is involved in the regulation of its expression.

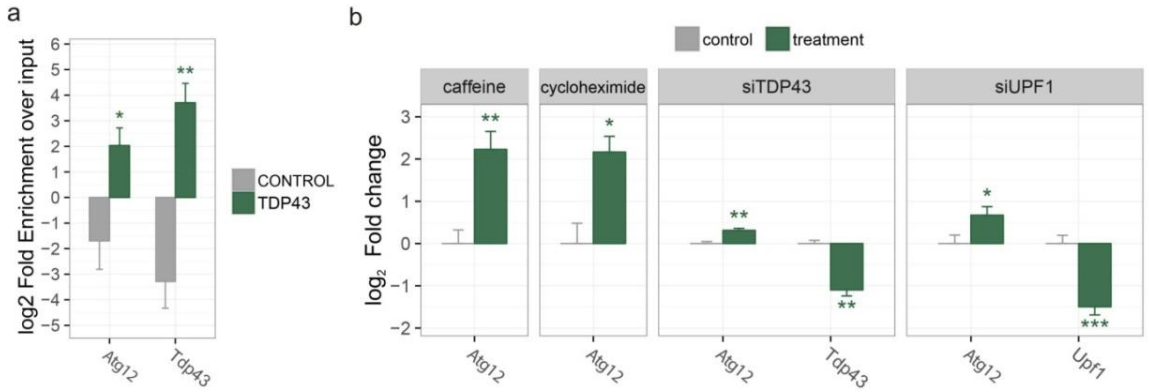

Figure 3.5 Analysis of TDP43 and NMD effects on the Atg12 transcript. (**a**) RNA immunoprecipitation analysis (RIP) of His-HA TDP43 in NSC-34. Atg12 mRNA was significantly enriched in TDP43 immunoprecipitation compared with the control (NSC-34 without tagged TDP43 expression). mRNA level was measured by RT-qPCR and normalized to Rpl10a. Fold enrichment was calculated versus the 5% input. The binding of Tdp43 transcript was used as a positive control of the experiment. Paired t-test was performed (* = p value < 0.05; ** = p value < 0.01; n = 3). (**b**) Quantitative real-time PCR (qRT-PCR) analysis of *Atg12* expression level when TDP43 or UPF1 are down-regulated, when translation is inhibited by cycloheximide treatment or when UPF1 phosphorylation is blocked by caffeine. siRNA for luciferase was used as a control in the silencing experiments. The relative quantification was determined via the ΔΔCt method and normalized to the endogenous controls Rpl10A and Ppia. Welch's t-test (one tail) was performed (* p value < 0.05; ** p value < 0.01; *** p value < 0.001, n = 4).

4. RESULTS: TDP43 AND ALTERNATIVE POLYADENYLATION

4.1 ALTERNATIVE POLYADENYLATION IS ALTERED IN TDP43^{Q331K} MOUSE MODEL

In 2015 Prudencio and colleagues added ALS to the list of human diseases associated with polyadenylation sites shifts, reporting an alternative polyadenylation (APA) alteration in sporadic ALS cases and c9ALS patients with a repeat expansion in *C9orf72* gene. From this evidence and supported by the fact that TDP43 can regulate the APA of its mRNA (Avendaño-Vázquez et al., 2012; Koyama et al., 2016), we investigated a possible APA change in TDP43^{Q331K} mice. This ALS mouse model expresses TDP43 with the ALS-linked mutation Q331K in the central nervous system, both in neurons and astrocytes (**Figure 4.1a**). It results in an age-dependent mild motor phenotype, not observed in TDP43^{wt} mouse (Arnold et al., 2013). Measurement of TDP43 protein expression in the spinal cord of these mice revealed a decrease of endogenous murine protein and an enrichment of the transgenic TDP43, which was found to be polyubiquitinated. This feature is evident in the late-stage of the pathology, at ten months of age (**Figure 4.1b**). We performed a behavioral characterization of this mouse model, assessing the motor deficit at different time points during the development of the disease. We tested the motor performance and the coordination skills by accelerating rotarod test. In our hands, this model develops a mild but significant motor deficit at early-stage (two months) in comparison with littermate mice, with a worsening of the performance during disease progression (**Figure 4.1c**). We attribute the decreased latency to fall observed in the non-transgenic mice at ten months to aging. An abnormal hind limb clasping is visible in 6-month-old TDP43^{Q331K} mice, but not in non-transgenic littermate mice (**Figure 4.1d**).

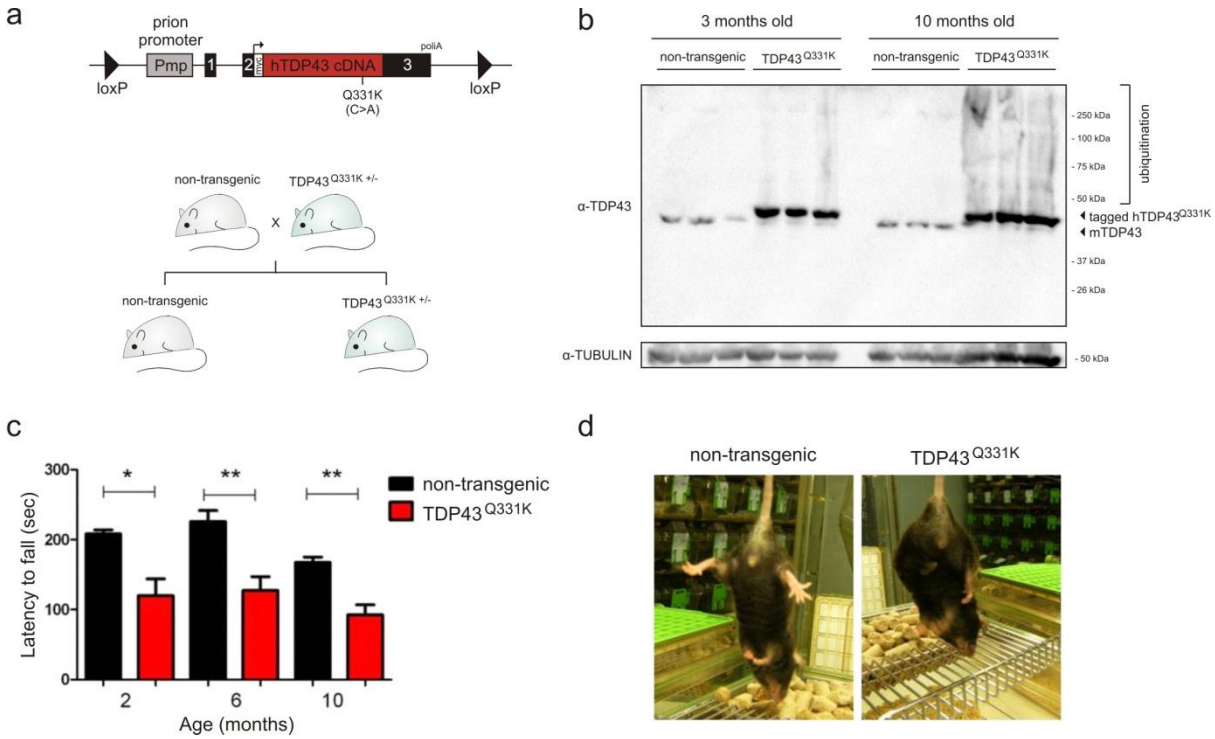

Figure 4.1 TDP43^{Q331K} mouse model. (**a**) Representation of the transgene expressed in the mouse model (B6N.Cg-Tg(Prnp-TARDBP*Q331K)103Dwc/J). The Myc-tagged human TDP43 carrying the ALS-linked Q331K mutation is directed to the brain and the spinal cord by the mouse prion protein promoter. Below, the mice breeding scheme is depicted. (**b**) Western blot analysis of the proteins extracted with Trizol from the spinal cord of three non-transgenic and three transgenic TDP43^{Q331K} mice at three and ten months of age. The antibody anti-TDP43 can recognize both the murine and the tagged human protein. At ten months the transgenic mice show a smear due to the polyubiquitination of TDP43. TUBULIN was used as a loading control. (**c**) Accelerating rotarod test performed on transgenic and littermate mice from two to ten months of age. TDP-43^{Q331K} mice displayed a significant impairment in motor performance and a lower latency to fall, compared to non-transgenic mice (* = p value < 0.05; ** = p value < 0.01). (**d**) Hind limb clasping tested at six months of age.

We sequenced the 3' end of polyadenylated RNAs extracted from spinal cords of ALS and littermate mice at three and ten months of age (**Figure 4.2a**). We considered the reads with 3' end mapping within 10bp from the transcript end (median 12 million reads, minimum 7 million, maximum 21 million), which represent the 95% of the signal (**Figure 4.2b**).

Among the detected polyadenylation sites, over 3000 genes (23.4%) have more than one PAS (**Figure 4.2c**). The same sequencing approach was previously used in HEK293 cells, where 3291 genes were annotated with multiple poly(A) sites (Rot et al., 2017).

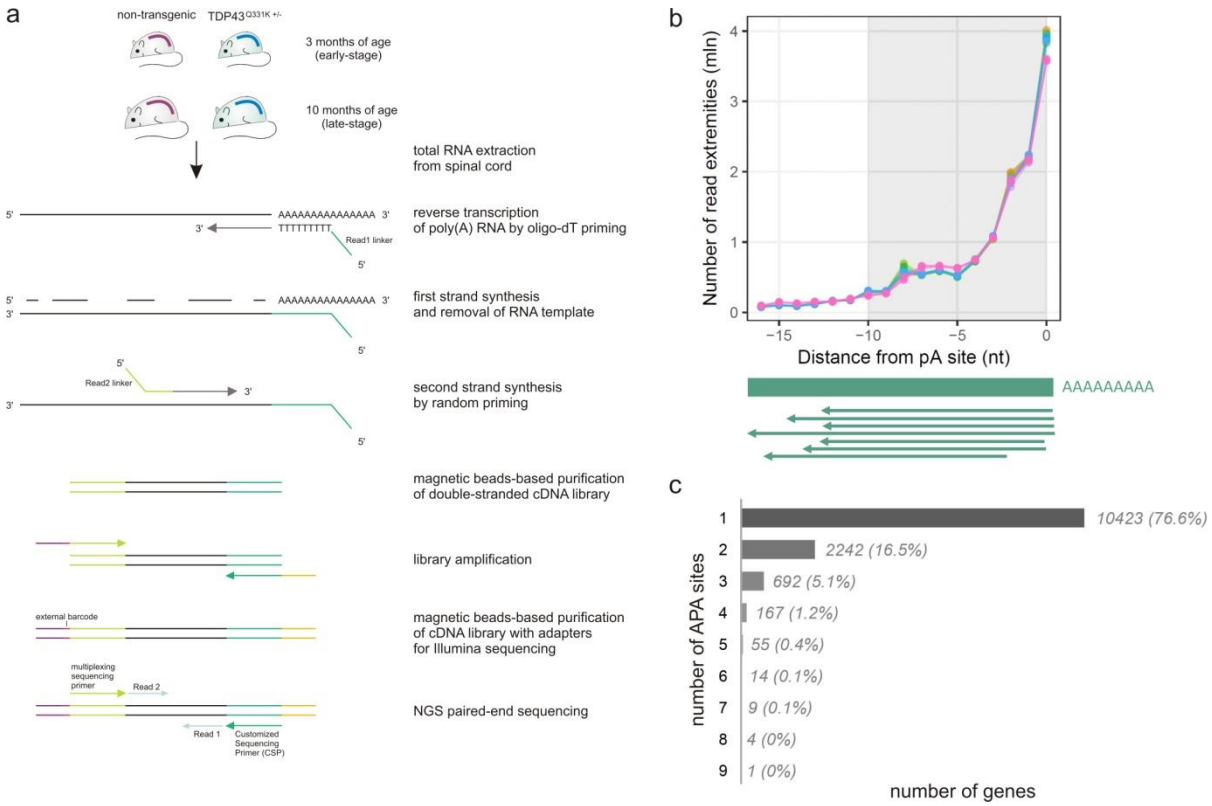

Figure 4.2 Analysis of APA in spinal cords of TDP43^{Q331K} transgenic and non-transgenic mice. (**a**) Experimental design and pipeline of QuantSeq Reverse 3' mRNA-Seq library preparation (Lexogen), which allows mapping the sequences close to the 3' end of polyadenylated RNAs at nucleotide resolution. We analyzed three mice for each condition. (**b**) Metaprofile plot of read-end sites distribution respect to known polyadenylation sites. From the quality control of 3'end analysis, 95% of the signal maps in a window of 10 nucleotides before the polyadenylation site (3 nucleotides of dispersion is allowed). The reads outside this region were not considered, excluding the false positives due to oligodT priming in sequences with long A-stretches. (**c**) Distribution of the number of detected PA sites per gene, considering all the classes of APA events (see Paragraph 1.4.2).

Our analysis showed a shift in the PAS selection, comparing the non-transgenic mice at ten and three months. Specifically, the process of aging is followed by preference in proximal PAS selection and the consequent production of shorter isoforms (**Figure 4.3a**). Previously, other biological processes were linked with broad APA modulation, as development, proliferation and neuron activity (Elkon et al., 2013), since this mechanism controls the gene expression.

Moreover, concerning the results from the transgenic mouse model, our study revealed an increase of differentially polyadenylated genes (DPGs) with the pathology progression. At the late-stage of the disease, ~20% of the genes characterized by the presence of more than one PAS have a different 3' end (**Figure 4.3b**). Examining the two alternative polyadenylation events (tandem or splicing-

dependent) separately, we didn't find an enrichment in one of the two classes among the differentially polyadenylated genes. The percentage of tandem APA with differential usage is 20% at three months and 34% at 10 months, considering a 36% of background, which represents the number of genes with more than one PAS because of a splicing-independent event. The analysis of the transcripts with a shift in the PAS usage revealed an enrichment in genes altered in ALS (**Figure 4.3c**).

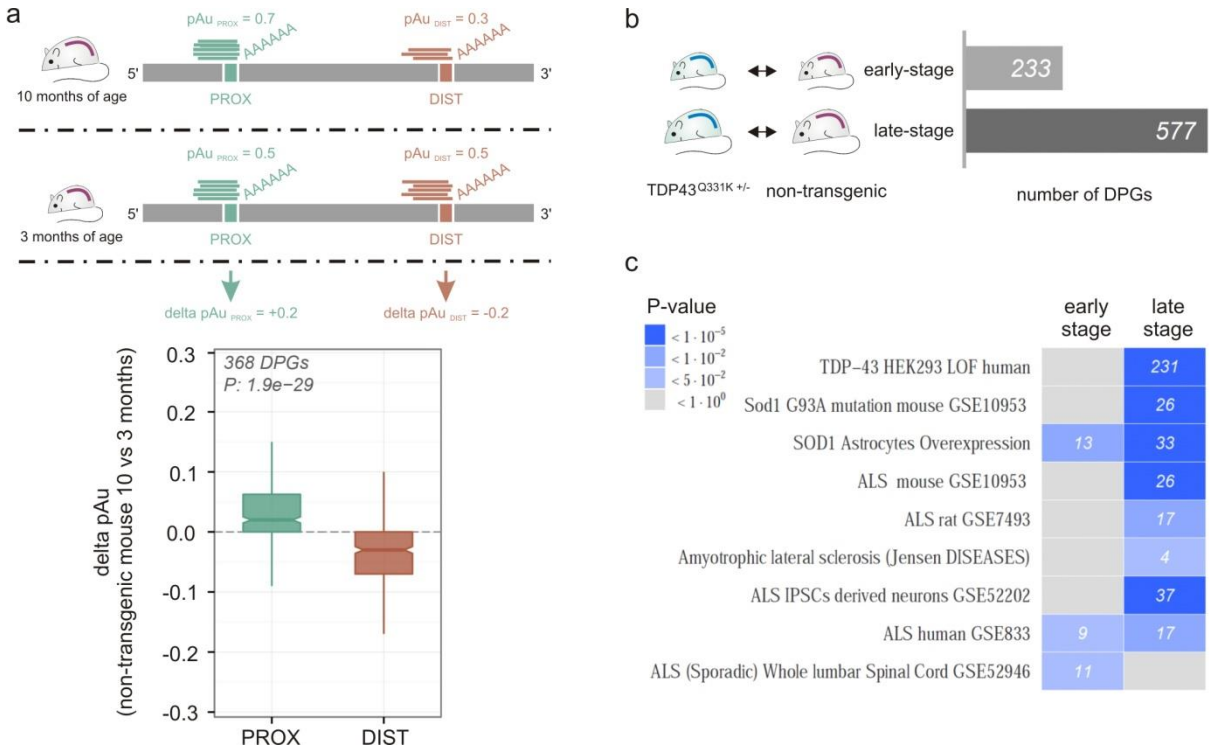

Figure 4.3 APA is altered during aging and ALS progression (**a**) Defining pAu as the polyadenylation site usage, quantified according to the number of reads, we calculated for the proximal (PROX) and the distal (DIST) polyadenylation site (PAS) the delta pAu as pAu (non-transgenic mouse ten months of age) - pAu (non-transgenic mouse three months of age). An example is reported. APA changes in non-transgenic mice comparing the two ages are shown in the bottom panel. (**b**) Number of differentially polyadenylated genes (DPGs) with two or more alternative polyadenylation sites in TDP43^{Q331K} transgenic mice at three and ten months of age and (**c**) their functional annotation enrichment analysis performed with the clusterProfiler Bioconductor package and the enrichR web server.

4.2 TDP43 MODULATES ALTERNATIVE POLYADENYLATION, PROMOTING THE PROXIMAL PAS USAGE OF ITS TARGETS

To study the molecular mechanism through which TDP43 modulates the alternative polyadenylation at the genome wide level, we performed 3' end sequencing of NSC-

34 cells knocked-down for TDP43. We identified 417 differentially polyadenylated genes (**Figure 4.4a**), involved in RNA processing and nervous system development (**Figure 4.4b**). Interestingly, analyzing the DPGs, we observed a statistically significant preference in the usage of the distal PAS when TDP43 is silenced (**Figure 4.4c**). This result suggests an involvement of TDP43 in the modulation of APA of a subset of transcripts.

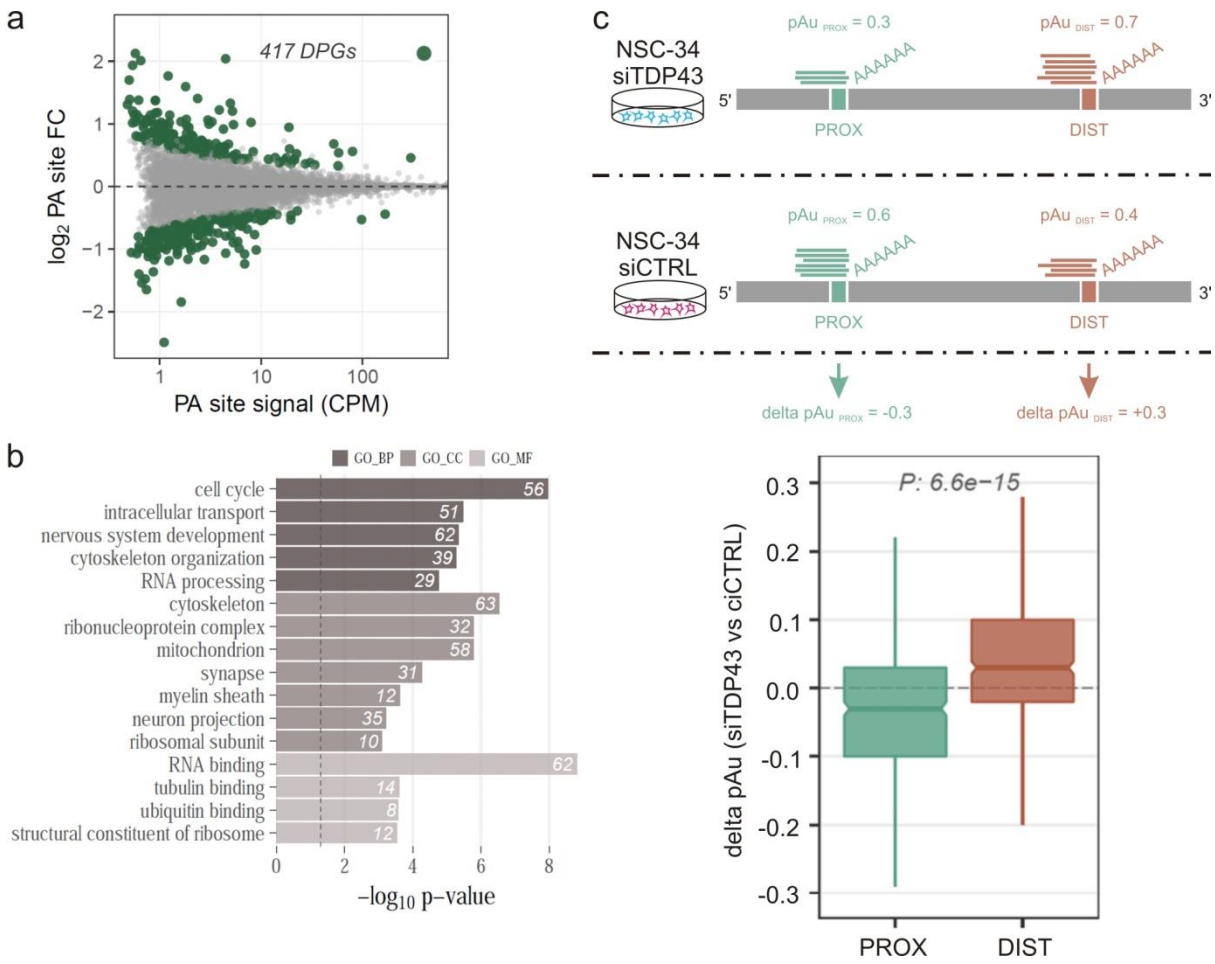

Figure 4.4 TDP43 depletion induces a shift in the polyadenylation site usage. (**a**) Scatter plot of differentially polyadenylated genes (DPGs) in NSC-34 cell line down-regulated for TDP43 and (**b**) the relative gene ontology (GO) analysis (BP, Biological Process; CC, Cellular Compartment, Molecular Function). (**c**) According to the number of reads, we quantified pAu for each DPG and calculated for the proximal (PROX) and the distal (DIST) polyadenylation site (PAS) the delta pAu as pAu (siTDP43) - pAu (siCTRL). An example is reported. We used siRNA for luciferase as a silencing control (siCTRL), conducting the experiment in duplicate. The bottom panel shows the delta pAu of DPGs in NSC-34 silenced for TDP43.

To find a functional model for TDP43, we crossed our sequencing data with the positional information of the TDP43 binding sites coming from published murine

brain HITS-CLIP data (Polymenidou et al., 2011). TDP43 depletion is known to be accompanied by alterations in alternative splicing (Xiao et al., 2011; Tollervey et al., 2011) and in cryptic splice site suppression (Ling et al., 2015). Therefore, we focused our analysis on significant tandem APA events to exclude an effect due to splicing involvement (**Figure 4.5a**). The percentage of DPGs produced by tandem APA is 37%, with a background of 36% as previously explained. From our analysis 22 known TDP43 targets emerged differentially polyadenylated in silenced NSC-34 cells and the position of the binding site turns out to be between the proximal and the distal PAS for all of them (**Figure 4.5b**). The Gene Ontology analysis revealed the presence of genes involved in cell differentiation, synapse organization and nervous system development (**Figure 4.5c**).

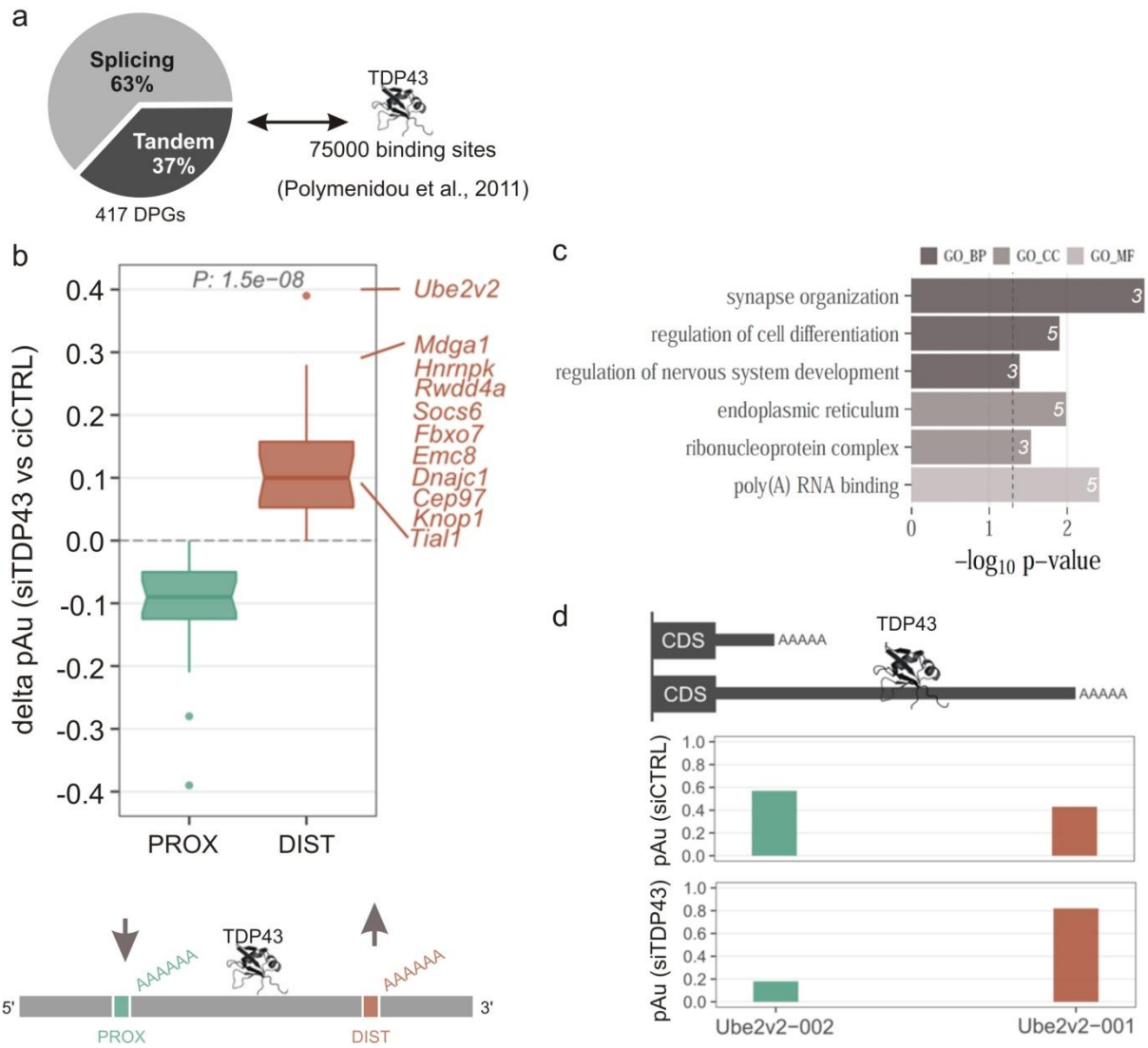

Figure 4.5 TDP43 promotes the proximal PAS usage of its mRNA targets (**a**) Pie chart representing the APA classes (tandem and splicing-dependent) of DPGs in NSC-34 cell line silenced for TDP43. An APA event is tandem when produces transcripts with the same start coordinate of the

last exon; otherwise, it is splicing-dependent. We crossed the genes characterized by a differential tandem APA, with a catalog of 75000 TDP43 binding sites in the mouse brain by HITS-CLIP (Polymenidou et al., 2011). The box whisker plot shows the delta pAu of DPGs in NSC-34 silenced for TDP43 produced by a tandem APA event and bound by TDP43. For all the genes, the binding site of TDP43 is between the proximal (PROX) and distal (DIST) PAS. The first 11 genes are listed on the right. (**c**) Gene ontology (GO) analysis showing the enriched Biological Processes (BP), Cellular Compartments (CC) and Molecular Functions (MF). (**d**) Representation of the different 3' ends of Ube2v2 and the TDP43 binding site. The pAu of each transcript calculated from the sequencing data is indicated in the graphs below.

We validated our sequencing data by real-time PCR focusing our attention on *Ube2v2*, one of the genes most differentially polyadenylated (**Figure 4.5d**). Using pairs of primers suitably designed to amplify the transcript with the long 3'UTR or to quantify the total expression level of the gene (**Figure 4.6a**), we confirmed that the distal PAS of Ube2v2 is preferred in TDP43 silenced NSC-34 cells (**Figure 4.6b** and **c**). We further verified that TDP43 binds the long isoform of Ube2v2 in our cells (**Figure 4.6d**).

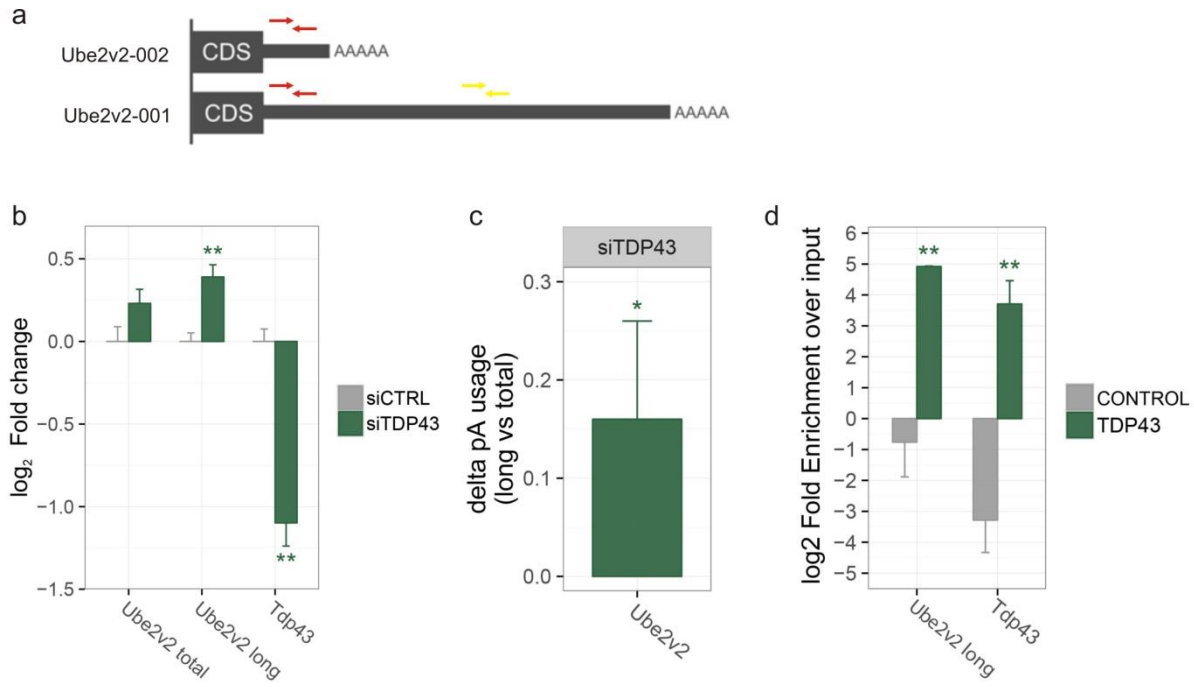

Figure 4.6 Validation of TDP43 effect on alternative polyadenylation of Ube2v2 transcript. (**a**) The two possible 3' ends of Ube2v2 are represented. The yellow arrows indicate the specific primers for the transcript with a long 3'UTR (Ube2v2-001); the red primers map on both transcripts (Ube2v2-001 and -002) and were used to quantify the total expression level of the gene. (**b**) Quantitative real-time PCR (qRT-PCR) analysis of Ube2v2 expression level upon TDP43 silencing. siRNA for

luciferase was used as a silencing control (siCTRL). The relative quantification was determined via the ΔΔCt method and normalized to the endogenous controls Rpl10a and Ppia. Paired t-test was performed on 3 biological replicates (** = p value < 0.01). (**c**) Quantification of the delta pAu of Ube2v2 in NSC-34 silenced for TDP43. Paired t-test was performed on 3 biological replicates (* = p value < 0.05) (**d**) RNA immunoprecipitation analysis (RIP) of His-HA TDP43. Ube2v2 mRNA was significantly enriched in TDP43 immunoprecipitation compared with the control (NSC-34 without tagged TDP43 expression). mRNA level was measured by RT-qPCR using the primers for the transcript with a long 3'UTR (Ube2v2-001; yellow primers in (a)) and normalized to Rpl10a. Fold enrichment was calculated versus the 5% input. The binding of TDP43 transcript was used as a positive control of the experiment. Paired t-test was performed (** = p value < 0.01; n = 3).

To confirm the role of TDP43 in alternative polyadenylation and to study the positional effects in the regulation of the PAS selection, we performed a tethering assay using a β-globin reporter, presenting 4MS2 binding sites in the 3'UTR between the cryptic proximal and the distal polyadenylation sites (**Figure 4.7a**). When the negative control GST is tethered, the distal PAS is used, since its sequence is stronger than the proximal one. The tethering of TDP43 and CSTF1, a component of the core polyadenylation machinery used as a positive control, reverses this situation. Both proteins promote the production of a shorter form of the reporter that can be distinguished by Northern blot analysis (**Figure 4.7b**). Moreover, we tested that TDP overexpression does not affect the β-globin transcript when it is not tethered (**Figure 4.7c**).

The 3' end processing occurs co-transcriptionally in the nuclear compartment. Performing a nucleus-cytoplasm fractionation of the transfected cells, we showed that the short isoform of the β-globin produced by the tethering of TDP43 and CSTF1 is present in both cellular fractions (**Figure 4.7d**).

The cryptic PAS mutagenesis converted the APA reporter (*β-globin 4MS2 APA*) in an NMD target (*β-globin 4MS2 Δproximal PAS*) when TDP43 is tetherd since the MS2 binding sites are located >50 nucleotides downstream the stop codon (**Figure 4.7e**). Y14 is not involved in the processing of the 3' end and, therefore, induces the degradation of both reporters. On the contrary, TDP43 plays a role in APA enhancing the 3'UTR cleavage upstream its binding site. In the absence of the proximal PAS, the MS2 binding sites are not removed and TDP43 can mediate the reporter decay through a post-transcriptional process.

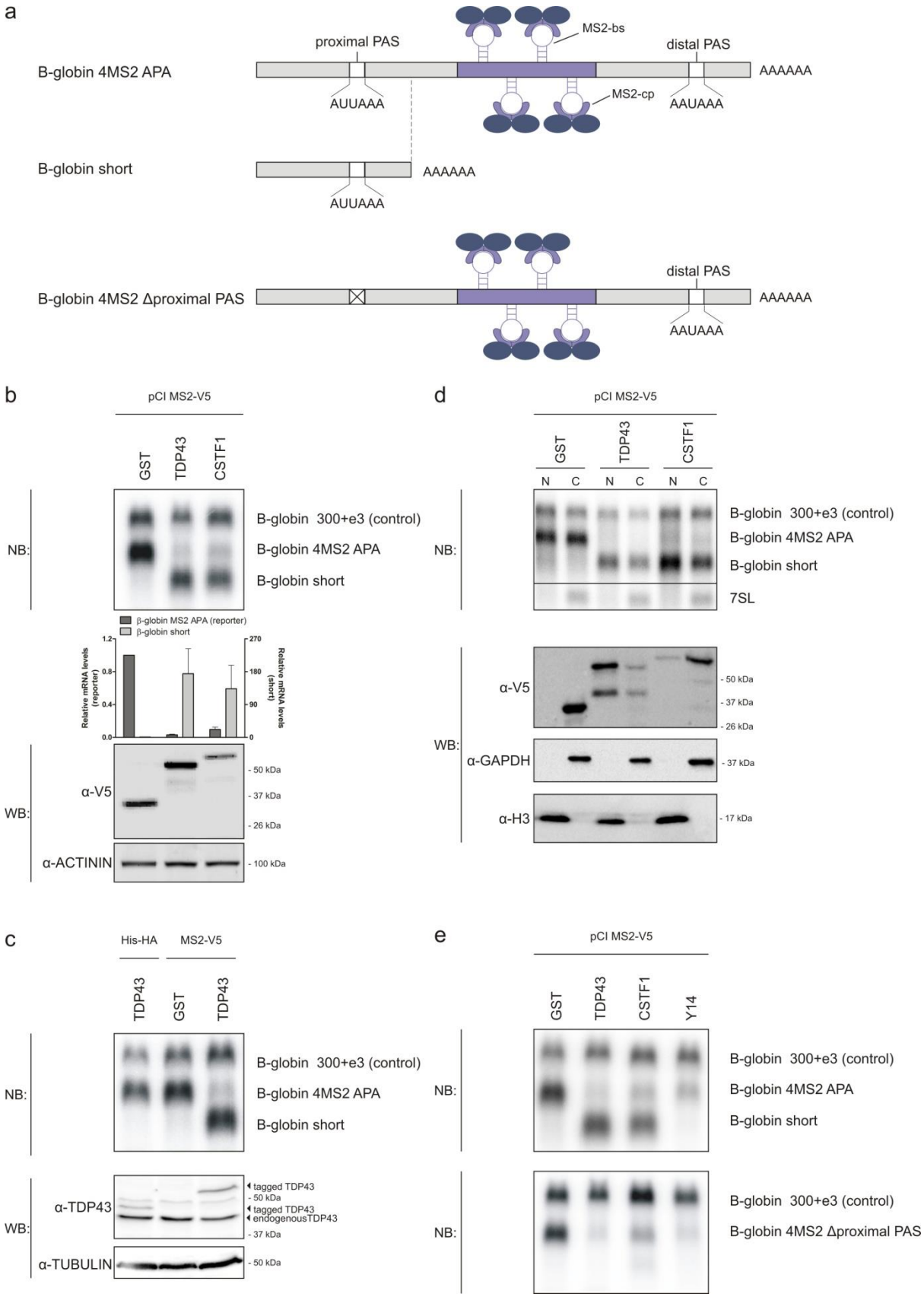

Figure 4.7 Validation of TDP43 involvement in alternative polyadenylation with a reporter assay

(**a**) Schematic representation of the β-globin reporters used in the tethering assay performed in HeLa

cells. 4 MS2 binding sites are located in the 3'UTR of the β-globin reporter, between its proximal and distal polyadenylation sites (*β-globin 4MS2 APA*). When a protein involved in APA is tethered in that region, it causes the production of a shorter reporter (*β-globin short*). *β-globin 4MS2 Δproximal PAS* was obtained by PCR site-directed mutagenesis of the proximal PAS and used in figure 4.7e. (**b**) Northern blot of TDP43 tethered between the proximal and the distal polyadenylation sites of the reporter *β-globin 4MS2 APA*. GST and CSTF1 tethering were used as negative and positive controls, respectively. An elongated human *β-globin* gene (*β-globin 300+e3*) without the MS2 binding sites served as a control for transfection efficiency. Western blot (bottom panel) validates the expression of the tethered V5 tagged proteins. ACTININ was used as a protein loading control. (**c**) Northern blot of His-HA and MS2-V5-TDP43 overexpression effect on *β-globin 4MS2 APA* . MS2-V5-GST is used as a control. Western blot (bottom panel) validates the expression of the tagged proteins (indicated by ◄) by using an antibody anti-TDP43. (**d**) Northern blot of tethering experiment performed with the *β-globin 4MS2 APA* reporter, after nucleus-cytoplasm fractionation. 7SL RNA marks specifically the cytoplasmic fraction (C) and is not detectable in the nuclear fraction (N). Western blot (bottom panel) validates the expression of the tethered V5 tagged proteins and the nucleus/cytoplasm fractionation. GAPDH and Histone 3 (H3) were used as cytoplasmic and nuclear markers, respectively. (**e**) Northern blot of TDP43 tethering performed with the *β-globin 4MS2 APA* and the *β-globin 4MS2 Δproximal PAS*.

4.3 ALS-LINKED Q331K MUTATION DOES NOT ALTER THE TDP43 EFFECT ON APA AND NMD

To investigate if the presence of Q331K point mutation in the C-terminal domain of TDP43 can alter its novel functions, we repeated the previous tethering assays on APA and NMD reporters. From the Northern blot data, we observed that the mutant is still able to influence the choice of the polyadenylation site (**Figure 4.8a**) and to degrade the reporter (**Figure 4.8b**). However, the expression of TDP43^{Q331K} for 48h in NSC-34 does not produce cytoplasmic aggregates (**Figure 4.8c**).

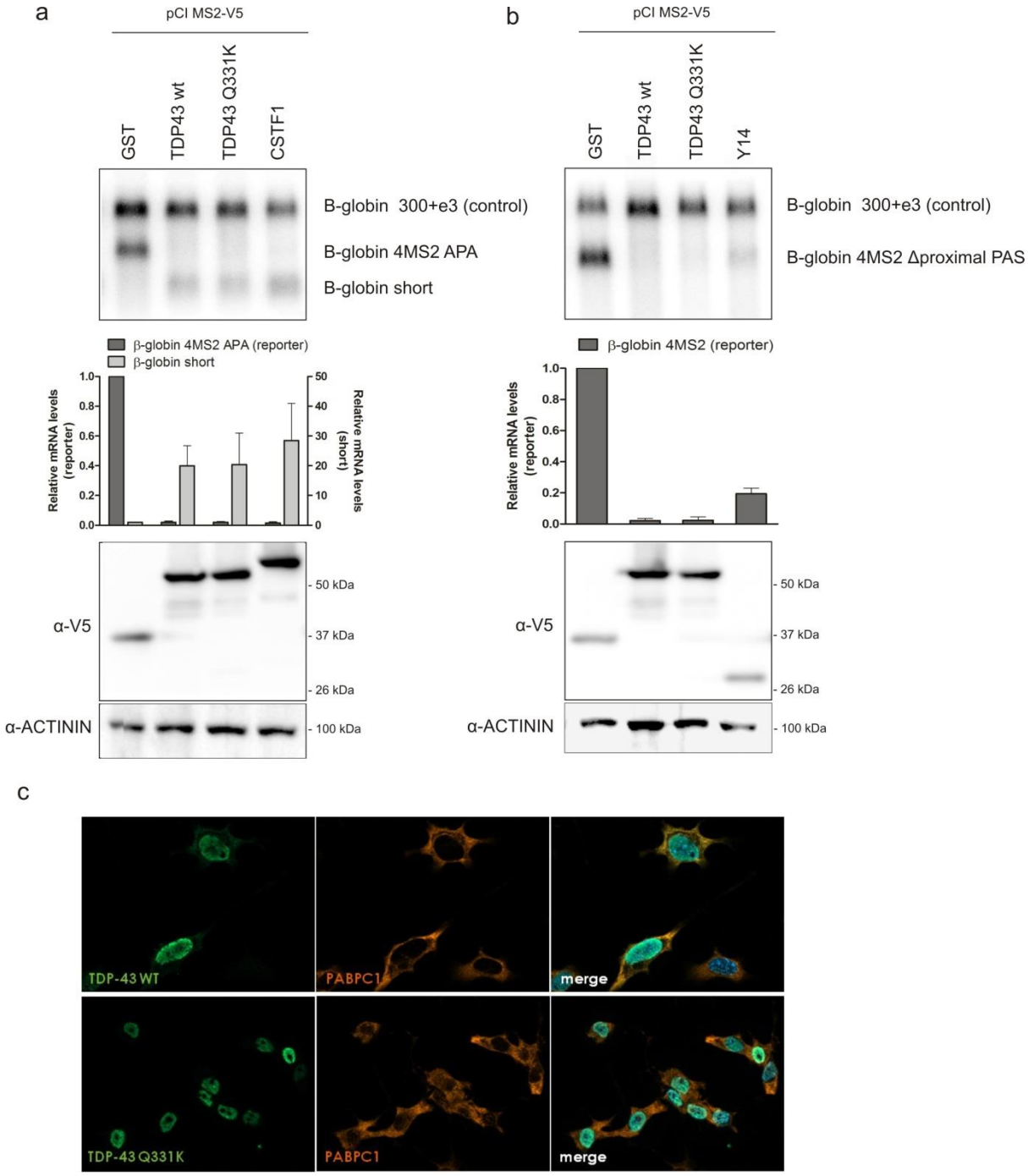

Figure 4.8 TDP43 Q331K is still able to affect the APA and NMD reporters. (**a**) Northern blot of TDP43 wt and Q331K tethered to (**a**) the *β-globin 4MS2 APA* and (**b**) the *β-globin 4MS2 Δproximal PAS*. In both experiments, β-globin 300+e3 served as a control for transfection efficiency. GST represents the negative control; CSTF1 and Y14 are used as positive controls of the two experiments. Western blots (bottom panels) show the expression level of the tethered V5 tagged proteins. ACTININ was used as a protein loading control. (**c**) Representative images of NSC-34 expressing TDP43 wt or TDP43Q331K. Antibody anti-PABPC1 is used as a marker of stress granules. The objective used for image acquisition was PlanApo oil immersion lens 63x/1.4.

4.4 THE GLYCINE-RICH DOMAIN OF TDP43 MEDIATES THE INTERACTION WITH THE CSTF COMPLEX AND THE TDP43 ACTIVITY IN ALTERNATIVE POLYADENYLATION REGULATION

We demonstrated by immunoprecipitation the direct interaction of TDP43 with the CSTF1 and CSTF3 components of the CSTF complex in the NSC-34 cell line (**Figure 4.9a**). We obtained the same outcome repeating the experiment in HeLa cells (data not shown). In both cases the interaction was found to be RNA-independent. This result is also supported by the interaction of TDP43 W113A-R151A with the complex (**Figure 4.9d**). These point mutations were reported to decrease the binding of TDP43 to UG repeats (Ayala et al., 2005; Ihara et al., 2013). As a further demonstration of this binding, we proved the TDP43 interaction with mVenus-CSTF1 (**Figure 4.9b**).

Using a truncated form of TDP43 lacking the glycine-rich C-terminal part (**Figure 4.9c**), we demonstrated that this domain is necessary for the interaction with CSTF1 (**Figure 4.9d**). Its absence causes a consistent reduction in proximal polyadenylation site selection (**Figure 4.9e**), without altering the nuclear localization of the protein (**Figure 4.9f**).

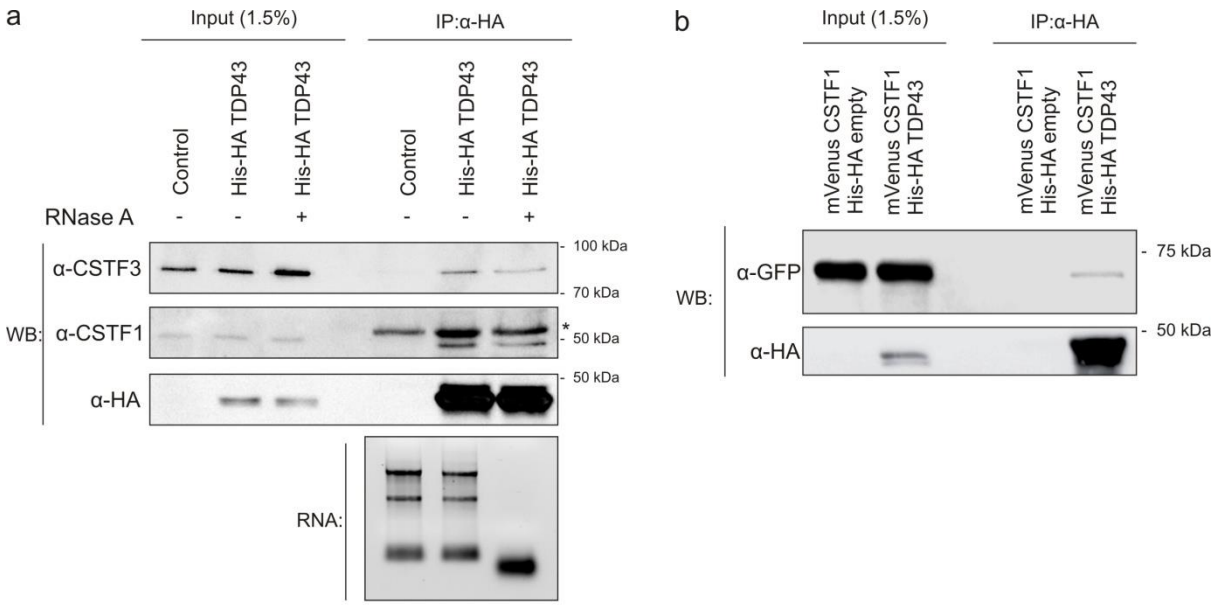

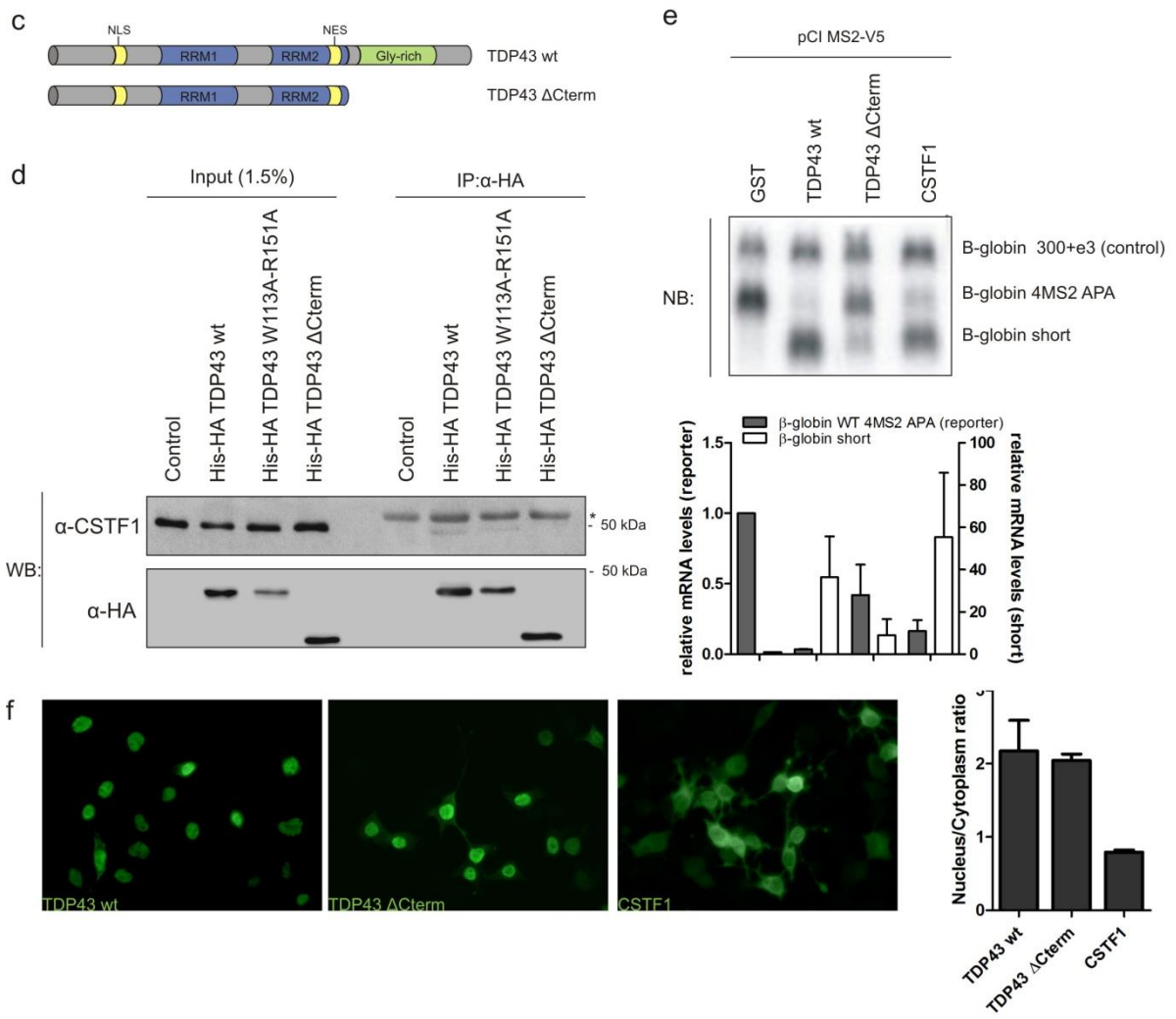

Figure 4.9 TDP43 interacts directly with the CSTF complex. (**a**) The interaction of TDP43 with CSTF1 and CSTF3 in NSC-34 cell line was proved by immunoprecipitation coupled with Western blot analysis in combination with RNase A treatment. 1.5% of input was loaded for each condition; the control represents NSC-34 without tagged protein expression. Antibody anti-HA tag was used as a control for the efficiency and specificity of TDP43 pull-down. * indicates the heavy chain of the IgG. RNA extracted from the flow through and run onto 1.5% agarose gel demonstrates the RNA degradation due to RNase A treatment (bottom panel). (**b**) We further confirmed the interaction of TDP43 with CSTF1 by immunoprecipitation coupled with Western blot analysis co-transfecting HeLa cells with His-HA TDP43 and mVenus CSTF1. Antibody anti-GFP was used to detect the tagged CSTF1. (**c**) Schematic representation of TDP43 wt and TDP43 ΔC-term, the fragment without the glycine-rich C-terminal part. (**d**) TDP43 wt, TDP43 W113A-R151A and TDP43 ΔC-term immunoprecipitation coupled with Western blot analysis in NSC-34 cells. (**e**) Northern blot of TDP43 wt and ΔC-term tethered between the proximal and the distal polyadenylation sites of the reporter β-globin 4MS2 APA. *β-globin short* is the short isoform produced by alternative polyadenylation. GST and CSTF1 tethering were used as negative and positive controls, respectively. An elongated human *β-globin* gene (*β-globin 300+e3*) without the MS2 binding sites served as a control for transfection efficiency. (**f**) Representative images of NSC-34 expressing mVenus-TDP43 wt, mVenus-TDP43 ΔC-

term, and mVenus-CSTF1. The cells were imaged on the High Content Screening System Operetta™ (PerkinElmer), through which we performed the cellular localization analysis of these proteins, quantifying the GFP intensity in the nucleus and the cytoplasm. The nuclei were identified by Hoechst staining. As previously shown by Western blot of nucleus-cytoplasm fractionation (Figure 4.7d), overexpressed CSTF1 is more cytoplasmic than nuclear.

5. DISCUSSION AND FUTURE WORK

TDP43 is a mostly nuclear RNA-binding protein ubiquitously expressed and found accumulated in the cytoplasm in sporadic and familial ALS patients (Neumann et al., 2006; Igaz et al., 2008). However, it is still unclear why this phenomenon, called TDP43 proteinopathy, causes selective motor neuron death.

The molecular function of TDP43 has been extensively investigated in the past. As a result, the protein has been implicated in several processes related to control of gene expression: transcription regulation, mRNA splicing, transport, stability and translation (Buratti et al., 2001; Fiesel et al., 2009; Freibaum et al., 2010; Tollervey et al., 2011; Polymenidou et al., 2011; Ling et al., 2015).

The analysis of protein-protein interactions (PPIs) is a widely used unbiased approach to study the role of a target protein inside the cell. It has been reported that more than 80% of proteins form complexes to elicit their functions (Berggård et al., 2007), and proteins involved in the same cellular process emerge as interactors from PPI studies (von Mering et al., 2002). Earlier studies investigated the interacting proteins of TDP43, demonstrating a strong association with mRNA splicing, microRNA processing and translation machinery (Freibaum et al., 2010; Ling et al., 2010; Blokhuis et al., 2016). To find out possible novel roles of TDP43, we adopted a SILAC-based proteomic approach for analyzing its protein interactome in NSC-34, a motor neuron-like cell line (**Figure 3.1**). The presence of known TDP43 binders in the list of its specific interactors, as the spliceosome and the ribosome components, supported the validity of our analysis. An entirely new result was the enrichment in several factors involved in the mRNA surveillance pathway and constituting the EJC-ome. It is interesting to observe how these four classes could belong to the same pathway. In fact, the Exon Junction Complex is assembled during the pre-mRNA splicing, is removed by the ribosome during the first round of translation, and allows the recognition and the degradation of mRNAs with a premature termination codon by the translation-dependent mRNA surveillance pathway, in particular the EJC-dependent Nonsense-mediated decay (**Figure 5.1**).

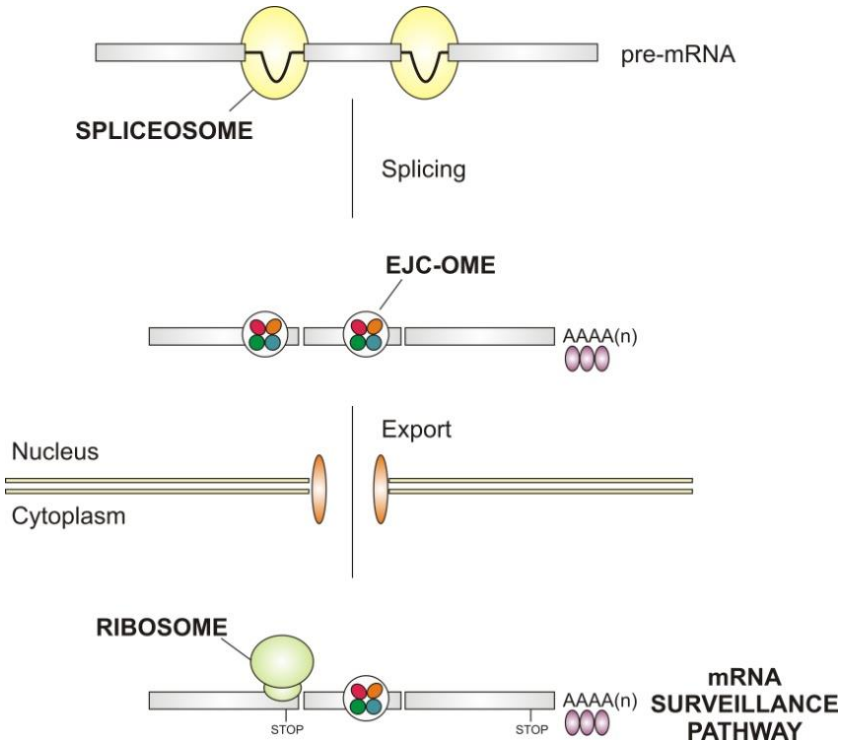

Figure 5.1 Enriched classes in the TDP43 protein interactome.

Recently, TDP43 has been indirectly linked to NMD by the elucidation of its role in suppression of cryptic splicing (Ling et al., 2015). TDP43 silencing increases the level of mature transcripts including cryptic exons of intronic origin. Consequently, it raises the frequency of transcripts with a premature termination codon subjected to NMD. Another finding suggesting a role of TDP43 in NMD comes from a genetic screen in yeast, which demonstrated that a yeast homolog of hUPF1 and hUPF1 itself prevent TDP43-mediated toxicity (Ju et al., unpublished). The overexpression of UPF1 counteracts TDP43 cytotoxicity in primary neuronal cultures (Barmada et al., 2013) and slows disease progression in an ALS model of rat (Jackson et al., 2015). These works support the involvement of UPF1 inactivation in TDP43-induced motor neuron degeneration *in vitro* and *in vivo*, and possibly, therefore, in NMD, even if functions of UPF1 other than that of NMD effector are known (Varsally et al., 2012).

Moreover, NMD was shown to be involved in the synaptic morphology and function maintenance. The loss of a central NMD player as SMG1 (Long et al., 2010) or an EJC core component as EIF4A3 (Bramham et al., 2008; Giorgi et al., 2007) leads to NMJ synaptic architectural and functional impairments, suggesting a possible involvement of NMD alteration in locomotor degeneration and ALS development.

Our data, particularly the interaction with cytoplasmic components of the mRNA surveillance pathway, suggest an involvement of TDP43 in the NMD pathway, that we substantiated adopting a classical approach (Gehring et al., 2008; Gehring et al., 2009). We tethered TDP43 in the 3'UTR of a β-globin reporter, in a position that triggers NMD. The presence of TDP43 more than 50 nucleotides downstream of the normal stop codon induces the reduction of the β-globin mRNA by a translation- and SMG1-dependent process (**Figure 3.2**). Moreover, we proved that TDP43 downregulation does not generally affect the NMD machinery, suggesting that the effect observed by the tethering assay depends on the direct binding of TDP43 to the mRNA undergoing NMD (**Figure 3.3**).

NMD can follow three different routes, which differ principally in their being dependent or not on the EJC. These alternative models are: (a) EJC-dependent NMD, which is activated in the presence of a premature termination codon. (b) EJC-independent NMD, which depends on the length of the 3'UTR and the distance between the stop codon and PABPC1. (c) STAU1-mediated decay, where STAUFEN1 binds its binding sites in the 3'UTR and recruits UPF1, eliciting the decay of the transcript.

Our genome-wide sequencing analysis of NSC-34 cells silenced for TDP43 (**Figure 3.4**) showed that the up-regulated mRNAs are characterized by a significant increase in the average 3'UTR size. Moreover, the use of a published list of TDP43 RNA interactions in the mouse brain highlighted an enrichment of its binding sites in the 3'UTR region of the up-regulated transcripts.

The identification of up-regulated transcripts with a long 3'UTR, the tethering results, and the directed interaction with PABPC1 could suggest the involvement of TDP43 in the EJC-independent NMD. As previously reported (Singh et al., 2008), a long 3'UTR is an important feature of "physiological" NMD targets. TDP43, binding the 3'UTR of its target and interacting with PABPC1, could interfere with a correct translation termination (**Figure 5.2a**). To confirm or disprove if the role of TDP43 in increasing NMD sensitivity of the bound mRNAs could be ascribed to its binding in the 3' UTR, we will clone after the β-globin coding sequence the 3'UTR of a transcript targeted by TDP43, presenting or not its binding site. The positivity of this result could allow us to move toward the demonstration that EJC-independent NMD is a target of TDP43.

On the other side, and even if it did not emerge from our SILAC-based proteomic

analysis, the interaction between TDP43 and STAUFEN1 has been reported in different studies (Yu et al., 2012; Milev et al., 2012). This raises the interesting possibility that they act together in favouring decay of their targets (**Figure 5.2b**), and therefore that TDP43-mediated decay and STAUFEN1-mediated decay are two special forms of NMD sharing a common mechanism of action. This hypothesis could be tested by combining the TDP43 tethering with the down-regulation of STAUFEN1. We could also cross our sequencing data with the binding sites not only of TDP43 but also STAUFEN1 to find common transcripts.

Another possible explanation of the results obtained from our tethering experiments could be that TDP43, as other RBPs (Singh et al., 2012; Le Hir et al., 2016), is able to influence the deposition, the assembly and/or the stability of the EJC (**Figure 5.2c**). To verify this option, we will combine the TDP43 tethering assay with the overexpression of the ribosome-associated protein PYM, which acts as an EJC disassembly factor (Gehring et al., 2009).

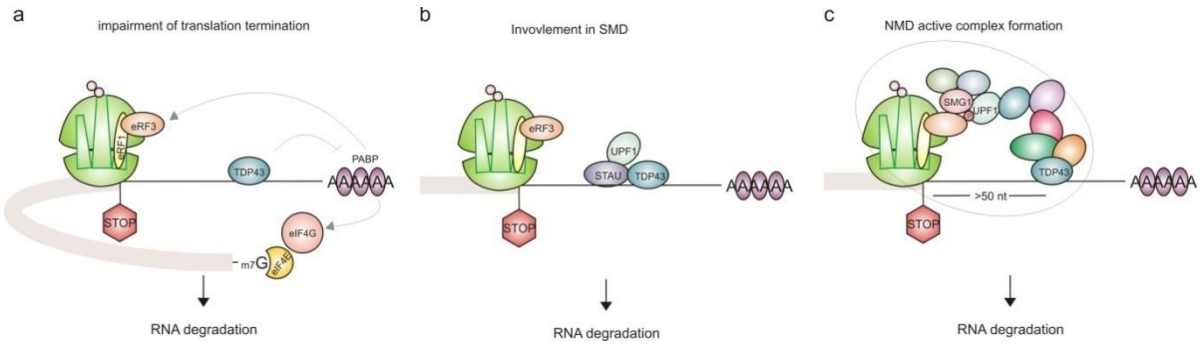

Figure 5.2 Possible mechanisms of action through which TDP43 could be involved in mRNA decay.

Even if the involved mechanism is still unclear, its impairment could play a pathological role in ALS. Since we propose TDP43 as an NMD enhancer, the loss of its function would induce an increase of its mRNA targets, and their higher expression could have a toxic effect on the cell.

The up-regulated transcripts upon TDP43 silencing resulted ontologically enriched in autophagy and apoptosis terms. Autophagy is an essential process to neuronal homeostasis, and it is involved in protein degradation, organelle turnover and stress response (Levine and Kroemer, 2008). Its dysregulation (excessive induction or deficiency), due to the impairment of the autophagic flux or its regulatory processes, is linked to ALS but also to other neurodegenerative diseases, such as Alzheimer's disease, Huntington's disease, Parkinson's disease and frontotemporal dementia

(Wong and Cuervo, 2010; Chen et al., 2012). The alteration of the autophagic process was previously linked to TDP43 neurodegeneration (Ying et al., 2016, Bose et al., 2011) and NMD pathway inhibition (Wengrod et al., 2013), highlighting a possible connection among these three conditions. Also, silencing of TDP43 has been already associated with apoptosis activation (Ayala et al., 2008). We showed that *Atg12* is up-regulated upon TDP43 silencing and NMD inhibition (**Figure 3.5**). It codifies for an autophagic protein, which also plays a proapoptotic role, inhibiting members of the anti-apoptotic Bcl-2 family (Rubinstein et al., 2011). For this reason, alteration of the ATG12 level could have an impact on these two processes.

To consolidate our findings and evaluate their impact on ALS, we are planning to perform further analysis on transcripts targeted by this novel TDP43 mechanism. We will evaluate the effect of enforced overexpression of validated TDP43 targets, as *Atg12*, on autophagy, apoptosis, and cell viability, using primary motor neurons and looking at specific markers. In this way, we will be able to propose causality between the impairment of NMD due to TDP43 loss, the increase of the transcripts level and cell features.

We will move to an *in vivo* system to consolidate our findings obtained in cell culture and clarify the role of NMD in ALS pathogenesis. We will silence in *Drosophila* key components of the NMD machinery, such as *NonC1* (the ortholog of *Smg1*) and *Upf1*, with a motor neuron specific driver (D42-Gal4). We will compare them to *Tbph* silencing (the ortholog of *Tardbp*), using a newly ALS *Drosophila* model established in our laboratory. Finally, we will assess the contribution to ALS of transcripts targeted by TDP43-dependent NMD in our *in vitro* experiments. We will silence their orthologs in *Drosophila* and evaluate the genetic interactions, the degeneration of the larval neuromuscular junctions, and the motor performance in the adult.

In the second session of this project, we showed that alternative polyadenylation changes with the aging and its alteration increases during the disease progression in the spinal cord of an ALS mouse model (**Figure 4.3**), where TDP43^{Q331K} is overexpressed causing an age-dependent mild motor phenotype (**Figure 4.1**).

We demonstrated by 3'end sequencing analysis of NSC-34 silenced for TDP43 and the use of a specific reporter, a novel mechanism through which this protein could modulate alternative polyadenylation, promoting the production of shorter transcripts.

Our sequencing data identified 417 genes differentially polyadenylated upon TDP43 silencing in neuronal cells. Among them, we observed a shift in the usage of the polyadenylation site, with a significant preference in the selection of the proximal PAS (**Figure 4.4**). This feature resulted much more evident analyzing only the tandem events (**Figure 4.5**). Since TDP43 is involved in alternative splicing regulation, excluding from the analysis the transcripts subjected to splicing dependent-APA, we reduced the possible involvement of other mechanisms.

Using the published TDP43 RNA interactome from mouse brain (Polymenidou et al., 2011), we found that TDP43 binds between the proximal and the distal PAS of all of its identified targets. The low number of genes (22) obtained crossing the two datasets could be ascribed to an intrinsic feature of the mechanism. Indeed, if TDP43 really promotes the usage of the proximal PAS, the longest isoform of the transcript will be less abundant, and therefore the TDP43 signal between the two PASs in these tandem transcripts will suffer a representation bias with respect to the other TDP43 binding sites. To provide a more consistent map of TDP43 binding sites to test our model, we are planning to perform iCLIP of endogenous TDP43 in our cells.

We demonstrated by a tethering experiment (**Figure 4.7**), how this protein could modulate alternative polyadenylation. We used a *β-globin* reporter presenting a cryptic proximal PAS (AUUAAA) and a distal PAS with a strong sequence (AAUAAA), which is usually preferred. Upon transfection, it leads to the expression of a long isoform predominantly (**Figure 5.3a**). As observed from our sequencing data, when TDP43 is tethered between the proximal and the distal PAS, it leads to the usage of the upstream PAS and the production of a shorter isoform (**Figure 5.3b**). This outcome suggests the TDP43 involvement in the promotion of the proximal polyadenylation site and/or the repression of the distal one. To identify the effective role of TDP43, we removed the cryptic sequence by mutagenesis (**Figure**

5.3c). Since, in this way, the MS2 binding sites are located more than 50 nucleotides after the stop codon, we obtained a TDP43-mediated decay sensitive reporter, which generates a long isoform when NMD is downregulated. However, the treatments resulted in having a lower effect on the tethering of TDP43, than that of Y14, a core component of the EJC (**Figure 3.2**). This observation leads us to suppose that TDP43 could enhance the upstream PAS selection, but also partially repress the downstream site usage, preventing the complete maturation of the transcript when the cryptic site is absent. The correctly processed mRNAs are transported from the nucleus to the cytoplasm, where they undergo NMD.

We can hypothesize to apply other modifications to the reporter to have more evidence about the positional effect of TDP43 in alternative polyadenylation modulation. Deletion of the distal PAS (**Figure 5.3d**) and TDP43 tethering downstream the distal PAS (**Figure 5.3e**) would not provide us more information on the mechanism. However, we could move the MS2 binding sites upstream the weaker PAS (**Figure 5.3f**) to obtain a reporter less sensitive to distal site inhibition and more suitable for NMD studies.

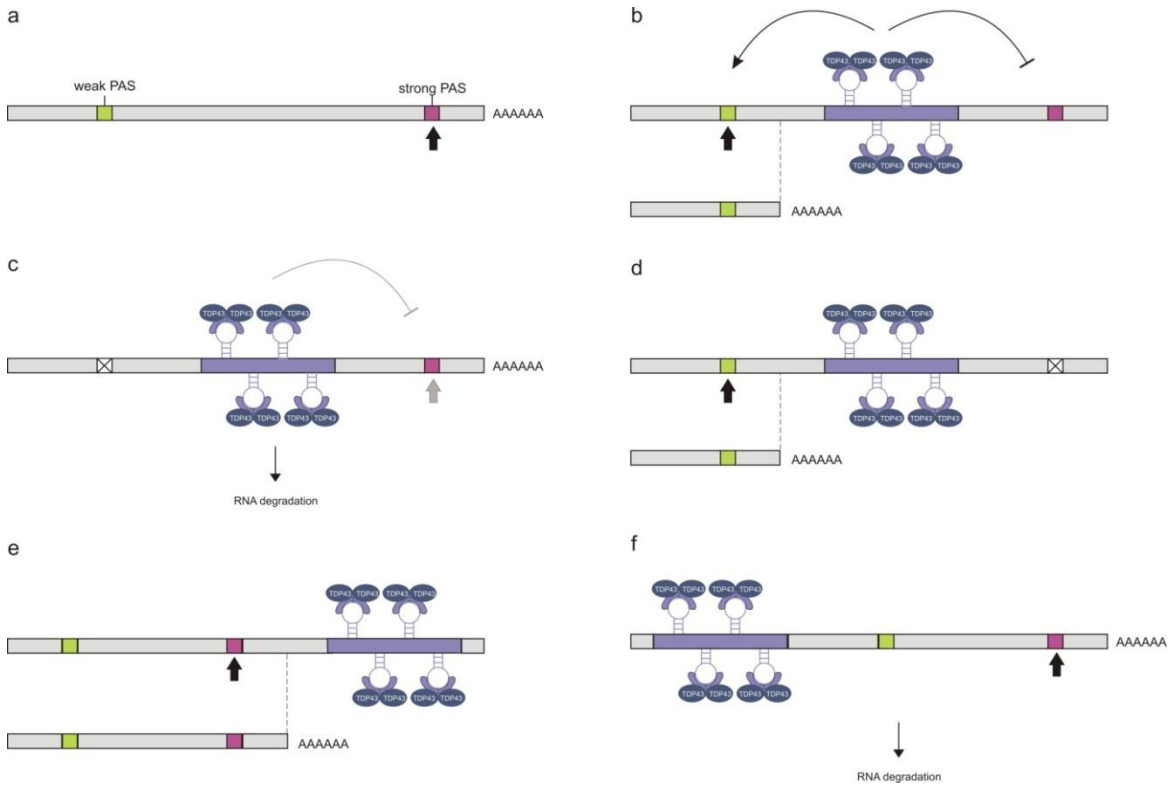

Figure 5.3 Different uses of the tethering approach to study how TDP43 modulates APA.

Our results obtained from the tethering experiments are supported by a recent study. Rot and co-workers integrated iCLIP and 3' mRNA sequencing data performed in

HEK293 cells. They found that TDP43 can bind upstream (40-80 nucleotides before the PAS) or near the proximal PAS (from 40 nucleotides before to 20 nucleotides after the PAS), preventing its selection and indirectly promoting the use of the distal site. They showed that TDP43 can also enhance the selection of the proximal site binding downstream sequences (20-80 nucleotides after the PAS). In their work a position-dependent regulatiory principle is presented, however they did not provide a demonstration of the involved mechanism.

Polyadenylation of the mRNA is a two-step reaction and needs the involvement of multiple cis- and trans-acting factors. The heterotrimer CSTF acts during the endonucleolytic cleavage and determines the polyadenylation efficiency. In 2009 Shi and co-workers purified and analyzed the protein composition of the human mRNA 3′ processing complexes, identifying a direct association with TDP43. In 2014 Costessi and colleagues failed to demonstrate the interaction between TDP43 and CSTF2, the member of the CSTF complex involved in the RNA-binding, rejecting the possible involvement of TDP43 in the regulation of polyA tail length. We were also unable to show this interaction, but we observed that TDP43 directly binds to the other two components of the CSTF complex (CSTF1 and CSTF3, **Figure 4.9**). The cause could be that, for technical reasons (e.g. buffer composition, antibody sensitivity), the interaction with CSTF2 cannot be detected. Another possibility could be that TDP43, which has the same binding site of CSTF2 (UG-stretches), forms a novel complex with CSTF1 and CSTF3 (the active components of the CSTF complex), which does not include component 2. We did not detect the CSFT complex in our SILAC based proteomic analysis of the TDP43 interactome, and this also occurred for the identification of TDP43 interaction with Barentsz (**Figure 3.1** and **Table 3.1**). Ionization biases and peptide mapping failures can be a common source of false negatives in protein identification by mass spectrometry. These proteins are absent in the list of specific TDP43 interactors, but also among the unspecific binders, so this would possibly mean that they were left out by the analysis. For this reason, we directly interrogated the TDP43 immunoprecipitation by Western blot. The combination of these high- and low-throughput proteomic approaches allowed us to circumvent their respective disadvantages.

The disease-related form of TDP43 is hyperphosphorylated, polyubiquitinated, and cleaved before the C-terminal domain (Neumann et al., 2006; Igaz et al., 2008). This region is also characterized by the presence of the most ALS-linked mutations

(Pesiridis et al., 2009) and is involved in several protein-protein interactions (Buratti et al., 2005; Ayala et al., 2005). From our analysis, the ALS-linked Q331K mutation does not affect the TDP43 functions and, as previously observed (Ling et al., 2010), its expression for 48h is not sufficient to significantly delocalize the protein to the cytoplasm or induce the formation of aggregates (**Figure 4.8**). For this reason, we focused on the truncated form of TDP43 lacking its C-terminal part by *in vitro* studies. The glycine-rich C-terminal domain resulted in playing a role in TDP43 interaction with CSTF1 and its deletion impaired TDP43 activity in the regulation of alternative polyadenylation (**Figure 4.9**).

Given the presented data, we propose a novel mechanism through which TDP43 acts on alternative polyadenylation. When TDP43 binds its mRNA target in the 3'UTR after the proximal polyA site, it prompts up there the recruitment of the CSTF complex, promoting the usage of the proximal PAS. The loss of the C-terminal domain in the pathological condition could be at the root of the alterations of alternative polyadenylation. To obtain a confirmation of the requirement of TDP43 interaction with the CSTF complex, we will combine the TDP43 tethering between the proximal and distal PAS with the silencing of its three components, alone or in combination. In this way, we will also be able to include or exclude the role of CSTF2 in the action of TDP43. Under the same silencing condition, we will also evaluate the effect on the alternative polyadenylation of TDP43 targets.

Genes involved in cellular differentiation, synapse organization and nervous system development resulted significantly enriched in our list of differentially polyadenylated genes targeted by TDP43, leading us to hypothesize a role of TDP43 in neuronal cells mediated through the modulation of the alternative polyadenylation of some of its targets. To understand how APA changes could impact on TDP43 targets in the neuronal environment, we will clone the 3'UTR (long and short) of some targets, engineering specific reporters without the presence of any additional polyA site. The long form will be mutagenized at the level of the proximal PAS and/or the TDP43 binding site. Then we will transfect them in primary culture of motor neurons, and we will analyze the expression, the translation efficiency, the cellular localization and the stability of the different isoforms. Moreover, we will test in *Drosophila* motor neurons if the silencing of the components of the CSTF complex could recapitulate the same phenotype observed in the absence of *Tbph*. In this way, we could suggest a direct link between alteration of alternative polyadenylation and neurodegeneration *in vivo*.

6. EXPERIMENTAL PROCEDURES

6.1 CELL CULTURE AND TREATMENTS

Murine motor neuron-like hybrid NSC-34 cells and human HeLa cells were cultured in DMEM (Gibco) supplemented with 10% FBS (Gibco), 100 U/ml penicillin streptomycin (Gibco) and 0.01 mM l-glutamine (Gibco) and were incubated at 37 °C, 5% CO_2.

For SILAC experiments, the cells were stable-isotope labeled under standard conditions as described in Paul et al., 2011. Heavy SILAC medium was prepared with DMEM lacking arginine and lysine (Gibco),10% dialyzed FBS (Gibco), 100 U/ml penicillin streptomycin (Gibco), 0.01 mM l-glutamine (Gibco),28 mg/l $^{13}C_6{}^{15}N_4$ L-arginine and 49 mg/l$^{13}C_6{}^{15}N_2$ L-lysine (Eurisotope). In 'Light' (L) SILAC medium were substituted with the corresponding non-labelled amino acids (Sigma).

NMD was inhibited by 10 mM caffeine or 50 µg/mLcycloheximide (Sigma, C1988) treatment for 18 h.

6.2 PLASMIDS CONSTRUCTS

The genes (or part of them) were amplified from SK-N- BE(2) cDNA or plasmid with AccuPrime™ DNA polymerase (Invitrogen), using the primers indicated in **Table 6.1**.

Table 6.1 Primers for cloning

Gene	Restriction site	Primer sequence (5'-3')	Template
hTDP43 Fw	SgfI	GAGGCGATCGCCTCTGAATATATTCGGGTAACC	Cdna
hTDP43 Rv	MluI	GCGACGCGTCTACATTCCCCAGCCAGAAGACTT	
hFus Fw	SgfI	GAGGCGATCGCCGCCTCAAACGATTATACCCAAC	Cdna
hFus Rv	MluI	GCGACGCGTTTAATACGGCCTCTCCCTGCGATC	
hTAF15 Fw	SgfI	GAGGCGATCGCCTCGGATTCTGGAAGTTACGGTCA	pDEST_TO_TAF15 (Addgene 26378)
hTAF15 Rv	MluI	GCGACGCGTTCAGTATGGTCGGTTGCGCTGAT	
hEWSR1 Fw	SgfI	GAGGCGATCGCCGCGTCCACGGATTACAGTACCTA	pDEST_TO_EWSR1 (Addgene 26376)
hEWSR1 Rv	MluI	GCGACGCGTCTAGTAGGGCCGATCTCTGCGCTC	
hTDP43 ΔCterm Rv	MluI	TTTTACGCGTATTGTGCTTAGGTTCGGC	pCMV6-AN- His-HA TDP43 wt
hTDP43 Fw	XhoI	CGAGCTCGAGTCTGAATATATTCGGGTAACCGAA	pCMV6-AN- His-HA TDP43 wt
hTDP43 Rv	NotI	GCGGCGGCCGCCTACATTCCCCAGCCAGAAGACTT	pCMV6-AN- His-HA TDP43 wt

Note: h = human

The amplified fragments were cloned using SgfI and MluI sites into the pCMV6-AN-His-HA plasmid (OriGene, PS100017). The generated vectors express the gene of interest in fusion with an amino-terminal polyhistidine (His) tag and an hemagglutinin (HA) epitope.

The vector pCI-MS2V5-TDP43 was generated using XhoI and NotI sites.

pCI-MS2V5 expressing GST, Y14 and CSTF1, pCI-mVenus empty vector, and the reporter genes used in the tethering experiments are a generous gift of Niels Gehring. The vectors pCI-mVenus-TDP43 wt, -TDP43 ΔCterm, and –CSTF1 were produced using XhoI and NotI sites.

The mutants were obtained via PCR-directed mutagenesis of the wild type template using the primers reported in **Table 6.2**.

Table 6.2 Primers for mutagenesis

Name	primer (5'-3')
TDP43 W113A sense	CTTTCAGGTCCTGTTCGGTTGTTTT**CGC**TGGGAGACCCAACAC
TDP43 W113A antisense	GTGTTGGGTCTCCCA**GCG**AAAACAACCGAACAGGACCTGAAAG
TDP43 R151A sense	TGTTTCATATTCCGTAAA**CGC**AACAAAGCCAAACCCCTTTG
TDP43 R151A antisense	AAGGGGTTTGGCTTTGTT**GCG**TTTACGGAATATGAAACAC
TDP43 Q331K sense	CCAGGCAGCACTAAAGAGCAGTTGGGGTA
TDP43 Q331K antisense	TACCCCAACTGCTCTTTAGTGCTGCCTGG
Globin_3UTR__XhoI asntisense	TTTTTTCTCGAGTGCATGAATATCCTC
Globin_delCrypt_polyA asntisense	GCTTAGGGAACAAAGGAACCCTCAACAGAAATTGGACAGCAAGAAA
Globin_EcoRI_exon3 sense	TTTTTTGAATTCACCCCACCAGTG

6.3 LENTIVIRUSES PRODUCTION

The His-HA tagged genes were excised from pCMV6-HIS-HA plasmids and subcloned into the BamHI and XhoI sites of the vector pENTR1A (w48-1, Addgene).

The resulting vectors were then recombined with pLenti CMV/TO Puro DEST (670-1, Addgene) using Gateway™ LR-Clonase (Life Technologies) to get the lentiviral vectors expressing tagged genes under the control of a doxycycline-inducible promoter. Lentiviruses were then prepared in accordance with the protocols detailed by Campeau et al., 2009.

6.4 TRANSDUCTION AND GENERATION OF TETRACYCLINE INDUCIBLE CELL LINES OVEREXPRESSING PROTEINS

NSC-34 cells were transduced with the pLentiCMV_TetR_Blast vector (Addgene, 716-1), constitutively expressing the tetracycline (Tet) repressor under the control of a CMV promoter, and selected for 10 days using 10 µg/ml Blasticidin (Sigma). The stable cells were infected with the lentiviral vectors in the presence of 4 µg/ml polybrene. The selection of transduced cells was then conducted by using 5 µg/ml puromycin. The protein overexpression was induced by adding 2 µg/ml doxycycline (Clontech) to the culture medium for 48 h and verified by Western blot analysis.
HeLa Flp-In T-REx cells β-globin xrRNA WT and PTC are a generous gift of Niels Gehring.

6.5 IMMUNOPRECIPITATION

Forty-eight hours after induction or transfection, cells were harvested in lysis buffer (150 mM NaCl, 25 mM Tris-HCl, 10 mM $MgCl_2$, 1% NP-40, 0.1% SDS,5% Glycerol) supplemented with complete protease inhibitor (Roche). Cell lysate was incubated with 30 µl (15 µl for Mass Spectrometry analysis) of anti-HA Magnetic Beads (Pierce) for 90' at 4°C. The beads were then washed with wash buffer (150 mM NaCl, 25 mM Tris-HCl, 10 mM $MgCl_2$, 0.025% NP-40). Bound proteins were eluted by boiling in SDS loading buffer and analyzed by Western blotting or with 8M guanidium hydrochloride and analyzed by MS. For SILAC-based quantitative immunoprecipitation beads from one heavy and one light experiment were mixed before elution and a label swap experiment was carried out (**Figure 3.1a**).

6.6 PROTEIN PRECIPITATION AND IN-SOLUTION DIGESTION

Eluted proteins from the immunoprecipitation were ethanol-precipitated and in solution-digested with lysyl endopeptidase (LysC) (Wako) and sequence-grade modified Trypsin (Promega). Stop and go extraction (STAGE) tips containing C_{18} empore disks (3M) were used to purify and store peptide extracts (Rappsilber et al., 2003).

6.7 LC-MS/MS AND DATA ANALYSIS

Peptide mixture (2 uL) was separated by reversed phase chromatography using the EASY-nLC2 system (Thermo Scientific) on 20 cm silica fritless microcolumn (75 µm inner diameter packed in-house with ReproSil-Pur C18-AQ 3-µm resin, Dr.Maisch GmbH). Peptides were separated on a 5-75% acetonitrile gradient with 0.5% formic acid (30 min) at a nano flow rate of 200 nl/min. Eluted peptides were ionized by electrospray ionization and sprayed into a Q Exactive Plus mass spectrometer (Thermo Scientific). The MS and MS/MS spectra were processed with the MaxQuant platform version 1.5.2.8 (Cox and Mann, 2008).

For SILAC experiments SILAC pairs were assembled from detected isotope patterns, recalibrated and quantified in the Quant module (heavy labels: Arg10 and Lys-8; maximum of 3 labelled aminoacids per peptide; maximum peptide charge of 6; top 6 MS/MS peaks per 100 Da; polymer detection enabled). A maximum of 2 missed cleavages were tolerated in the *in silico* digestion of the protein sequences. For protein identification, a minimum peptide length of 7 amino acids was required. Maximum false discovery rate was set at 1% for both peptide and protein identifications, estimated based on the reverse hits matched in the target-decoy database. Carbamidomethylation of cysteine was used as fixed modification. Oxidation of methionine and acetylation of the protein N-terminus were set as variable modifications. MS/MS spectra were searched by the internal Andromeda search engine against the *Mus musculus* protein database (ID UP000000589) and the database of common contaminants.

6.8 WESTERN BLOT

Protein samples derived from cells lysated with RIPA buffer, from immunoprecipitation or from TriFast extractions were resolved on SDS-PAGE and transferred to nitrocellulose membrane. Immunoblot analysis was performed with the following antibodies: anti-ACTININ (Santa Cruz Biotechnology, H-300), anti-BARENTSZ (Sigma, HPA024592,a generous gift from Macchi's lab), anti-CSTF1 (Bethyl, A301-250A), anti-CSTF3 (Bethyl, A301-096A), anti-EIF4A3 (homemade antibody, a generous gift from Macchi's lab), anti-GAPDH (Santa Cruz

Biotechnology, 6C5), anti-H3 (Abcam, ab1791), anti-HA (Bethyl, A190-108A), anti-PABPC1 (Sigma, SAB2101708), anti-SMG1 (Santa Cruz Biotechnology, E-4), anti-TDP43 (Proteintech, 10782-2-AP), anti-TUBULIN (Sigma, T6199), anti-UPF1 (Bethyl, A301-902A), anti-V5 (QED Bioscience, 18870), anti-Y14 (Bethyl, A301-033A), anti-mouse IgG-HRP (Santa CruzBiotechnology, sc-2005), anti-rabbit IgG-HRP (Santa Cruz Biotechnology, sc-2004). ECL Prime and Select Western blotting detection reagents (GE Healthcare) in combination with Chemidoc (Biorad) were used for visualization.

6.9 IMMUNOFLUORESCENCE MICROSCOPY

After fixation in 4% PFA, cells were permeabilized in PBS + 0.1% Triton X-100 for 5 min and incubated in blocking solution (2% bovine serum albumin, 2% fetal bovine serum, 0.2% gelatin in PBS) for 1 hour at RT. Primary antibodies were incubated overnight at RT in blocking solution diluted 1:10 in PBS. The following primary antibodies were used: rabbit anti-PABPC1 1:500 (Ab21060, Abcam), mouse anti-HA 1:500 (Sigma). The following secondary antibodies, diluted 1:800, were used: goat anti-rabbit Alexa Fluor® 594 (A11012, Thermo Fisher Scientific), goat anti-mouse Alexa Fluor® 488 (A11017, Thermo Fisher Scientific). Nuclei were stained with DAPI. Images were acquired with Zeiss Observer Z.1 Microscope implemented with the Zeiss ApoTome device. Pictures were acquired using AxioVision imaging software package (Zeiss). Images were not modified other than adjustments of levels and brightness.

6.10 TETHERING ASSAY

$2.7x10^5$ HeLa cells were seeded in 6-well plates 24 h before transient transfection by calcium phosphate precipitation with 2 µg reporter plasmid, 1 µg of MS2V5-tagged expression plasmid, 0.5 µg transfection control plasmid (β-globin 300 + E3) and 0.5 µg of pCI-mVenus plasmid.

6.11 siRNA TRANSFECTION

HeLa cells (2,5x10^5 cells/well) or NSC-34 cells (4x10^5cells/well) were reverse transfected in 6-well plates using 2.5 ml Lipofectamine RNAiMAX (Thermo Fisher) and 60 pmol siRNA (**Table 6.3**), following the manufacturer's protocol.

Table 6.3 siRNA target sequences

Target gene	siRNA (5'-3')	Reference
Luciferase	CGUACGCGGAAUACUUCGAdTdT	Miyagishi and Taira., 2002
hSMG1	GUGUAUGUGCGCCAAAGUAdTdT	Usuki et al., 2006
hTDP43	GCAAAGCCAAGAUGAGCCUdTdT	De Conti et al., 2015
mUPF1	CAGUUACUGUGGAAUCCAUdTdT	Mino et al., 2015
mTDP43	CGAUGAACCCAUUGAAAUAdTdT	Colombrita et al., 2012

6.12 RNA EXTRACTION

Total RNA was isolated using EUROGOLD TriFast (Euroclone) according to the manufacturer's instructions. For cytoplasm-nucleus fractionation, the cells were harvested in polysome buffer (10 mMNaCl, 10 mM MgCl2, 10 mMTris-HCl pH 7.4, 1% Triton X-100, 1% Na-deoxycholate and 1 mM DTT) and the fractions were separated by centrifugation before RNA purification. The RNA extraction from mouse spinal cord was performed after tissue homogenization with FastPrep®-24 system.

6.13 NORTHERN BLOT

RNA was resolved on a 1% agarose and 0.4 M formaldehyde gel using the tricine-triethanolamine buffer system (Mansour et al., 2013) and analysed by Northern blotting.[α-32P]-GTP body-labelled RNA probes were used for reporter and control RNAs detection and in vitro transcribed using BamHI-linearized PSP65-globin plasmid as a template.7SL endogenous RNA was detected using a 5'-32P-labelled oligonucleotide (5'-TGCTCCGTTTCCGACCTGGGCCGGTTCACCCCTCCTT-3'). Signals were scanned with Typhoon FLA 7000 (GE Healthcare) and raw unmodified scans were quantified with ImageQuant TL (GE Healthcare).

6.14 RNA IMMUNOPRECIPITATION (RIP)

Cells were harvested in polysome lysis buffer (100 mM KCl, 5 mM $MgCl_2$, 10 mM HEPES pH 7.4, 0.5%NP-40) supplemented with 100 U RNase Out (Invitrogen) and complete protease inhibitor (Roche). 30 µl of anti-HA Magnetic Beads (Pierce) were added to500 µg of cell lysate in NT2 buffer (50 mM Tris–HCl pH 7.4, 150 mM NaCl, 1 mM $MgCl_2$,0.05%NP-40 supplemented with fresh 200 U RNase Out (Invitrogen), 20 mM EDTA). 5% of the reaction mix was saved as input. After 3h of incubation at 4°C, the immunoprecipitated complexes were washed 4 times with cold NT2 buffer supplemented with 0.5% Urea, 4 times with cold NT2 bufferand resuspended in 100 µl NT2. RNA from immunoprecipitate and input was isolated with EUROGOLD TriFast (Euroclone) and analyzed by quantitative PCR.

6.15 QUANTITATIVE PCR

500 ng of total RNA were retrotranscribed with the iScript cDNA synthesis kit (Biorad). The obtained cDNA was used as template in qPCR reaction performed with KAPA SYBR FAST qPCR (Kapa Biosystem) and specific primers (**Table 6.4**). PCR conditions were 3 min at 95°C for initial denaturing, followed by 39 cycles of 10 sec at 95°C,20 sec at 60°C and 10 sec at 72°C. Ppia and Rpl10A were used as reference genes. The relative expression was calculated with the delta delta Ct method.

Table 6.4 Primers for quantitative PCR

target name	forward primer (5'-3')	reverse primer (5'-3')
mAtg12	GAAATGGGCTGTGGAGCGAA	TGCAGTAATGCAGGACCAGTT
mGabarapl2	CATGGTGGCTCACAACCGTA	TCTGTATGAATGCCCTATCTGC
mPpia	AACACAAACGGTTCCCAGTT	CTTCCCAAAGACCACATGCT
mRpl10a	GAAGAAGGTGCTGTGTTTGGC	TCGGTCATCTTCACGTGGC
mScg2	TGCTTGGAGCCTTCCACATAA	AAGCTGCTTCGGCTCCAGA
mTdp43	AGAGCTTTTGCCTTCGTCACCT	AAGAGACTGGGCAACCTTATCATC
mUbe2v2 (long)	CTTGTGTGAAGATCAGAGGT	CCTTGTTGACACGCATGGTA
mUbe2v2 (total)	GTGTCTTAAGAGACTGTGCTA	GCTGGCCAGGAACTTGTAAT
mUpf1	AGATCACGGCACAGCAGAT	CTCCAGAGTGGCTGAAGGAT

6.16 LIBRARY PREPARATION AND NEXT GENERATION SEQUENCING DATA ANALYSIS

QuantSeq 3' mRNA-Seq Library Prep Kit REV (Lexogen) was used starting from 500 ng of total RNA. For protocol details see **Figure 4.2a**. Paired end sequencing was performed with the Illumina HiSeq 2500 platform (Mus musculus, GPL17021). Fastq files were checked for quality control with FastQC. Adapter removal and flexible quality trimming was performed with Trimmomatic version 0.36. Processed reads generated from each sample were aligned to the mouse transcriptome with Bowtie2 (version 2.2.6), using the Gencode M6 transcript annotation. All programs were used with default settings unless otherwise specified. Read pairs with 3'end mapping within 10bp from transcript end, corresponding to the polyadenylation cleavage site, were considered for quantification and estimation of transcript expression levels (using bedtools utilities version 2.17.0). Normalization among samples was performed with the edgeR Bioconductor package, using the TMM method (trimmed mean of M values). Only transcripts with signal exceeding 1 CPM (count per million) in at least one condition were kept for further analysis.

6.16.1 FOR NMD (SIMPLE DIFFERENTIAL EXPRESSION ANALYSIS)

Differential expression analysis was performed with edgeR using the glmQLFit method (Genewise Negative Binomial Generalized Linear Models With Quasi-Likelihood Tests), selecting transcripts with statistical significance < 0.05.

6.16.2 FOR APA (DIFFERENTIAL POLYADENYLATION ANALYSIS)

Differential polyadenylation analysis was performed with edgeR using the diffSpliceDGE method, selecting transcripts with statistical significance < 0.1. P-values were not corrected for multiple testing. Within each gene, only isoforms with transcript 3’ ends more distant than 10bp (in genomic coordinates) were considered as distinct polyadenylation sites. Polyadenylation usage values were defined as the percentage of signal associated with each isoform with respect to the total signal of the gene.

6.17 ANIMALS AND MOTOR TESTS

Mice carrying a mutated TDP43 gene (B6N.Cg-Tg(Prnp-TARDBP*Q331K)103Dwc/J) and non-transgenic littermate C57B6JN were purchased from Jackson Laboratories (Bar Harbor, ME, USA). The breeding and maintenance of the mouse colony were conducted in consultation with the veterinary staff. Animal care and experimental procedures were conducted in accordance with the University of Trento ethics committee and were approved by the Italian Ministry of Health.

Cohorts of male transgenic and non-transgenic mice were followed weekly for general health and motor phenotype. For the hindlimb-clasping test, the mice were gently lifted by their tail for up to 10 s and extension of the limbs was tested for abnormal reflex. To evaluate motor coordination and balance, mice were tested for time to fall on accelerating rotarod test (Ugo Basile Instruments) starting from 3 weeks of age until 10 months of age. Following a 1 week training session, trials were repeated weekly. Each session consisted of three tests of 300 s with an acceleration period (2–40 rpm) and a 5 min interval between trials. The time spent on the spinning wheel before falling was averaged over three trials. Statistical analysis was performed using one-way ANOVA test.

For the tissue collection, mice were sacrificed at 3 months and 10 months of age using carbon dioxide euthanasia. The spinal cords were rapidly isolated with the ejection method (Meikle et al., 1981), flash frozen in liquid nitrogen and stored at -80°C for RNA and protein extraction.

7. ADDENDUM

Within the “AXonomIX project” (http://www.axonomix.eu/), whose aim is to identify the translational networks altered in motor neuron diseases, a large collection of cell models (**Table 7.1**) for Motor Neuron Diseases (MNDs) were produced. Amyotrophic Lateral Sclerosis (ALS), Spinal Muscular Atrophy (SMA) and Distal Spinal Muscular Atrophy type1 (DSMA type1) are a group of untreatable and lethal disorders characterized by progressive degeneration of upper and lower motor neurons in the central nervous system and weakness of muscles.

Several RNA binding proteins involved in MNDs were cloned and mutagenized into double tagged-lentiviral vectors. These proteins are directly or indirectly associated with RNA processing (splicing, stability, transport and translation) and they are affected by MNDs-linked mutations. Mutations in TDP43, FUS, Angiogenin, TAF15, EWSR1, Ataxin-2 are associated with amyotrophic lateral sclerosis (ALS), disruption of SMN causes spinal muscular atrophy (SMA), and genetic alterations in IGHMBP2 lead to distal spinal muscular atrophy type 1 (DSMA1).

NSC-34 cell line was engeneered for the inducible expression of tagged wild type or mutant protein of interst.

In addition to the cell models for MNDs-linked proteins overexpression, an *in vitro* model for Spinal Muscular Atrophy was generated by using CRISPR-Cas9 technology (**Figure 7.1a**). SMA is caused by loss or mutation of the *survival motor neuron1* gene (*SMN1*), which leads to insufficient expression of the functional full-length SMN protein (lower than 20%) and motor neuron dysfunction (Burghes and Beattie, 2009). The *Survival Motor Neuron* (*SMN*) gene was knocked-out in NSC-34 cells (**Figure 7.1b**); after clonal expansion, several cell lines with a defined SMN protein expression level were derived (**Figure 7.1c**).

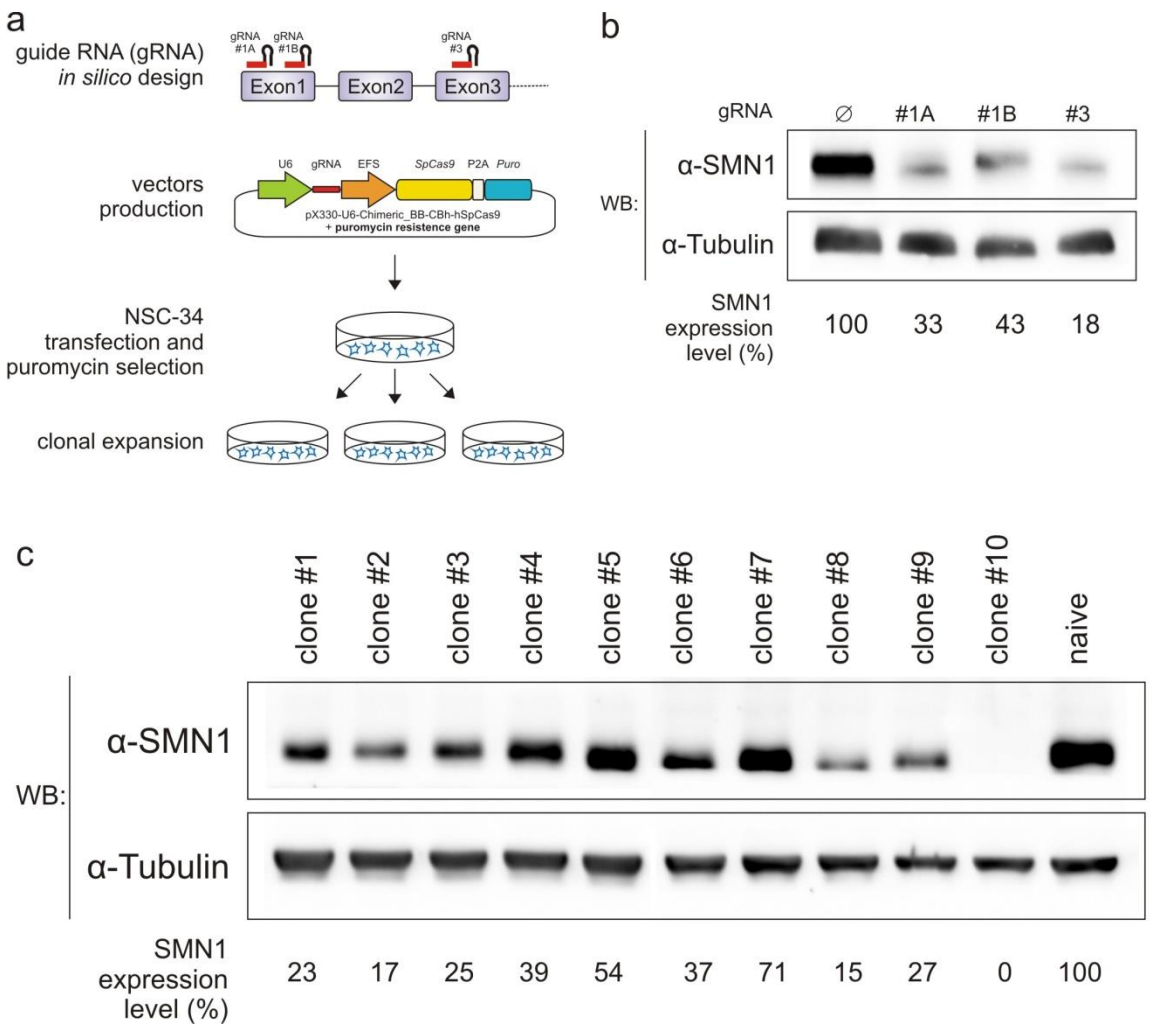

Figure 7.1 SMA cell model. The RNA-guided Cas9 nuclease from the microbial clustered regularly interspaced short palindromic repeats (CRISPR) adaptive immune system was used to knockout the *Survival Motor Neuron* (*SMN*) in NSC-34 cell line. Cas9, guided by a RNA of 20 nucleotides, recognizes and binds a specific locus in the genome and produces a double strand break, which is repaired by non-homologous end joining (NHEJ). An indel mutation can be introduced, generating a premature stop codon. (**a**) NSC-34 cells, transfected with pX330 vector expressing Cas9 and 3 different *in silico* designed guide RNAs (1A, 1B and 3), were selected with puromycin for 48 hrs. Starting from the pool of cells transfected with the guide 3, we performed a clonal expansion to derive cell lines with a defined SMN expression level. The SMN protein level was tested in the pool populations (**b**) and in 10 clones (**c**) by Western blot analysis. TUBULIN was used as protein loading control.

Table 7.1 Panel of produced plasmids and MND cell models

		Genetagging	Gataway System		
	Gene	pCMV6-AN-His-HA	pENTR	pLENTI CMV/TO Puro DEST	Cell line NSC34
ALS	hTDP43 wt	✓	✓	✓	✓
	hTDP43 Q331K		✓	✓	✓
	hTDP43 A315T		✓	✓	✓
	hTDP43 M337V		✓	✓	✓
	hFUS wt	✓	✓	✓	✓
	hFUS R521C		✓	✓	✓
	hFUS R521H		✓	✓	✓
	hFUS P525L		✓	✓	✓
	hEWSR1 wt	✓	✓	✓	✓
	hEWSR1 G511A		✓	✓	✓
	hEWSR1 P552L		✓	✓	✓
	hEWSR1 G584S		✓	✓	✓
	hTAF15 wt	✓	✓	✓	✓
	hTAF15 G391E		✓	✓	✓
	hTAF15 R408C		✓	✓	✓
	hMATRIN3 wt	✓	✓	✓	✓
	hMATRIN3 S85C		✓	✓	✓
	hATXN2 22Q	✓	✓	✓	✓
	hATXN2 31Q	✓	✓	✓	✓
	hSOD1 wt	✓	✓	✓	✓
	hSOD1 A4V		✓	✓	✓
	hSOD1 G93A		✓	✓	✓
	hSOD1 G37R		✓	✓	✓
	hANGIOGENIN wt	✓	✓	✓	✓
	hANGIOGENIN S28N		✓	✓	✓
	hANGIOGENIN K40I		✓	✓	✓
	hANGIOGENIN H114R		✓	✓	✓
DSMA1	hIGHMBP2	✓	✓	✓	✓
SMA	hSMN1	✓	✓	✓	✓
	ΔSMN1				✓
Control	EGFP	✓	✓	✓	✓

Using some of these cell lines, we performed a label-free quantitative mass spectrometry analysis (**Figure 7.2a**) of the protein interactors of several MNDs-linked RBPs: FUS (**Figure 7.2b**), MATR3 (**Figure 7.2c**), EWSR1 (**Figure 7.2d**), TAF15 (**Figure 7.2e**), ATXN2 (**Figure 7.2f**), and IGHMBP2 (**Figure 7.2g**).

This high-throughput analysis provided a low number of significant specific interactors (**Table 7.2**), compared to the SILAC-based analysis performed on the TDP43 interactome (**Table 3.1**). However, our results evidenced, for some of the analyzed proteins, enrichment in components of NMD and mRNA 3'end processing

(**Figure 7.2h**, **i** and **l**), suggesting their possible involvement in these pathways, even if more validations are needed.

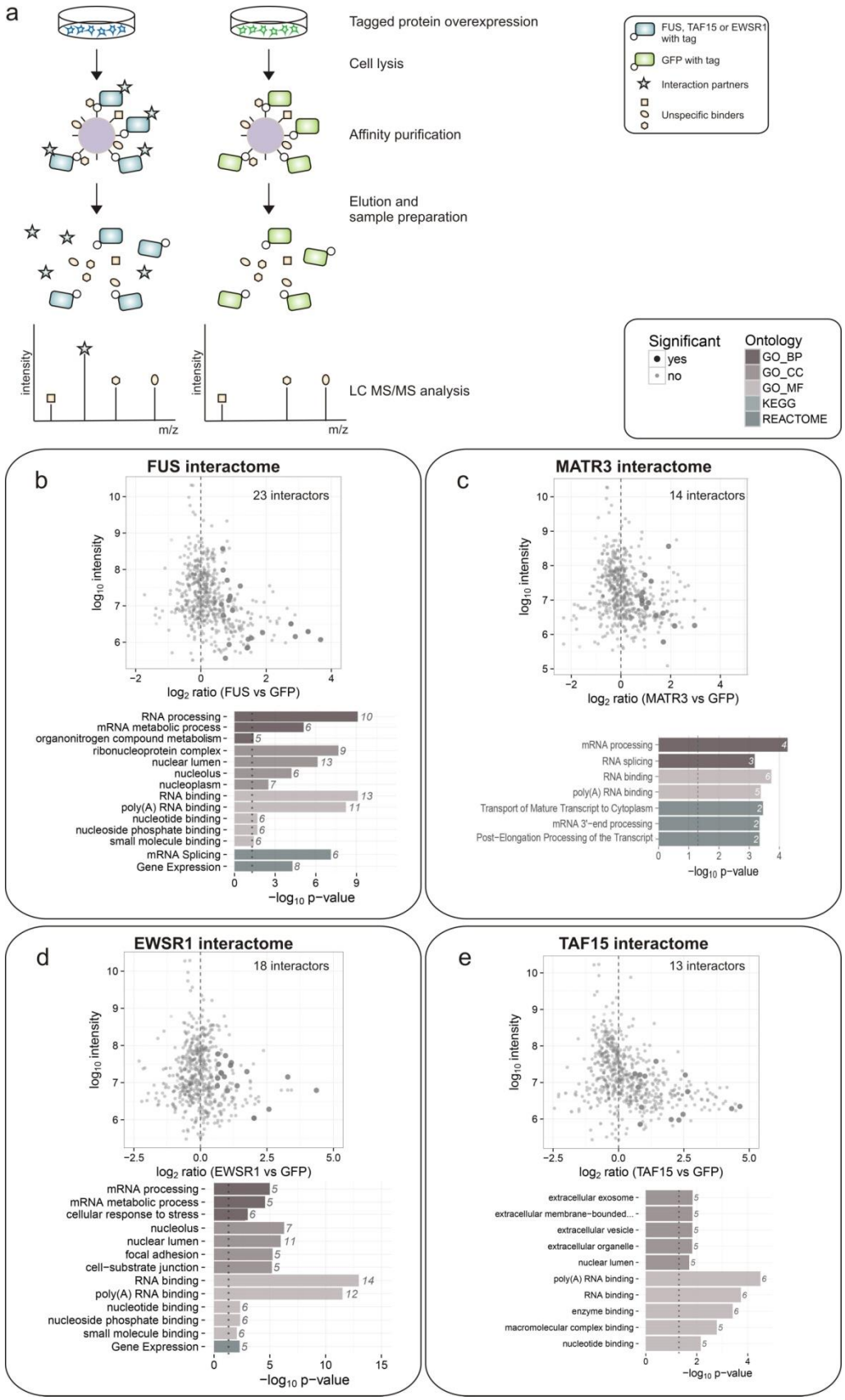

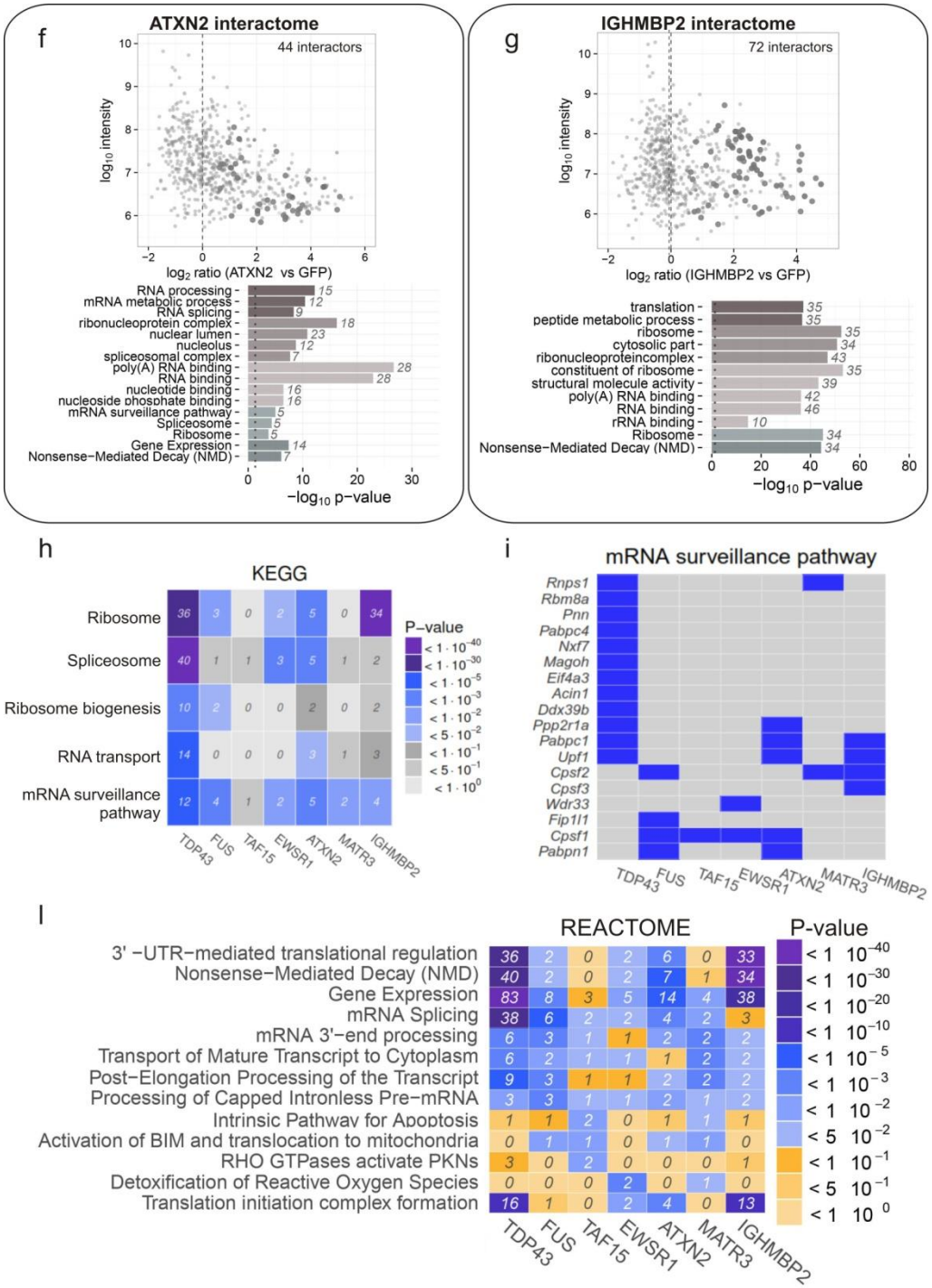

Figure 7.2 Protein interactome analysis of RBPs involved in MNDs. (**a**) Workflow of protein-protein interaction analysis by label-free quantitative Mass Spectrometry. His-HA RBPs and His-HA GFP were overexpressed for 48 h in NSC-34 cell line. After the pull-down, captured bait/prey complexes were eluted and analyzed by LC-MS/MS. We performed the analysis in three independent experiments, without any treatment. For each quantified protein, the LFQ intensity (y axis) and the fold change between RBP pull-down and GFP pull-down (used as negative control, x-axis) are represented in the scatter plot. The number of identified high-confidence interacting proteins (highlighted in bigger dots) are indicated (fold-change > 1.5 and the t-test p value < 0.1). The enrichment analysis is presented in the bottom panel. We performed the interactome proteomic

analysis of (**b**) FUS, (**c**) MATR3, (**d**) EWSR1, (**e**) TAF15, (**f**) ATXN2, and (**g**) IGHMBP2. (**h** and **I**) Comparison between the TDP43 interactome analyzed by SILAC based approach and the protein interactors of other RBPs involved in MNDs identified by LFQ proteomics. (**i**) List of the proteins of the mRNA surveillance pathway (KEGG mmu03015) interacting with MNDs-linked RBPs.

Table 7.2 Protein interactors of RBPs involved in MNDs

RBP	Interactors
FUS	1810009A15Rik, AU019823, Bcar1, Cpsf1, Cpsf2, Csnk2b, Ddx17, Dynll1, Fip1l1, Mphosph10, Mrpl34, Nop2, Pabpn1, Pgk1, Ptbp1, Rpl10a, Rps27, Snrnp70, Ssb, Taf15, Tmcc3, Usp28, Wdr46
MATR3	Bcar1, Chgb, Cpsf2, Dynll1, Hnrnpll, Krt76, Prdx1, Prpf38a, Psma2, Rnps1, Skp1, Tmcc3, Tmod3, Usp28
EWSR1	Anxa1, Anxa2, Bcar1, Caap1, Cat, Cpsf1, Ddx18, Prdx1, Prmt1, Prpf38a, Rps18, Rps9, Snrnp70, Srsf10, Txn, Usp28, Wdr33, Zcchc17
TAF15	Bcar1, Cpsf1, Ddx17, Dnaja1, Dynll1, Hdgfrp2, Myh14, Prmt1, Serping1, Snrnp70, Tecr, Tmcc3, Ywhaz
ATXN2	Aen, Atad3, Bcas2, Cpsf1, Csnk2b, Cyc1, Ddx18, Ddx46, Ddx52, Dync1h1, Dynll1, Eif4b, Fam195b, Fbl, Flii, Hdgfrp2, Hsd17b12, Hsph1, Khsrp, Larp4, Lsm12, Mfap1, Mrps5, Mybbp1a, Pabpc1, Pabpn1, Parp1, Pcbp2, Ppp2r1a, Prpf40a, Rbm25, Rbmx2, Rpl10a, Rpl7, Rps2, Rps9, Rsbn1, Rsrc2, Skp1, Srek1, Top2a, Tra2a, Upf1, Wdr46
IGHMBP2	Actr2, Add3, Bcar1, Caprin1, Capza1, Cherp, Cpsf2, Cpsf3, Csnk2b, Ddx17, Dstn, Flii, Fxr1, G3bp1, G3bp2, Gm17669, Gnb2l1, Lima1, Llph, Lrrfip2, Mprip, Myl1, Pabpc1, Prpf31, Ptbp1, Rbm28, Rcn2, Rpl10a, Rpl12, Rpl13, Rpl13a, Rpl14, Rpl15, Rpl18, Rpl18a, Rpl19, Rpl27, Rpl28, Rpl3, Rpl34, Rpl35a, Rpl37a, Rpl4, Rpl5, Rpl6, Rpl7, Rplp1, Rplp2, Rps10, Rps12, Rps15a, Rps16, Rps19, Rps21, Rps27, Rps27l, Rps28, Rps3, Rps5, Rps8, Rps9, Serbp1, Skp1, Tmcc3, Tpm1, Tpm2, Tpm4, Upf1, Vgf, Vimp, Wdr1, Ywhaq

The produced cell lines represent a valuable resource and are suitable for *in vitro* studies, protein and RNA interactome analysis. Some of them were used in different projects that led to the following articles, and other papers are in preparation:

Exosome derived from murine adipose-derived stromal cells: neuroprotective effect on in vitro model of amyotrophic lateral sclerosis. Raffaella Mariotti, Roberta Bonafede, Ilaria Scambi, Daniele Peroni, Valentina Potrich, Federico Boschi, Donatella Benati, Bruno Bonetti, Experimental Cell Research, 2016 Jan 1;340(1):150-8. doi: 10.1016/j.yexcr.2015.12.009

In vivo translatome profiling reveals early defects in ribosome biology underlying SMA pathogenesis. Paola Bernabò, Toma Tebaldi, Ewout JN Groen, Fiona M Lane, Elena Perenthaler, Francesca Mattedi, Helen J Newbery, Haiyan Zhou, Paola Zuccotti, Valentina Potrich, Francesco Muntoni, Alessandro Quattrone, Thomas H Gillingwater, Gabriella Viero. Submitted doi: https://doi.org/10.1101/103481

REFERENCES

- Amrani N, Dong S, He F, Ganesan R, Ghosh S, Kervestin S, Li C, Mangus DA, Spatrick P, Jacobson A. Aberrant termination triggers nonsense-mediated mRNA decay. Biochem Soc Trans. 2006 Feb;34(Pt 1):39-42. Review. PubMed PMID: 16246174.
- Amrani N, Ganesan R, Kervestin S, Mangus DA, Ghosh S, Jacobson A. A faux 3'-UTR promotes aberrant termination and triggers nonsense-mediated mRNA decay. Nature. 2004 Nov 4;432(7013):112-8. PubMed PMID: 15525991.
- An J, Zhu X, Wang H, Jin X. A dynamic interplay between alternative polyadenylation and microRNA regulation: implications for cancer (Review). Int J Oncol. 2013 Oct;43(4):995-1001. doi: 10.3892/ijo.2013.2047. Epub 2013 Aug 1. Review. PubMed PMID: 23913120.
- Anders KR, Grimson A, Anderson P. SMG-5, required for C.elegans nonsense-mediated mRNA decay, associates with SMG-2 and protein phosphatase 2A. EMBO J. 2003 Feb 3;22(3):641-50. PubMed PMID: 12554664; PubMed Central PMCID:PMC140740.
- Arai T, Hasegawa M, Akiyama H, Ikeda K, Nonaka T, Mori H, Mann D, Tsuchiya K, Yoshida M, Hashizume Y, Oda T. TDP-43 is a component of ubiquitin-positive tau-negative inclusions in frontotemporal lobar degeneration and amyotrophic lateral sclerosis. Biochem Biophys Res Commun. 2006 Dec 22;351(3):602-11. Epub 2006 Oct 30. PubMed PMID: 17084815.
- Arnold ES, Ling SC, Huelga SC, Lagier-Tourenne C, Polymenidou M, Ditsworth D, Kordasiewicz HB, McAlonis-Downes M, Platoshyn O, Parone PA, Da Cruz S, Clutario KM, Swing D, Tessarollo L, Marsala M, Shaw CE, Yeo GW, Cleveland DW. ALS-linked TDP-43 mutations produce aberrant RNA splicing and adult-onset motor neuron disease without aggregation or loss of nuclear TDP-43. Proc Natl Acad Sci U S A. 2013 Feb 19;110(8):E736-45. doi: 10.1073/pnas.1222809110. Epub 2013 Feb 4. PubMed PMID: 23382207; PubMed Central PMCID: PMC3581922.
- Avendaño-Vázquez SE, Dhir A, Bembich S, Buratti E, Proudfoot N, Baralle FE. Autoregulation of TDP-43 mRNA levels involves interplay between transcription, splicing, and alternative polyA site selection. Genes Dev. 2012 Aug 1;26(15):1679-84. doi: 10.1101/gad.194829.112. PubMed PMID: 22855830; PubMed Central PMCID: PMC3418585.
- Ayala YM, De Conti L, Avendaño-Vázquez SE, Dhir A, Romano M, D'Ambrogio A, Tollervey J, Ule J, Baralle M, Buratti E, Baralle FE. TDP-43 regulates its mRNA levels through a negative feedback loop. EMBO J. 2011 Jan 19;30(2):277-88. doi:10.1038/emboj.2010.310. Epub 2010 Dec 3. PubMed PMID: 21131904; PubMed Central PMCID: PMC3025456
- Ayala YM, Misteli T, Baralle FE. TDP-43 regulates retinoblastoma protein phosphorylation through the repression of cyclin-dependent kinase 6 expression. Proc Natl Acad Sci U S A. 2008 Mar 11;105(10):3785-9. doi:10.1073/pnas.0800546105. Epub 2008 Feb 27. PubMed PMID: 18305152; PubMed Central PMCID: PMC2268791.
- Ayala YM, Pantano S, D'Ambrogio A, Buratti E, Brindisi A, Marchetti C, Romano M, Baralle FE. Human, Drosophila, and C.elegans TDP43: nucleic acid binding properties and splicing regulatory function. J Mol Biol. 2005 May 6;348(3):575-88. PubMed PMID: 15826655.
- Barmada S, Ju S, Arjun A, Batarse A, Qu H, Huang EE, et al. RNA helicases ameliorate ALS- and FTD related neurotoxicity. Ann Neurol 2013; 74:S93.
- Batra R, Charizanis K, Manchanda M, Mohan A, Li M, Finn DJ, Goodwin M, Zhang C, Sobczak K, Thornton CA, Swanson MS. Loss of MBNL leads to disruption of developmentally regulated alternative polyadenylation in RNA-mediated disease. Mol Cell. 2014 Oct 23;56(2):311-22. doi: 10.1016/j.molcel.2014.08.027. Epub 2014 Sep 25. PubMed PMID: 25263597; PubMed Central PMCID: PMC4224598.
- Bava FA, Eliscovich C, Ferreira PG, Miñana B, Ben-Dov C, Guigó R, Valcárcel J, Méndez R. CPEB1 coordinates alternative 3'-UTR formation with translational regulation. Nature. 2013 Mar 7;495(7439):121-5. doi: 0.1038/nature11901. Epub 2013 Feb 24. PubMed PMID: 23434754.
- Behm-Ansmant I, Kashima I, Rehwinkel J, Saulière J, Wittkopp N, Izaurralde E. mRNA quality control: an ancient machinery recognizes and degrades mRNAs with nonsense codons. FEBS Lett. 2007 Jun 19;581(15):2845-53. Epub 2007 May 21. Review. PubMed PMID: 17531985.
- Bembich S, Herzog JS, De Conti L, Stuani C, Avendaño-Vázquez SE, Buratti E, Baralle M, Baralle FE. Predominance of spliceosomal complex formation over polyadenylation site selection in TDP-43 autoregulation. Nucleic Acids Res. 2014 Mar;42(5):3362-71. doi: 10.1093/nar/gkt1343.

Epub 2013 Dec 24. PubMed PMID:24369426; PubMed Central PMCID: PMC3950720.

- Berggård T, Linse S, James P. Methods for the detection and analysis of protein-protein interactions. Proteomics. 2007 Aug;7(16):2833-42. Review. PubMed PMID: 17640003. von Mering C, Krause R, Snel B, Cornell M, Oliver SG, Fields S, Bork P. Comparative assessment of large-scale data sets of protein-protein interactions. Nature. 2002 May 23;417(6887):399-403. Epub 2002 May 8. PubMed PMID: 12000970.
- Bettencourt C, HouldenH.Exome sequencing uncovers hidden pathways in familial and sporadic ALS.NatNeurosci. 2015 May;18(5):611-3. doi: 10.1038/nn.4012.
- Bhardwaj A, Myers MP, Buratti E, Baralle FE. Characterizing TDP-43 interaction with its RNA targets. Nucleic Acids Res. 2013 May;41(9):5062-74. doi: 10.1093/nar/gkt189. Epub 2013 Mar 21. PubMed PMID: 23519609; PubMed Central PMCID: PMC3643599.
- Bhattacharya A, Czaplinski K, Trifillis P, He F, Jacobson A, Peltz SW. Characterization of the biochemical properties of the human Upf1 gene product that is involved in nonsense-mediated mRNA decay. RNA. 2000 Sep;6(9):1226-35. PubMed PMID: 10999600; PubMed Central PMCID: PMC1369996
- Bhattacharya A, Czaplinski K, Trifillis P, He F, Jacobson A, Peltz SW. Characterization of the biochemical properties of the human Upf1 gene product that is involved in nonsense-mediated mRNA decay. RNA. 2000 Sep;6(9):1226-35. PubMed PMID: 10999600; PubMed Central PMCID: PMC1369996.
- Blokhuis AM, Koppers M, Groen EJ, van den Heuvel DM, Dini Modigliani S, Anink JJ, Fumoto K, van Diggelen F, Snelting A, Sodaar P, Verheijen BM, Demmers JA, Veldink JH, Aronica E, Bozzoni I, den Hertog J, van den Berg LH, Pasterkamp RJ. Comparative interactomics analysis of different ALS-associated proteins identifies converging molecular pathways. Acta Neuropathol. 2016 Aug;132(2):175-96. doi: 10.1007/s00401-016-1575-8. Epub 2016 May 10. PubMed PMID: 27164932; PubMed Central PMCID: PMC4947123.
- Boehm V, Gerbracht JV, Marx MC, Gehring NH. Interrogating the degradation pathways of unstable mRNAs with XRN1-resistant sequences. Nat Commun. 2016 Dec 5;7:13691. doi: 10.1038/ncomms13691. PubMed PMID: 27917860; PubMed Central PMCID:PMC5150221.
- Boehm V, Haberman N, Ottens F, Ule J, Gehring NH. 3' UTR length and messenger ribonucleoprotein composition determine endocleavage efficiencies at termination codons. Cell Rep. 2014 Oct 23;9(2):555-68. doi: 10.1016/j.celrep.2014.09.012. Epub 2014 Oct 9. PubMed PMID: 25310981.
- Bono F, Ebert J, Unterholzner L, Güttler T, Izaurralde E, Conti E. Molecular insights into the interaction of PYM with the Mago-Y14 core of the exon junction complex. EMBO Rep. 2004 Mar;5(3):304-10. Epub 2004 Feb 13. PubMed PMID: 14968132; PubMed Central PMCID: PMC1299003.
- Bose JK, Huang CC, Shen CK. Regulation of autophagy by neuropathological protein TDP-43. J Biol Chem. 2011 Dec 30;286(52):44441-8. doi:10.1074/jbc.M111.237115. Epub 2011 Nov 3. PubMed PMID: 22052911; PubMed Central PMCID: PMC3247982.
- Bramham, C. R., Worley, P. F., Moore, M. J. and Guzowski, J. (2008). The immediate early gene arc/arg3.1: regulation, mechanisms, and function. J. Neurosci. 28, 1176011767.
- Budini M, Buratti E, Stuani C, Guarnaccia C, Romano V, De Conti L, Baralle FE. Cellular model of TAR DNA-binding protein 43 (TDP-43) aggregation based on its C-terminal Gln/Asn-rich region. J Biol Chem. 2012 Mar 2;287(10):7512-25. doi: 10.1074/jbc.M111.288720. Epub 2012 Jan 10. PubMed PMID: 22235134; PubMed Central PMCID: PMC3293573.
- Buratti E, Baralle FE. Characterization and functional implications of the RNA binding properties of nuclear factor TDP-43, a novel splicing regulator of CFTR exon 9. J Biol Chem. 2001 Sep 28;276(39):36337-43. Epub 2001 Jul 24. PubMed PMID: 11470789.
- Buratti E, Brindisi A, Giombi M, Tisminetzky S, Ayala YM, Baralle FE. TDP-43 binds heterogeneous nuclear ribonucleoprotein A/B through its C-terminal tail: an important region for the inhibition of cystic fibrosis transmembrane conductance regulator exon 9 splicing. J Biol Chem. 2005 Nov 11;280(45):37572-84. Epub 2005 Sep 12. PubMed PMID: 16157593.
- Buratti E, Dörk T, Zuccato E, Pagani F, Romano M, Baralle FE. Nuclear factor TDP-43 and SR proteins promote in vitro and in vivo CFTR exon 9 skipping. EMBO J. 2001 Apr 2;20(7):1774-84. PubMed PMID: 11285240; PubMed Central PMCID: PMC145463.
- Burghes AH, Beattie CE. Spinal muscular atrophy: why do low levels of survival motor neuron protein make motor neurons sick? Nat Rev Neurosci. 2009 Aug;10(8):597-609. doi: 10.1038/nrn2670. Epub 2009 Jul 8. Review. PubMed PMID:19584893; PubMed Central PMCID: PMC2853768.

- Campeau E, Ruhl VE, Rodier F, Smith CL, Rahmberg BL, Fuss JO, Campisi J, Yaswen P, Cooper PK, Kaufman PD. A versatile viral system for expression and depletion of proteins in mammalian cells. PLoS One. 2009 Aug 6;4(8):e6529. doi:10.1371/journal.pone.0006529. PubMed PMID: 19657394; PubMed Central PMCID:PMC2717805.
- Castelo-Branco P, Furger A, Wollerton M, Smith C, Moreira A, Proudfoot N. Polypyrimidine tract binding protein modulates efficiency of polyadenylation. Mol Cell Biol. 2004 May;24(10):4174-83. Erratum in: Mol Cell Biol. 2004 Aug;24(15):6889. PubMed PMID: 15121839; PubMed Central PMCID: PMC400487.
- Chamieh H, Ballut L, Bonneau F, Le Hir H. NMD factors UPF2 and UPF3 bridge UPF1 to the exon junction complex and stimulate its RNA helicase activity. Nat Struct Mol Biol. 2008 Jan;15(1):85-93. Epub 2007 Dec 9. PubMed PMID: 18066079.
- Chang JC, Kan YW. beta 0 thalassemia, a nonsense mutation in man. Proc Natl Acad Sci U S A. 1979 Jun;76(6):2886-9. PubMed PMID: 88735; PubMed Central PMCID: PMC383714.
- Chen S, Zhang X, Song L, Le W. Autophagy dysregulation in amyotrophic lateral sclerosis. Brain Pathol. 2012 Jan;22(1):110-6. doi:10.1111/j.1750-3639.2011.00546.x. Review. PubMed PMID: 22150926.
- Chiu SY, Serin G, Ohara O, Maquat LE. Characterization of human Smg5/7a: a protein with similarities to Caenorhabditis elegans SMG5 and SMG7 that functions in the dephosphorylation of Upf1. RNA. 2003 Jan;9(1):77-87. PubMed PMID:12554878; PubMed Central PMCID: PMC1370372.
- Colombrita C, Onesto E, Megiorni F, Pizzuti A, Baralle FE, Buratti E, Silani V, Ratti A. TDP-43 and FUS RNA-binding proteins bind distinct sets of cytoplasmicmessenger RNAs and differently regulate their post-transcriptional fate inmotoneuron-like cells. J Biol Chem. 2012 May 4;287(19):15635-47. doi:10.1074/jbc.M111.333450. Epub 2012 Mar 16. PubMed PMID: 22427648; PubMed Central PMCID: PMC3346140.
- Colombrita C, Zennaro E, Fallini C, Weber M, Sommacal A, Buratti E, Silani V, Ratti A. TDP-43 is recruited to stress granules in conditions of oxidative insult. J Neurochem. 2009 Nov;111(4):1051-61. doi: 10.1111/j.1471-4159.2009.06383.x. Epub 2009 Sep 16. PubMed PMID: 19765185.
- Costessi L, Porro F, Iaconcig A, Muro AF. TDP-43 regulates β-adducin (Add2) transcript stability. RNA Biol. 2014;11(10):1280-90. doi:10.1080/15476286.2014.996081. PubMed PMID: 25602706; PubMed Central PMCID:PMC4615836.
- Cox J, Mann M. MaxQuant enables high peptide identification rates, individualized p.p.b.-range mass accuracies and proteome-wide protein quantification. Nat Biotechnol. 2008 Dec;26(12):1367-72. doi: 10.1038/nbt.1511. Epub 2008 Nov 30. PubMed PMID: 19029910.
- Czaplinski K, Weng Y, Hagan KW, Peltz SW. Purification and characterization of the Upf1 protein: a factor involved in translation and mRNA degradation. RNA. 1995 Aug;1(6):610-23. PubMed PMID: 7489520; PubMed Central PMCID: PMC1369305.
- Dai W, Zhang G, Makeyev EV. RNA-binding protein HuR autoregulates its expression by promoting alternative polyadenylation site usage. Nucleic Acids Res. 2012 Jan;40(2):787-800. doi: 10.1093/nar/gkr783. Epub 2011 Sep 24. PubMed PMID: 21948791; PubMed Central PMCID: PMC3258158.
- De Conti L, Akinyi MV, Mendoza-Maldonado R, Romano M, Baralle M, Buratti E. TDP-43 affects splicing profiles and isoform production of genes involved in the apoptotic and mitotic cellular pathways. Nucleic Acids Res. 2015 Oct15;43(18):8990-9005. doi: 10.1093/nar/gkv814. Epub 2015 Aug 10. PubMed PMID: 26261209; PubMed Central PMCID: PMC4605304.
- De Conti L, Akinyi MV, Mendoza-Maldonado R, Romano M, Baralle M, Buratti E. TDP-43 affects splicing profiles and isoform production of genes involved in the apoptotic and mitotic cellular pathways. Nucleic Acids Res. 2015 Oct15;43(18):8990-9005. doi: 10.1093/nar/gkv814. Epub 2015 Aug 10. PubMed PMID: 26261209; PubMed Central PMCID: PMC4605304.
- Derti A, Garrett-Engele P, Macisaac KD, Stevens RC, Sriram S, Chen R, Rohl CA, Johnson JM, Babak T. A quantitative atlas of polyadenylation in five mammals. Genome Res. 2012 Jun;22(6):1173-83. doi: 10.1101/gr.132563.111. Epub 2012 Mar 27. PubMed PMID: 22454233; PubMed Central PMCID: PMC3371698.
- Derti A, Garrett-Engele P, Macisaac KD, Stevens RC, Sriram S, Chen R, Rohl CA, Johnson JM, Babak T. A quantitative atlas of polyadenylation in five mammals. Genome Res. 2012 Jun;22(6):1173-83. doi: 10.1101/gr.132563.111. Epub 2012 Mar 27.PubMed PMID: 22454233; PubMed Central PMCID: PMC3371698.
- Di Giammartino DC, Nishida K, Manley JL. Mechanisms and consequences of alternative

polyadenylation. Mol Cell. 2011 Sep 16;43(6):853-66. doi:10.1016/j.molcel.2011.08.017. Review. PubMed PMID: 21925375; PubMed CentralPMCID: PMC3194005.

- Dittmar KA, Jiang P, Park JW, Amirikian K, Wan J, Shen S, Xing Y, Carstens RP. Genome-wide determination of a broad ESRP-regulated posttranscriptional network by high-throughput sequencing. Mol Cell Biol. 2012 Apr;32(8):1468-82. doi:10.1128/MCB.06536-11. Epub 2012 Feb 21. PubMed PMID: 22354987; PubMed Central PMCID: PMC3318588.
- Dostie J, Dreyfuss G. Translation is required to remove Y14 from mRNAs in the cytoplasm. Curr Biol. 2002 Jul 9;12(13):1060-7. PubMed PMID: 12121612.
- Eberle AB, Lykke-Andersen S, Mühlemann O, Jensen TH. SMG6 promotes endonucleolytic cleavage of nonsense mRNA in human cells. Nat Struct Mol Biol. 2009 Jan;16(1):49-55. doi: 10.1038/nsmb.1530. Epub 2008 Dec 7. PubMed PMID:19060897.
- Elkon R, Ugalde AP, Agami R. Alternative cleavage and polyadenylation: extent, regulation and function. Nat Rev Genet. 2013 Jul;14(7):496-506. doi:10.1038/nrg3482. Review. PubMed PMID: 23774734..
- Elkon R, Ugalde AP, Agami R. Alternative cleavage and polyadenylation: extent, regulation and function. Nat Rev Genet. 2013 Jul;14(7):496-506. doi:10.1038/nrg3482. Review. PubMed PMID: 23774734.
- Erson-Bensan AE. Alternative polyadenylation and RNA-binding proteins. J Mol Endocrinol. 2016 Aug;57(2):F29-34. doi: 10.1530/JME-16-0070. Epub 2016 May 20. Review. PubMed PMID: 27208003.
- Estes PS, Boehringer A, Zwick R, Tang JE, Grigsby B, Zarnescu DC. Wild-type and A315T mutant TDP-43 exert differential neurotoxicity in a Drosophila model of ALS. Hum Mol Genet. 2011 Jun 15;20(12):2308-21. doi: 10.1093/hmg/ddr124. Epub 2011 Mar 26. PubMed PMID: 21441568; PubMed Central PMCID: PMC3098735.
- Feiguin F, Godena VK, Romano G, D'Ambrogio A, Klima R, Baralle FE. Depletion of TDP-43 affects Drosophila motoneurons terminal synapsis and locomotive behavior. FEBS Lett. 2009 May 19;583(10):1586-92. doi: 10.1016/j.febslet.2009.04.019. Epub 2009 Apr 19. PubMed PMID: 19379745.
- Fiesel FC, Voigt A, Weber SS, Van den Haute C, Waldenmaier A, Görner K, Walter M, Anderson ML, Kern JV, Rasse TM, Schmidt T, Springer W, Kirchner R, Bonin M, Neumann M, Baekelandt V, Alunni-Fabbroni M, Schulz JB, Kahle PJ. Knockdown of transactive response DNA-binding protein (TDP-43) downregulates histone deacetylase 6. EMBO J. 2010 Jan 6;29(1):209-21. doi: 10.1038/emboj.2009.324. Epub 2009 Nov 12. PubMed PMID: 19910924; PubMed Central PMCID: PMC2808372.
- Fiorini F, Boudvillain M, Le Hir H. Tight intramolecular regulation of the human Upf1 helicase by its N- and C-terminal domains. Nucleic Acids Res. 2013 Feb 1;41(4):2404-15. doi: 10.1093/nar/gks1320. Epub 2012 Dec 28. PubMed PMID:23275559; PubMed Central PMCID: PMC3575847.
- Fox-Walsh K, Davis-Turak J, Zhou Y, Li H, Fu XD. A multiplex RNA-seq strategy to profile poly(A+) RNA: application to analysis of transcription response and 3'end formation. Genomics. 2011 Oct;98(4):266-71. doi: 10.1016/j.ygeno.2011.04.003.Epub 2011 Apr 15. PubMed PMID: 21515359; PubMed Central PMCID: PMC3160523.
- Franks TM, Singh G, Lykke-Andersen J. Upf1 ATPase-dependent mRNP disassembly is required for completion of nonsense- mediated mRNA decay. Cell. 2010 Dec 10;143(6):938-50. doi: 10.1016/j.cell.2010.11.043. PubMed PMID: 21145460; PubMed Central PMCID: PMC3357093.
- Freibaum BD, Chitta RK, High AA, Taylor JP. Global analysis of TDP-43 interacting proteins reveals strong association with RNA splicing and translation machinery. J Proteome Res. 2010 Feb 5;9(2):1104-20. doi: 10.1021/pr901076y. PubMed PMID: 20020773; PubMed Central PMCID: PMC2897173.
- Fu Y, Sun Y, Li Y, Li J, Rao X, Chen C, Xu A. Differential genome-wide profiling of tandem 3' UTRs among human breast cancer and normal cells by high-throughput sequencing. Genome Res. 2011 May;21(5):741-7. doi:10.1101/gr.115295.110. Epub 2011 Apr 7. PubMed PMID: 21474764; PubMed Central PMCID: PMC3083091.
- Gawande B, Robida MD, Rahn A, Singh R. Drosophila Sex-lethal protein mediates polyadenylation switching in the female germline. EMBO J. 2006 Mar 22;25(6):1263-72. Epub 2006 Mar 2. PubMed PMID: 16511567; PubMed Central PMCID:PMC1422161.
- Gehring NH, Hentze MW, Kulozik AE. Tethering assays to investigate nonsense-mediated mRNA decay activating proteins. Methods Enzymol. 2008;448:467-82. doi: 10.1016/S0076-

6879(08)02623-2. PubMed PMID: 19111190.

- Gehring NH, Lamprinaki S, Hentze MW, Kulozik AE. The hierarchy of exon-junction complex assembly by the spliceosome explains key features of mammalian nonsense-mediated mRNA decay. PLoS Biol. 2009 May 26;7(5):e1000120. doi: 10.1371/journal.pbio.1000120. Epub 2009 May 26. PubMed PMID: 19478851; PubMed Central PMCID: PMC2682485.
- Gehring NH, Lamprinaki S, Hentze MW, Kulozik AE. The hierarchy of exon-junction complex assembly by the spliceosome explains key features of mammalian nonsense-mediated mRNA decay. PLoS Biol. 2009 May 26;7(5):e1000120. doi: 10.1371/journal.pbio.1000120. Epub 2009 May 26. PubMed PMID: 19478851; PubMed Central PMCID: PMC2682485.
- Gehring NH, Neu-Yilik G, Schell T, Hentze MW, Kulozik AE. Y14 and hUpf3b form an NMD-activating complex. Mol Cell. 2003 Apr;11(4):939-49. PubMed PMID:12718880.
- Giorgi C, Yeo GW, Stone ME, Katz DB, Burge C, Turrigiano G, Moore MJ. The EJC factor eIF4AIII modulates synaptic strength and neuronal protein expression. Cell. 2007 Jul 13;130(1):179-91. PubMed PMID: 17632064.
- Gong C, Maquat LE. lncRNAs transactivate STAU1-mediated mRNA decay by duplexing with 3' UTRs via Alu elements. Nature. 2011 Feb 10;470(7333):284-8. doi: 10.1038/nature09701. PubMed PMID: 21307942; PubMed Central PMCID:PMC3073508.
- Gregersen LH, Schueler M, Munschauer M, Mastrobuoni G, Chen W, Kempa S, Dieterich C, Landthaler M. MOV10 Is a 5' to 3' RNA helicase contributing to UPF1 mRNA target degradation by translocation along 3' UTRs. Mol Cell. 2014 May 22;54(4):573-85. doi: 10.1016/j.molcel.2014.03.017. Epub 2014 Apr 10. PubMed PMID: 24726324.
- Gruber AR, Martin G, Keller W, Zavolan M. Means to an end: mechanisms of alternative polyadenylation of messenger RNA precursors. Wiley Interdiscip Rev RNA. 2014 Mar-Apr;5(2):183-96. doi: 10.1002/wrna.1206. Epub 2013 Nov 14. Review. PubMed PMID: 24243805; PubMed Central PMCID: PMC4282565.
- Gruber AR, Martin G, Keller W, Zavolan M. Means to an end: mechanisms of alternative polyadenylation of messenger RNA precursors. Wiley Interdiscip Rev RNA. 2014 Mar-Apr;5(2):183-96. doi: 10.1002/wrna.1206. Epub 2013 Nov 14. Review. PubMed PMID: 24243805; PubMed Central PMCID: PMC4282565.
- Hafner M, Renwick N, Brown M, Mihailović A, Holoch D, Lin C, Pena JT, Nusbaum JD, Morozov P, Ludwig J, Ojo T, Luo S, Schroth G, Tuschl T. RNA-ligase-dependent biases in miRNA representation in deep-sequenced small RNA cDNA libraries. RNA. 2011 Sep;17(9):1697-712. doi: 10.1261/rna.2799511. Epub 2011 Jul 20. PubMed PMID:21775473; PubMed Central PMCID: PMC3162335.
- Hilgers V, Lemke SB, Levine M. ELAV mediates 3' UTR extension in the Drosophila nervous system. Genes Dev. 2012 Oct 15;26(20):2259-64. doi:10.1101/gad.199653.112. Epub 2012 Sep 27. PubMed PMID: 23019123; PubMed Central PMCID: PMC3475798.
- Hogg JR, Goff SP. Upf1 senses 3'UTR length to potentiate mRNA decay. Cell. 2010 Oct 29;143(3):379-89. doi: 10.1016/j.cell.2010.10.005. PubMed PMID: 21029861; PubMed Central PMCID: PMC2981159.
- Hoque M, Ji Z, Zheng D, Luo W, Li W, You B, Park JY, Yehia G, Tian B. Analysis of alternative cleavage and polyadenylation by 3' region extraction and deep sequencing. Nat Methods. 2013 Feb;10(2):133-9. doi: 10.1038/nmeth.2288. Epub 2012 Dec 16. PubMed PMID: 23241633; PubMed Central PMCID: PMC3560312.
- Hoshino S, Imai M, Mizutani M, Kikuchi Y, Hanaoka F, Ui M, Katada T. Molecular cloning of a novel member of the eukaryotic polypeptide chain-releasing factors (eRF). Its identification as eRF3 interacting with eRF1. J Biol Chem. 1998 Aug 28;273(35):22254-9. PubMed PMID: 9712840.
- Huntzinger E, Kashima I, Fauser M, Saulière J, Izaurralde E. SMG6 is the catalytic endonuclease that cleaves mRNAs containing nonsense codons in metazoan. RNA. 2008 Dec;14(12):2609-17. doi: 10.1261/rna.1386208. Epub 2008 Oct 30. PubMed PMID: 18974281; PubMed Central PMCID: PMC2590965.
- Hurt JA, Robertson AD, Burge CB. Global analyses of UPF1 binding and function reveal expanded scope of nonsense-mediated mRNA decay. Genome Res. 2013 Oct;23(10):1636-50. doi: 10.1101/gr.157354.113. Epub 2013 Jun 13. PubMed PMID:23766421; PubMed Central PMCID: PMC3787261.
- Igaz LM, Kwong LK, Lee EB, Chen-Plotkin A, Swanson E, Unger T, Malunda J, Xu Y, Winton MJ, Trojanowski JQ, Lee VM. Dysregulation of the ALS-associated gene TDP-43 leads to neuronal death and degeneration in mice. J Clin Invest. 2011 Feb;121(2):726-38. doi: 10.1172/JCI44867.

Epub 2011 Jan 4. PubMed PMID: 21206091; PubMed Central PMCID: PMC3026736.

- Igaz LM, Kwong LK, Xu Y, Truax AC, Uryu K, Neumann M, Clark CM, Elman LB, Miller BL, Grossman M, McCluskey LF, Trojanowski JQ, Lee VM. Enrichment of C-terminal fragments in TAR DNA-binding protein-43 cytoplasmic inclusions in brain but not in spinal cord of frontotemporal lobar degeneration and amyotrophic lateral sclerosis. Am J Pathol. 2008 Jul;173(1):182-94. doi: 10.2353/ajpath.2008.080003. Epub 2008 Jun 5. PubMed PMID: 18535185; PubMed Central PMCID: PMC2438296.
- Ihara R, Matsukawa K, Nagata Y, Kunugi H, Tsuji S, Chihara T, Kuranaga E, Miura M, Wakabayashi T, Hashimoto T, Iwatsubo T. RNA binding mediates neurotoxicity in the transgenic Drosophila model of TDP-43 proteinopathy. Hum Mol Genet. 2013 Nov 15;22(22):4474-84. doi: 10.1093/hmg/ddt296. Epub 2013 Jun 25. PubMed PMID: 238047
- Ivanov PV, Gehring NH, Kunz JB, Hentze MW, Kulozik AE. Interactions between UPF1, eRFs, PABP and the exon junction complex suggest an integrated model for mammalian NMD pathways. EMBO J. 2008 Mar 5;27(5):736-47. doi:10.1038/emboj.2008.17. Epub 2008 Feb 7. PubMed PMID: 18256688; PubMed Central PMCID: PMC2265754.
- Jackson KL, Dayton RD, Orchard EA, Ju S, Ringe D, Petsko GA, Maquat LE, Klein RL. Preservation of forelimb function by UPF1 gene therapy in a rat model of TDP-43-induced motor paralysis. Gene Ther. 2015 Jan;22(1):20-8. doi:10.1038/gt.2014.101. Epub 2014 Nov 6. PubMed PMID: 25354681; PubMed Central PMCID: PMC4924570.
- Jan CH, Friedman RC, Ruby JG, Bartel DP. Formation, regulation and evolution of Caenorhabditis elegans 3'UTRs. Nature. 2011 Jan 6;469(7328):97-101. doi:10.1038/nature09616. Epub 2010 Nov 17. PubMed PMID: 21085120; PubMed Central PMCID: PMC3057491.
- Jenal M, Elkon R, Loayza-Puch F, van Haaften G, Kühn U, Menzies FM, Oude Vrielink JA, Bos AJ, Drost J, Rooijers K, Rubinsztein DC, Agami R. The poly(A)-binding protein nuclear 1 suppresses alternative cleavage and polyadenylation sites. Cell. 2012 Apr 27;149(3):538-53. doi:10.1016/j.cell.2012.03.022. Epub 2012 Apr 12. PubMed PMID: 22502866.
- Kabashi E, Lin L, Tradewell ML, Dion PA, Bercier V, Bourgouin P, Rochefort D, Bel Hadj S, Durham HD, Vande Velde C, Rouleau GA, Drapeau P. Gain and loss of function of ALS-related mutations of TARDBP (TDP-43) cause motor deficits in vivo. Hum Mol Genet. 2010 Feb 15;19(4):671-83. doi: 10.1093/hmg/ddp534. Epub 2009 Dec 3. Erratum in: Hum Mol Genet. 2010 Aug 1;19(15):3102. PubMed PMID: 19959528.
- Kashima I, Yamashita A, Izumi N, Kataoka N, Morishita R, Hoshino S, Ohno M, Dreyfuss G, Ohno S. Binding of a novel SMG-1-Upf1-eRF1-eRF3 complex (SURF) to the exon junction complex triggers Upf1 phosphorylation and nonsense-mediated mRNA decay. Genes Dev. 2006 Feb 1;20(3):355-67. PubMed PMID: 16452507; PubMed Central PMCID: PMC1361706.
- Katz Y, Wang ET, Airoldi EM, Burge CB. Analysis and design of RNA sequencing experiments for identifying isoform regulation. Nat Methods. 2010 Dec;7(12):1009-15. doi: 10.1038/nmeth.1528. Epub 2010 Nov 7. PubMed PMID:21057496; PubMed Central PMCID: PMC3037023.
- Kenna KP, van Doormaal PT, Dekker AM, Ticozzi N, Kenna BJ, Diekstra FP, vanRheenen W, van Eijk KR, Jones AR, Keagle P, Shatunov A, Sproviero W, Smith BN,van Es MA, Topp SD, Kenna A, Miller JW, Fallini C, Tiloca C, McLaughlin RL, VanceC, Troakes C, Colombrita C, Mora G, Calvo A, Verde F, Al-Sarraj S, King A, CaliniD, de Belleroche J, Baas F, van der Kooi AJ, de Visser M, Ten Asbroek AL, SappPC, McKenna-Yasek D, Polak M, Asress S, Muñoz-Blanco JL, Strom TM, Meitinger T,Morrison KE; SLAGEN Consortium, Lauria G, Williams KL, Leigh PN, Nicholson GA,Blair IP, Leblond CS, Dion PA, Rouleau GA, Pall H, Shaw PJ, Turner MR, Talbot K, Taroni F, Boylan KB, Van Blitterswijk M, Rademakers R, Esteban-Pérez J,García-Redondo A, Van Damme P, Robberecht W, Chio A, Gellera C, Drepper C,Sendtner M, Ratti A, Glass JD, Mora JS, Basak NA, Hardiman O, Ludolph AC,Andersen PM, Weishaupt JH, Brown RH Jr, Al-Chalabi A, Silani V, Shaw CE, van den Berg LH, Veldink JH, Landers JE. NEK1 variants confer susceptibility toamyotrophic lateral sclerosis. Nat Genet. 2016 Sep;48(9):1037-42. doi:10.1038/ng.3626. Epub 2016 Jul 25. PubMed PMID: 27455347.
- Kervestin S, Jacobson A. NMD: a multifaceted response to premature translational termination. Nat Rev Mol Cell Biol. 2012 Nov;13(11):700-12. doi:10.1038/nrm3454. Epub 2012 Oct 17. Review. PubMed PMID: 23072888; PubMed Central PMCID: PMC3970730.
- Kim YK, Furic L, Desgroseillers L, Maquat LE. Mammalian Staufen1 recruits Upf1 to specific mRNA 3'UTRs so as to elicit mRNA decay. Cell. 2005 Jan 28;120(2):195-208. PubMed PMID: 15680326.

- Koyama A, Sugai A, Kato T, Ishihara T, Shiga A, Toyoshima Y, Koyama M, Konno T, Hirokawa S, Yokoseki A, Nishizawa M, Kakita A, Takahashi H, Onodera O. Increased cytoplasmic TARDBP mRNA in affected spinal motor neurons in ALS caused by abnormal autoregulation of TDP-43. Nucleic Acids Res. 2016 Jul 8;44(12):5820-36. doi: 10.1093/nar/gkw499. Epub 2016 Jun 2. PubMed PMID:27257061; PubMed Central PMCID: PMC4937342.
- Kraemer BC, Schuck T, Wheeler JM, Robinson LC, Trojanowski JQ, Lee VM, Schellenberg GD. Loss of murine TDP-43 disrupts motor function and plays an essential role in embryogenesis. Acta Neuropathol. 2010 Apr;119(4):409-19. doi:10.1007/s00401-010-0659-0. Epub 2010 Mar 3. PubMed PMID: 20198480; PubMed Central PMCID: PMC2880609.
- Kumar DR, Aslinia F, Yale SH, Mazza JJ. Jean-Martin Charcot: The Father of Neurology. Clinical Medicine & Research. 2011;9(1):46-49. doi:10.3121/cmr.2009.883.
- Kumar V, Sami N, Kashav T, Islam A, Ahmad F, Hassan MI. Protein aggregation and neurodegenerative diseases: From theory to therapy. Eur J Med Chem. 2016 Nov 29;124:1105-1120. doi: 10.1016/j.ejmech.2016.07.054. Epub 2016 Jul 26. Review. PubMed PMID: 27486076.
- Kurosaki T, Li W, Hoque M, Popp MW, Ermolenko DN, Tian B, Maquat LE. A post-translational regulatory switch on UPF1 controls targeted mRNA degradation. Genes Dev. 2014 Sep 1;28(17):1900-16. doi: 10.1101/gad.245506.114. PubMed PMID:25184677; PubMed Central PMCID: PMC4197951.
- Kurosaki T, Li W, Hoque M, Popp MW, Ermolenko DN, Tian B, Maquat LE. A post-translational regulatory switch on UPF1 controls targeted mRNA degradation. Genes Dev. 2014 Sep 1;28(17):1900-16. doi: 10.1101/gad.245506.114. PubMed PMID:25184677; PubMed Central PMCID: PMC4197951.
- Kurosaki T, Maquat LE. Rules that govern UPF1 binding to mRNA 3' UTRs. Proc Natl Acad Sci U S A. 2013 Feb 26;110(9):3357-62. doi: 10.1073/pnas.1219908110. Epub 2013 Feb 12. PubMed PMID: 23404710; PubMed Central PMCID: PMC3587222.
- Lalmansingh AS, Urekar CJ, Reddi PP. TDP-43 is a transcriptional repressor: the testis-specific mouse acrv1 gene is a TDP-43 target in vivo. J Biol Chem. 2011 Apr 1;286(13):10970-82. doi: 10.1074/jbc.M110.166587. Epub 2011 Jan 20. PubMed PMID: 21252238; PubMed Central PMCID: PMC3064152.
- Le Hir H, Izaurralde E, Maquat LE, Moore MJ. The spliceosome deposits multiple proteins 20-24 nucleotides upstream of mRNA exon-exon junctions. EMBO J. 2000 Dec 15;19(24):6860-9. PubMed PMID: 11118221; PubMed Central PMCID: PMC305905.
- Le Hir H, Saulière J, Wang Z. The exon junction complex as a node of post-transcriptional networks. Nat Rev Mol Cell Biol. 2016 Jan;17(1):41-54. doi:10.1038/nrm.2015.7. Epub 2015 Dec 16. Review. PubMed PMID: 26670016.
- Lee EB, Lee VM, Trojanowski JQ. Gains or losses: molecular mechanisms of TDP43-mediated neurodegeneration. Nat Rev Neurosci. 2011 Nov 30;13(1):38-50. doi:10.1038/nrn3121. Review. PubMed PMID: 22127299; PubMed Central PMCID: PMC3285250.
- Lee SR, Pratt GA, Martinez FJ, Yeo GW, Lykke-Andersen J. Target Discrimination in Nonsense-Mediated mRNA Decay Requires Upf1 ATPase Activity. Mol Cell. 2015 Aug 6;59(3):413-25. doi: 10.1016/j.molcel.2015.06.036. PubMed PMID: 26253027; PubMed Central PMCID: PMC4673969.
- Lee SR, Pratt GA, Martinez FJ, Yeo GW, Lykke-Andersen J. Target Discrimination in Nonsense-Mediated mRNA Decay Requires Upf1 ATPase Activity. Mol Cell. 2015 Aug 6;59(3):413-25. doi: 10.1016/j.molcel.2015.06.036. PubMed PMID: 26253027; PubMed Central PMCID: PMC4673969.
- Levine B, Kroemer G. Autophagy in the pathogenesis of disease. Cell. 2008 Jan 11;132(1):27-42. doi: 10.1016/j.cell.2007.12.018. Review. PubMed PMID: 18191218; PubMed Central PMCID: PMC2696814.
- Li Y, Ray P, Rao EJ, Shi C, Guo W, Chen X, Woodruff EA 3rd, Fushimi K, Wu JY. A Drosophila model for TDP-43 proteinopathy. Proc Natl Acad Sci U S A. 2010 Feb 16;107(7):3169-74. doi: 10.1073/pnas.0913602107. Epub 2010 Jan 26. PubMed PMID:20133767; PubMed Central PMCID: PMC2840283.
- Licatalosi DD, Mele A, Fak JJ, Ule J, Kayikci M, Chi SW, Clark TA, Schweitzer AC, Blume JE, Wang X, Darnell JC, Darnell RB. HITS-CLIP yields genome-wide insights into brain alternative RNA processing. Nature. 2008 Nov 27;456(7221):464-9. doi: 10.1038/nature07488. Epub 2008 Nov 2. PubMed PMID: 18978773; PubMed Central PMCID: PMC2597294.
- Ling SC, Albuquerque CP, Han JS, Lagier-Tourenne C, Tokunaga S, Zhou H, Cleveland DW. ALS-associated mutations in TDP-43 increase its stability and promote TDP-43 complexes with

FUS/TLS. Proc Natl Acad Sci U S A. 2010 Jul 27;107(30):13318-23. doi: 10.1073/pnas.1008227107. Epub 2010 Jul 12. PubMed PMID: 20624952; PubMed Central PMCID: PMC2922163.

- Ling JP, Pletnikova O, Troncoso JC, Wong PC. TDP-43 repression of nonconserved cryptic exons is compromised in ALS-FTD. Science. 2015 Aug 7;349(6248):650-5. doi: 10.1126/science.aab0983. PubMed PMID: 26250685; PubMed Central PMCID:PMC4825810.
- Liu-Yesucevitz L, Bilgutay A, Zhang YJ, Vanderweyde T, Citro A, Mehta T, Zaarur N, McKee A, Bowser R, Sherman M, Petrucelli L, Wolozin B. Tar DNA binding protein-43 (TDP-43) associates with stress granules: analysis of cultured cells and pathological brain tissue. PLoS One. 2010 Oct 11;5(10):e13250. doi:10.1371/journal.pone.0013250. Erratum in: PLoS One. 2011;6(9). doi:10.1371/annotation/7d880410-06e3-4fe3-a8f1-e84c89bcf8d0. Vanderwyde, Tara [corrected to Vanderweyde, Tara]. PubMed PMID: 20948999; PubMed Central PMCID:PMC2952586.
- Long AA, Mahapatra CT, Woodruff EA 3rd, Rohrbough J, Leung HT, Shino S, An L, Doerge RW, Metzstein MM, Pak WL, Broadie K. The nonsense-mediated decay pathway maintains synapse architecture and synaptic vesicle cycle efficacy. J Cell Sci.2010 Oct 1;123(Pt 19):3303-15. doi: 10.1242/jcs.069468. Epub 2010 Sep 7. PubMedPMID: 20826458; PubMed Central PMCID: PMC2939802.
- Losson R, Lacroute F. Interference of nonsense mutations with eukaryotic messenger RNA stability. Proc Natl Acad Sci U S A. 1979 Oct;76(10):5134-7. PubMed PMID: 388431; PubMed Central PMCID: PMC413094.
- Lu Y, Ferris J, Gao FB. Frontotemporal dementia and amyotrophic lateral sclerosis-associated disease protein TDP-43 promotes dendritic branching. Mol Brain. 2009 Sep 25;2:30. doi: 10.1186/1756-6606-2-30. PubMed PMID: 19781077; PubMed Central PMCID: PMC2762964.
- Lukavsky PJ, Daujotyte D, Tollervey JR, Ule J, Stuani C, Buratti E, Baralle FE, Damberger FF, Allain FH. Molecular basis of UG-rich RNA recognition by the human splicing factor TDP-43. Nat Struct Mol Biol. 2013 Dec;20(12):1443-9. doi:10.1038/nsmb.2698. Epub 2013 Nov 17. PubMed PMID: 24240615.
- Lutz CS, Moreira A. Alternative mRNA polyadenylation in eukaryotes: an effective regulator of gene expression. Wiley Interdiscip Rev RNA. 2011 Jan-Feb;2(1):22-31. doi: 10.1002/wrna.47. Epub 2010 Sep 20. Review. PubMed PMID:21956967.
- Lykke-Andersen J, Shu MD, Steitz JA. Communication of the position of exon-exon junctions to the mRNA surveillance machinery by the protein RNPS1. Science. 2001 Sep 7;293(5536):1836-9. PubMed PMID: 11546874.
- Lykke-Andersen J, Shu MD, Steitz JA. Human Upf proteins target an mRNA for nonsense-mediated decay when bound downstream of a termination codon. Cell. 2000 Dec 22;103(7):1121-31. PubMed PMID: 11163187.
- Mangone M, Manoharan AP, Thierry-Mieg D, Thierry-Mieg J, Han T, Mackowiak SD, Mis E, Zegar C, Gutwein MR, Khivansara V, Attie O, Chen K, Salehi-Ashtiani K, Vidal M, Harkins TT, Bouffard P, Suzuki Y, Sugano S, Kohara Y, Rajewsky N, Piano F, Gunsalus KC, Kim JK. The landscape of C. elegans 3'UTRs. Science. 2010 Jul 23;329(5990):432-5. doi: 10.1126/science.1191244. Epub 2010 Jun 3. PubMed PMID: 20522740; PubMed Central PMCID: PMC3142571.
- Mansfield KD, Keene JD. Neuron-specific ELAV/Hu proteins suppress HuR mRNA during neuronal differentiation by alternative polyadenylation. Nucleic Acids Res. 2012 Mar;40(6):2734-46. doi: 10.1093/nar/gkr1114. Epub 2011 Dec 1. PubMed PMID: 22139917; PubMed Central PMCID: PMC3315332.
- Mansour, F. H. &Pestov, D. G. Separation of long RNA by agaroseformaldehyde gel electrophoresis. Anal. Biochem. 441, 18–20 (2013).
- Maquat LE, Kinniburgh AJ, Rachmilewitz EA, Ross J. Unstable beta-globin mRNA in mRNA-deficient beta o thalassemia. Cell. 1981 Dec;27(3 Pt 2):543-53. PubMed PMID: 6101206.
- Maquat LE, Kinniburgh AJ, Rachmilewitz EA, Ross J. Unstable beta-globin mRNA in mRNA-deficient beta o thalassemia. Cell. 1981 Dec;27(3 Pt 2):543-53. PubMed PMID: 6101206.
- Masamha CP, Xia Z, Yang J, Albrecht TR, Li M, Shyu AB, Li W, Wagner EJ. CFIm25 links alternative polyadenylation to glioblastoma tumour suppression. Nature. 2014 Jun 19;510(7505):412-6. doi: 10.1038/nature13261. Epub 2014 May 11. PubMed PMID: 24814343; PubMed Central PMCID: PMC4128630.
- Masuda A, Takeda J, Okuno T, Okamoto T, Ohkawara B, Ito M, Ishigaki S, Sobue G, Ohno K. Position-specific binding of FUS to nascent RNA regulates mRNA length. Genes Dev. 2015 May

15;29(10):1045-57. doi: 10.1101/gad.255737.114. PubMed PMID: 25995189; PubMed Central PMCID: PMC4441052.

- Meikle AD, Martin AH. A rapid method for removal of the spinal cord. Stain Technol. 1981 Jul;56(4):235-7. PubMed PMID: 7029784.
- Mendell JT, Sharifi NA, Meyers JL, Martinez-Murillo F, Dietz HC. Nonsense surveillance regulates expression of diverse classes of mammalian transcripts and mutes genomic noise. Nat Genet. 2004 Oct;36(10):1073-8. Epub 2004 Sep 26. Erratum in: Nat Genet. 2004 Nov;36(11):1238. PubMed PMID: 15448691.
- Mendell JT, Sharifi NA, Meyers JL, Martinez-Murillo F, Dietz HC. Nonsense surveillance regulates expression of diverse classes of mammalian transcripts and mutes genomic noise. Nat Genet. 2004 Oct;36(10):1073-8. Epub 2004 Sep 26. Erratum in: Nat Genet. 2004 Nov;36(11):1238. PubMed PMID: 15448691.
- Milev MP, Ravichandran M, Khan MF, Schriemer DC, Mouland AJ. Characterization of staufen1 ribonucleoproteins by mass spectrometry and biochemical analyses reveal the presence of diverse host proteins associated with human immunodeficiency virus type 1. Front Microbiol. 2012 Oct 25;3:367. doi:10.3389/fmicb.2012.00367. eCollection 2012. PubMed PMID: 23125841; PubMed Central PMCID: PMC3486646.
- Mino T, Murakawa Y, Fukao A, Vandenbon A, Wessels HH, Ori D, Uehata T, Tartey S, Akira S, Suzuki Y, Vinuesa CG, Ohler U, Standley DM, Landthaler M, Fujiwara T, Takeuchi O. Regnase-1 and Roquin Regulate a Common Element in Inflammatory mRNAs by Spatiotemporally Distinct Mechanisms. Cell. 2015 May 21;161(5):1058-73. doi:10.1016/j.cell.2015.04.029. PubMed PMID: 26000482.
- Mino T, Murakawa Y, Fukao A, Vandenbon A, Wessels HH, Ori D, Uehata T, Tartey S, Akira S, Suzuki Y, Vinuesa CG, Ohler U, Standley DM, Landthaler M, Fujiwara T, Takeuchi O. Regnase-1 and Roquin Regulate a Common Element in Inflammatory mRNAs by Spatiotemporally Distinct Mechanisms. Cell. 2015 May 21;161(5):1058-73. doi:10.1016/j.cell.2015.04.029. PubMed PMID: 26000482.
- Miyagishi M, Taira K. U6 promoter-driven siRNAs with four uridine 3' overhangsefficiently suppress targeted gene expression in mammalian cells. Nat Biotechnol.2002 May;20(5):497-500. PubMed PMID: 11981564.
- Miyagishi M, Taira K. U6 promoter-driven siRNAs with four uridine 3' overhangs efficiently suppress targeted gene expression in mammalian cells. Nat Biotechnol. 2002 May;20(5):497-500. PubMed PMID: 11981564.
- Moll P, Ante M, Seitz A, Reda T. QuantSeq 3′ mRNA sequencing for RNA quantification. Nat Methods. 2014
- Mühlemann O. Intimate liaison with SR proteins brings exon junction complexes to unexpected places. Nat Struct Mol Biol. 2012 Dec;19(12):1209-11. doi:10.1038/nsmb.2454. PubMed PMID: 23211765.
- Nagy E, Maquat LE. A rule for termination-codon position within intron-containing genes: when nonsense affects RNA abundance. Trends Biochem Sci. 1998 Jun;23(6):198-9. Review. PubMed PMID: 9644970.
- Neumann M, Sampathu DM, Kwong LK, Truax AC, Micsenyi MC, Chou TT, Bruce J, Schuck T, Grossman M, Clark CM, McCluskey LF, Miller BL, Masliah E, Mackenzie IR, Feldman H, Feiden W, Kretzschmar HA, Trojanowski JQ, Lee VM. Ubiquitinated TDP-43 in frontotemporal lobar degeneration and amyotrophic lateral sclerosis. Science. 2006 Oct 6;314(5796):130-3. PubMed PMID: 17023659.
- Nicholson P, Yepiskoposyan H, Metze S, Zamudio Orozco R, Kleinschmidt N, Mühlemann O. Nonsense-mediated mRNA decay in human cells: mechanistic insights, functions beyond quality control and the double-life of NMD factors. Cell Mol Life Sci. 2010 Mar;67(5):677-700. doi: 10.1007/s00018-009-0177-1. Epub 2009 Oct 27. Review. PubMed PMID: 19859661.
- Ohnishi T, Yamashita A, Kashima I, Schell T, Anders KR, Grimson A, Hachiya T, Hentze MW, Anderson P, Ohno S. Phosphorylation of hUPF1 induces formation of mRNA surveillance complexes containing hSMG-5 and hSMG-7. Mol Cell. 2003 Nov;12(5):1187-200. PubMed PMID: 14636577.
- Okada-Katsuhata Y, Yamashita A, Kutsuzawa K, Izumi N, Hirahara F, Ohno S. N- and C-terminal Upf1 phosphorylations create binding platforms for SMG-6 and SMG-5:SMG-7 during NMD. Nucleic Acids Res. 2012 Feb;40(3):1251-66. doi:10.1093/nar/gkr791. Epub 2011 Sep 29. PubMed PMID: 21965535; PubMed Central PMCID: PMC3273798.
- Ou SH, Wu F, Harrich D, García-Martínez LF, Gaynor RB. Cloning and characterization of a

novel cellular protein, TDP-43, that binds to human immunodeficiency virus type 1 TAR DNA sequence motifs. J Virol. 1995 Jun;69(6):3584-96. PubMed PMID: 7745706; PubMed Central PMCID: PMC189073.

- Ozsolak F, Kapranov P, Foissac S, Kim SW, Fishilevich E, Monaghan AP, John B, Milos PM. Comprehensive polyadenylation site maps in yeast and human reveal pervasive alternative polyadenylation. Cell. 2010 Dec 10;143(6):1018-29. doi:10.1016/j.cell.2010.11.020. PubMed PMID: 21145465; PubMed Central PMCID:PMC3022516.
- Ozsolak F, Milos PM. RNA sequencing: advances, challenges and opportunities. Nat Rev Genet. 2011 Feb;12(2):87-98. doi: 10.1038/nrg2934. Epub 2010 Dec 30. Review. PubMed PMID: 21191423; PubMed Central PMCID: PMC3031867.
- Palacios IM, Gatfield D, St Johnston D, Izaurralde E. An eIF4AIII-containing complex required for mRNA localization and nonsense-mediated mRNA decay. Nature. 2004 Feb 19;427(6976):753-7. PubMed PMID: 14973490.
- Park E, Gleghorn ML, Maquat LE. Staufen2 functions in Staufen1-mediated mRNA decay by binding to itself and its paralog and promoting UPF1 helicase but not ATPase activity. Proc Natl Acad Sci U S A. 2013 Jan 8;110(2):405-12. doi:10.1073/pnas.1213508110. Epub 2012 Dec 20. PubMed PMID: 23263869; PubMed Central PMCID: PMC3545820.
- Park E, Maquat LE. Staufen-mediated mRNA decay. Wiley Interdiscip Rev RNA. 2013 Jul-Aug;4(4):423-35. doi: 10.1002/wrna.1168. Epub 2013 May 16. Review. PubMed PMID: 23681777; PubMed Central PMCID: PMC3711692.
- Paul FE, Hosp F, Selbach M. Analyzing protein-protein interactions byquantitative mass spectrometry. Methods. 2011 Aug;54(4):387-95. doi:10.1016/j.ymeth.2011.03.001. Epub 2011 Mar 5. Review. PubMed PMID: 21382495.
- Pesiridis GS, Lee VM, Trojanowski JQ. Mutations in TDP-43 link glycine-rich domain functions to amyotrophic lateral sclerosis. Hum Mol Genet. 2009 Oct 15;18(R2):R156-62. doi: 10.1093/hmg/ddp303. Review. PubMed PMID: 19808791; PubMed Central PMCID: PMC2758707.
- Polymenidou M, Cleveland DW. The seeds of neurodegeneration: prion-like spreading in ALS. Cell. 2011 Oct 28;147(3):498-508. doi:10.1016/j.cell.2011.10.011. PubMed PMID: 22036560; PubMed Central PMCID: PMC3220614.
- Polymenidou M, Lagier-Tourenne C, Hutt KR, Huelga SC, Moran J, Liang TY, Ling SC, Sun E, Wancewicz E, Mazur C, Kordasiewicz H, Sedaghat Y, Donohue JP, Shiue L, Bennett CF, Yeo GW, Cleveland DW. Long pre-mRNA depletion and RNA missplicing contribute to neuronal vulnerability from loss of TDP-43. Nat Neurosci. 2011 Apr;14(4):459-68. doi: 10.1038/nn.2779. Epub 2011 Feb 27. PubMed PMID: 21358643; PubMed Central PMCID: PMC3094729.
- Prudencio M, Belzil VV, Batra R, Ross CA, Gendron TF, Pregent LJ, Murray ME, Overstreet KK, Piazza-Johnston AE, Desaro P, Bieniek KF, DeTure M, Lee WC, Biendarra SM, Davis MD, Baker MC, Perkerson RB, van Blitterswijk M, Stetler CT, Rademakers R, Link CD, Dickson DW, Boylan KB, Li H, Petrucelli L. Distinct brain transcriptome profiles in C9orf72-associated and sporadic ALS. Nat Neurosci. 2015 Aug;18(8):1175-82. doi: 10.1038/nn.4065. Epub 2015 Jul 20. PubMed PMID: 26192745; PubMed Central PMCID: PMC4830686.
- Rappsilber J, Ishihama Y, Mann M. Stop and go extraction tips for matrix-assisted laser desorption/ionization, nanoelectrospray, and LC/MS sample pretreatment in proteomics. Anal Chem. 2003 Feb 1;75(3):663-70. PubMed PMID:12585499.
- Rot G, Wang Z, Huppertz I, Modic M, Lenče T, Hallegger M, Haberman N, Curk T, von Mering C, Ule J. High-Resolution RNA Maps Suggest Common Principles of Splicing and Polyadenylation Regulation by TDP-43. Cell Rep. 2017 May 2;19(5):1056-1067. doi: 10.1016/j.celrep.2017.04.028. PubMed PMID: 28467899; PubMed Central PMCID: PMC5437728.
- Rubinstein AD, Eisenstein M, Ber Y, Bialik S, Kimchi A. The autophagy protein Atg12 associates with antiapoptotic Bcl-2 family members to promote mitochondrial apoptosis. Mol Cell. 2011 Dec 9;44(5):698-709. doi: 10.1016/j.molcel.2011.10.014.PubMed PMID: 22152474.
- Sato H, Maquat LE. Remodeling of the pioneer translation initiation complex involves translation and the karyopherin importin beta. Genes Dev. 2009 Nov 1;23(21):2537-50. doi: 10.1101/gad.1817109. PubMed PMID: 19884259; PubMed Central PMCID: PMC2779746.
- Saulière J, Murigneux V, Wang Z, Marquenet E, Barbosa I, Le Tonquèze O, Audic Y, Paillard L, Roest Crollius H, Le Hir H. CLIP-seq of eIF4AIII reveals transcriptome-wide mapping of the human exon junction complex. Nat Struct Mol Biol. 2012 Nov;19(11):1124-31. doi: 10.1038/nsmb.2420. Epub 2012 Oct 21. PubMed PMID: 23085716.

- Schmidt SA, Foley PL, Jeong DH, Rymarquis LA, Doyle F, Tenenbaum SA, Belasco JG, Green PJ. Identification of SMG6 cleavage sites and a preferred RNA cleavage motif by global analysis of endogenous NMD targets in human cells. Nucleic Acids Res. 2015 Jan;43(1):309-23. doi: 10.1093/nar/gku1258. Epub 2014 Nov 27. PubMed PMID: 25429978; PubMed Central PMCID: PMC4288159.
- Sephton CF, Good SK, Atkin S, Dewey CM, Mayer P 3rd, Herz J, Yu G. TDP-43 is a developmentally regulated protein essential for early embryonic development. J Biol Chem. 2010 Feb 26;285(9):6826-34. doi: 10.1074/jbc.M109.061846. Epub 2009 Dec 29. Erratum in: J Biol Chem. 2010 Dec 3;285(49):38740. PubMed PMID: 20040602; PubMed Central PMCID: PMC2825476.
- Shepard PJ, Choi EA, Lu J, Flanagan LA, Hertel KJ, Shi Y. Complex and dynamic landscape of RNA polyadenylation revealed by PAS-Seq. RNA. 2011 Apr;17(4):761-72.doi: 10.1261/rna.2581711. Epub 2011 Feb 22. PubMed PMID: 21343387; PubMed Central PMCID: PMC3062186.
- Sherstnev A, Duc C, Cole C, Zacharaki V, Hornyik C, Ozsolak F, Milos PM, Barton GJ, Simpson GG. Direct sequencing of Arabidopsis thaliana RNA reveals patterns of cleavage and polyadenylation. Nat Struct Mol Biol. 2012 Aug;19(8):845-52. doi: 10.1038/nsmb.2345. Epub 2012 Jul 22. PubMed PMID:22820990; PubMed Central PMCID: PMC3533403.
- Shi Y, Di Giammartino DC, Taylor D, Sarkeshik A, Rice WJ, Yates JR 3rd, Frank J, Manley JL. Molecular architecture of the human pre-mRNA 3' processing complex. Mol Cell. 2009 Feb 13;33(3):365-76. doi: 10.1016/j.molcel.2008.12.028. PubMed PMID: 19217410; PubMed Central PMCID: PMC2946185.
- Shi Y. Alternative polyadenylation: new insights from global analyses. RNA. 2012 Dec;18(12):2105-17. doi: 10.1261/rna.035899.112. Epub 2012 Oct 24. Review. PubMed PMID: 23097429; PubMed Central PMCID: PMC3504663
- Shigeoka T, Kato S, Kawaichi M, Ishida Y. Evidence that the Upf1-related molecular motor scans the 3'-UTR to ensure mRNA integrity. Nucleic Acids Res. 2012 Aug;40(14):6887-97. doi: 10.1093/nar/gks344. Epub 2012 May 2. PubMed PMID:22554850; PubMed Central PMCID: PMC3413143.
- Singh G, Kucukural A, Cenik C, Leszyk JD, Shaffer SA, Weng Z, Moore MJ. The cellular EJC interactome reveals higher-order mRNP structure and an EJC-SR protein nexus. Cell. 2012 Nov 9;151(4):750-64. doi: 10.1016/j.cell.2012.10.007. Epub 2012 Oct 18. Erratum in: Cell. 2012 Nov 9;151(4):915-6. PubMed PMID:23084401; PubMed Central PMCID: PMC3522173.
- Singh G, Rebbapragada I, Lykke-Andersen J. A competition between stimulators and antagonists of Upf complex recruitment governs human nonsense-mediated mRNA decay. PLoS Biol. 2008 Apr 29;6(4):e111. doi: 10.1371/journal.pbio.0060111. PubMed PMID: 18447585; PubMed Central PMCID: PMC2689706.
- Smibert P, Miura P, Westholm JO, Shenker S, May G, Duff MO, Zhang D, Eads BD, Carlson J, Brown JB, Eisman RC, Andrews J, Kaufman T, Cherbas P, Celniker SE, Graveley BR, Lai EC. Global patterns of tissue-specific alternative polyadenylation in Drosophila. Cell Rep. 2012 Mar 29;1(3):277-89. Erratum in: Cell Rep. 2013 Mar 28;3(3):969. PubMed PMID: 22685694; PubMed Central PMCID:PMC3368434.
- Stallings NR, Puttaparthi K, Luther CM, Burns DK, Elliott JL. Progressive motor weakness in transgenic mice expressing human TDP-43. Neurobiol Dis. 2010 Nov;40(2):404-14. doi: 10.1016/j.nbd.2010.06.017. Epub 2010 Aug 2. PubMed PMID:20621187.
- Svetoni F, Frisone P, Paronetto MP. Role of FET proteins in neurodegenerative disorders. RNA Biol. 2016 Nov;13(11):1089-1102. Epub 2016 Jul 14. Review. PubMed PMID: 27415968; PubMed Central PMCID: PMC5100351.
- Takagaki Y, Seipelt RL, Peterson ML, Manley JL. The polyadenylation factor CstF-64 regulates alternative processing of IgM heavy chain pre-mRNA during B cell differentiation. Cell. 1996 Nov 29;87(5):941-52. PubMed PMID: 8945520.
- Taylor JP, Brown RH Jr, Cleveland DW. Decoding ALS: from genes to mechanism. Nature. 2016 Nov 10;539(7628):197-206. doi: 10.1038/nature20413
- Thermann R, Neu-Yilik G, Deters A, Frede U, Wehr K, Hagemeier C, Hentze MW, Kulozik AE. Binary specification of nonsense codons by splicing and cytoplasmic translation. EMBO J. 1998 Jun 15;17(12):3484-94. PubMed PMID: 9628884; PubMed Central PMCID: PMC1170685.
- Tian B, Hu J, Zhang H, Lutz CS. A large-scale analysis of mRNA polyadenylation of human and mouse genes. Nucleic Acids Res. 2005 Jan 12;33(1):201-12. Print 2005. PubMed PMID: 15647503; PubMed Central PMCID: PMC546146.

- Tian B, Manley JL. Alternative cleavage and polyadenylation: the long and short of it. Trends Biochem Sci. 2013 Jun;38(6):312-20. doi: 10.1016/j.tibs.2013.03.005. Epub 2013 Apr 27. Review. PubMed PMID: 23632313; PubMed Central PMCID: PMC3800139.
- Tian B, Manley JL. Alternative polyadenylation of mRNA precursors. Nat Rev Mol Cell Biol. 2017 Jan;18(1):18-30. doi: 10.1038/nrm.2016.116. Epub 2016 Sep 28. Review. PubMed PMID: 27677860.
- Tollervey JR, Curk T, Rogelj B, Briese M, Cereda M, Kayikci M, König J, Hortobágyi T, Nishimura AL, Zupunski V, Patani R, Chandran S, Rot G, Zupan B, Shaw CE, Ule J. Characterizing the RNA targets and position-dependent splicing regulation by TDP-43. Nat Neurosci. 2011 Apr;14(4):452-8. doi: 10.1038/nn.2778. Epub 2011 Feb 27. PubMed PMID: 21358640; PubMed Central PMCID: PMC3108889.
- Trcek T, Sato H, Singer RH, Maquat LE. Temporal and spatial characterization of nonsense-mediated mRNA decay. Genes Dev. 2013 Mar 1;27(5):541-51. doi:10.1101/gad.209635.112. Epub 2013 Feb 21. PubMed PMID: 23431032; PubMed Central PMCID: PMC3605467.
- Ulitsky I, Shkumatava A, Jan CH, Subtelny AO, Koppstein D, Bell GW, Sive H,Bartel DP. Extensive alternative polyadenylation during zebrafish development. Genome Res. 2012 Oct;22(10):2054-66. doi: 10.1101/gr.139733.112. Epub 2012 Jun 21. PubMed PMID: 22722342; PubMed Central PMCID: PMC3460199.
- Unterholzner L, Izaurralde E. SMG7 acts as a molecular link between mRNA surveillance and mRNA decay. Mol Cell. 2004 Nov 19;16(4):587-96. PubMed PMID:15546618.
- Usuki F, Yamashita A, Kashima I, Higuchi I, Osame M, Ohno S. Specificinhibition of nonsense-mediated mRNA decay components, SMG-1 or Upf1, rescues thephenotype of Ullrich disease fibroblasts. MolTher. 2006 Sep;14(3):351-60. Epub2006 Jun 27. PubMed PMID: 16807116.
- Usuki F, Yamashita A, Kashima I, Higuchi I, Osame M, Ohno S. Specific inhibition of nonsense-mediated mRNA decay components, SMG-1 or Upf1, rescues the phenotype of Ullrich disease fibroblasts. Mol Ther. 2006 Sep;14(3):351-60. Epub 2006 Jun 27. PubMed PMID: 16807116.
- Van Nostrand EL, Pratt GA, Shishkin AA, Gelboin-Burkhart C, Fang MY, Sundararaman B, Blue SM, Nguyen TB, Surka C, Elkins K, Stanton R, Rigo F, Guttman M, Yeo GW. Robust transcriptome-wide discovery of RNA-binding protein binding sites with enhanced CLIP (eCLIP). Nat Methods. 2016 Jun;13(6):508-14. doi:10.1038/nmeth.3810. Epub 2016 Mar 28. PubMed PMID: 27018577; PubMed Central PMCID: PMC4887338.
- Van Rheenen W, Shatunov A, Dekker AM, McLaughlin RL, Diekstra FP, Pulit SL,van der Spek RA, Võsa U, de Jong S, Robinson MR, Yang J, Fogh I, van Doormaal PT,Tazelaar GH, Koppers M, Blokhuis AM, Sproviero W, Jones AR, Kenna KP, van EijkKR, Harschnitz O, Schellevis RD, Brands WJ, Medic J, Menelaou A, Vajda A, TicozziN, Lin K, Rogelj B, Vrabec K, Ravnik-Glavač M, Koritnik B, Zidar J, Leonardis L, Grošelj LD, Millecamps S, Salachas F, Meininger V, de Carvalho M, Pinto S, MoraJS, Rojas-García R, Polak M, Chandran S, Colville S, Swingler R, Morrison KE,Shaw PJ, Hardy J, Orrell RW, Pittman A, Sidle K, Fratta P, Malaspina A, Topp S,Petri S, Abdulla S, Drepper C, Sendtner M, Meyer T, Ophoff RA, Staats KA,Wiedau-Pazos M, Lomen-Hoerth C, Van Deerlin VM, Trojanowski JQ, Elman L,McCluskey L, Basak AN, Tunca C, Hamzeiy H, Parman Y, Meitinger T, Lichtner P,Radivojkov-Blagojevic M, Andres CR, Maurel C, Bensimon G, Landwehrmeyer B, Brice A, Payan CA, Saker-Delye S, Dürr A, Wood NW, Tittmann L, Lieb W, Franke A,Rietschel M, Cichon S, Nöthen MM, Amouyel P, Tzourio C, Dartigues JF,Uitterlinden AG, Rivadeneira F, Estrada K, Hofman A, Curtis C, Blauw HM, van der Kooi AJ, de Visser M, Goris A, Weber M, Shaw CE, Smith BN, Pansarasa O, Cereda C,Del Bo R, Comi GP, D'Alfonso S, Bertolin C, Sorarù G, Mazzini L, Pensato V,Gellera C, Tiloca C, Ratti A, Calvo A, Moglia C, Brunetti M, Arcuti S, Capozzo R,Zecca C, Lunetta C, Penco S, Riva N, Padovani A, Filosto M, Muller B, Stuit RJ;PARALS Registry; SLALOM Group; SLAP Registry; FALS Sequencing Consortium; SLAGEN Consortium; NNIPPS Study Group, Blair I, Zhang K, McCann EP, Fifita JA, NicholsonGA, Rowe DB, Pamphlett R, Kiernan MC, Grosskreutz J, Witte OW, Ringer T, Prell T,Stubendorff B, Kurth I, Hübner CA, Leigh PN, Casale F, Chio A, Beghi E, PupilloE, Tortelli R, Logroscino G, Powell J, Ludolph AC, Weishaupt JH, Robberecht W,Van Damme P, Franke L, Pers TH, Brown RH, Glass JD, Landers JE, Hardiman O,Andersen PM, Corcia P, Vourc'h P, Silani V, Wray NR, Visscher PM, de Bakker PI,van Es MA, Pasterkamp RJ, Lewis CM, Breen G, Al-Chalabi A, van den Berg LH,Veldink JH. Genome-wide association analyses identify new risk variants and thegenetic architecture of amyotrophic lateral sclerosis. Nat Genet. 2016Sep;48(9):1043-8. doi: 10.1038/ng.3622. Epub 2016 Jul 25. PubMed PMID: 27455348.
- Vanden Broeck L, Callaerts P, Dermaut B. TDP-43-mediated neurodegeneration: towards a loss-of-function hypothesis? Trends Mol Med. 2014 Feb;20(2):66-71.

doi:10.1016/j.molmed.2013.11.003. Epub 2013 Dec 16. PubMed PMID: 24355761.

- Varsally W, Brogna S. UPF1 involvement in nuclear functions. Biochem Soc Trans. 2012 Aug;40(4):778-83. doi: 10.1042/BST20120052. Review. PubMed PMID:22817733.
- Wang DB, Gitcho MA, Kraemer BC, Klein RL. Genetic strategies to study TDP-43 in rodents and to develop preclinical therapeutics for amyotrophic lateral sclerosis. Eur J Neurosci. 2011 Oct;34(8):1179-88. doi: 10.1111/j.1460-9568.2011.07803.x. Epub 2011 Jul 21. Review. PubMed PMID: 21777407; PubMed Central PMCID: PMC3196044.
- Wang IF, Reddy NM, Shen CK. Higher order arrangement of the eukaryotic nuclear bodies. Proc Natl Acad Sci U S A. 2002 Oct 15;99(21):13583-8. Epub 2002 Oct 2. PubMed PMID: 12361981; PubMed Central PMCID: PMC129717.
- Wang IF, Wu LS, Chang HY, Shen CK. TDP-43, the signature protein of FTLD-U, is a neuronal activity-responsive factor. J Neurochem. 2008 May;105(3):797-806. Epub 2007 Dec 15. PubMed PMID: 18088371.
- Wang ET, Sandberg R, Luo S, Khrebtukova I, Zhang L, Mayr C, Kingsmore SF, Schroth GP, Burge CB. Alternative isoform regulation in human tissue transcriptomes. Nature. 2008 Nov 27;456(7221):470-6. doi: 10.1038/nature07509. PubMed PMID: 18978772; PubMed Central PMCID: PMC2593745.
- Wegorzewska I, Bell S, Cairns NJ, Miller TM, Baloh RH. TDP-43 mutant transgenic mice develop features of ALS and frontotemporal lobar degeneration. Proc Natl Acad Sci U S A. 2009 Nov 3;106(44):18809-14. doi: 10.1073/pnas.0908767106. Epub 2009 Oct 15. PubMed PMID: 19833869; PubMed Central PMCID: PMC2762420.
- Wengrod J, Martin L, Wang D, Frischmeyer-Guerrerio P, Dietz HC, Gardner LB. Inhibition of nonsense-mediated RNA decay activates autophagy. Mol Cell Biol. 2013 Jun;33(11):2128-35. doi: 10.1128/MCB.00174-13. Epub 2013 Mar 18. PubMed PMID: 23508110; PubMed Central PMCID: PMC3648072.
- Wils H, Kleinberger G, Janssens J, Pereson S, Joris G, Cuijt I, Smits V, Ceuterick-de Groote C, Van Broeckhoven C, Kumar-Singh S. TDP-43 transgenic mice develop spastic paralysis and neuronal inclusions characteristic of ALS and frontotemporal lobar degeneration. Proc Natl Acad Sci U S A. 2010 Feb 23;107(8):3858-63. doi: 10.1073/pnas.0912417107. Epub 2010 Feb 3. PubMed PMID:20133711; PubMed Central PMCID: PMC2840518.
- Wittmann J, Hol EM, Jäck HM. hUPF2 silencing identifies physiologic substrates of mammalian nonsense-mediated mRNA decay. Mol Cell Biol. 2006 Feb;26(4):1272-87. PubMed PMID: 16449641; PubMed Central PMCID: PMC1367210.
- Wong E, Cuervo AM. Autophagy gone awry in neurodegenerative diseases. Nat Neurosci. 2010 Jul;13(7):805-11. doi: 10.1038/nn.2575. Review. PubMed PMID:20581817; PubMed Central PMCID: PMC4038747.
- Wu LS, Cheng WC, Hou SC, Yan YT, Jiang ST, Shen CK. TDP-43, a neuro-pathosignature factor, is essential for early mouse embryogenesis. Genesis. 2010 Jan;48(1):56-62. doi: 10.1002/dvg.20584. PubMed PMID: 20014337.
- Xiao S, Sanelli T, Dib S, Sheps D, Findlater J, Bilbao J, Keith J, Zinman L, Rogaeva E, Robertson J. RNA targets of TDP-43 identified by UV-CLIP are deregulated in ALS. Mol Cell Neurosci. 2011 Jul;47(3):167-80. doi:10.1016/j.mcn.2011.02.013. Epub 2011 Mar 21. PubMed PMID: 21421050.
- Xu YF, Gendron TF, Zhang YJ, Lin WL, D'Alton S, Sheng H, Casey MC, Tong J, Knight J, Yu X, Rademakers R, Boylan K, Hutton M, McGowan E, Dickson DW, Lewis J, Petrucelli L. Wild-type human TDP-43 expression causes TDP-43 phosphorylation, mitochondrial aggregation, motor deficits, and early mortality in transgenic mice. J Neurosci. 2010 Aug 11;30(32):10851-9. doi: 10.1523/JNEUROSCI.1630-10.2010. PubMed PMID: 20702714; PubMed Central PMCID:PMC3056148.
- Xu YF, Zhang YJ, Lin WL, Cao X, Stetler C, Dickson DW, Lewis J, Petrucelli L. Expression of mutant TDP-43 induces neuronal dysfunction in transgenic mice. Mol Neurodegener. 2011 Oct 26;6:73. doi: 10.1186/1750-1326-6-73. PubMed PMID: 22029574; PubMed Central PMCID: PMC3216869.
- Yamashita A, Izumi N, Kashima I, Ohnishi T, Saari B, Katsuhata Y, Muramatsu R, Morita T, Iwamatsu A, Hachiya T, Kurata R, Hirano H, Anderson P, Ohno S. SMG-8 and SMG-9, two novel subunits of the SMG-1 complex, regulate remodeling of the mRNA surveillance complex during nonsense-mediated mRNA decay. Genes Dev. 2009 May 1;23(9):1091-105. doi: 10.1101/gad.1767209. PubMed PMID: 19417104; PubMed Central PMCID: PMC2682953.
- Yamashita A, Ohnishi T, Kashima I, Taya Y, Ohno S. Human SMG-1, a novel

phosphatidylinositol 3-kinase-related protein kinase, associates with components of the mRNA surveillance complex and is involved in the regulation of nonsense-mediated mRNA decay. Genes Dev. 2001 Sep 1;15(17):2215-28. PubMed PMID: 11544179; PubMed Central PMCID: PMC312771.

- Yepiskoposyan H, Aeschimann F, Nilsson D, Okoniewski M, Mühlemann O. Autoregulation of the nonsense-mediated mRNA decay pathway in human cells. RNA. 2011 Dec;17(12):2108-18. doi: 10.1261/rna.030247.111. Epub 2011 Oct 25. PubMed PMID: 22028362; PubMed Central PMCID: PMC3222124.
- Ying Z, Xia Q, Hao Z, Xu D, Wang M, Wang H, Wang G. TARDBP/TDP-43 regulates autophagy in both MTORC1-dependent and MTORC1-independent manners. Autophagy.2016;12(4):707-8. doi: 10.1080/15548627.2016.1151596. PubMed PMID: 27050460;PubMed Central PMCID: PMC4836031.
- Yu Z, Fan D, Gui B, Shi L, Xuan C, Shan L, Wang Q, Shang Y, Wang Y. Neurodegeneration-associated TDP-43 interacts with fragile X mental retardation protein (FMRP)/Staufen (STAU1) and regulates SIRT1 expression in neuronal cells. J Biol Chem. 2012 Jun 29;287(27):22560-72. doi: 10.1074/jbc.M112.357582. Epub 2012 May 14. PubMed PMID: 22584570; PubMed Central PMCID: PMC3391095.
- Zhang J, Sun X, Qian Y, LaDuca JP, Maquat LE. At least one intron is required for the nonsense-mediated decay of triosephosphate isomerase mRNA: a possible link between nuclear splicing and cytoplasmic translation. Mol Cell Biol. 1998 Sep;18(9):5272-83. PubMed PMID: 9710612; PubMed Central PMCID: PMC109113.
- Zhang J, Sun X, Qian Y, Maquat LE. Intron function in the nonsense-mediated decay of beta-globin mRNA: indications that pre-mRNA splicing in the nucleus can influence mRNA translation in the cytoplasm. RNA. 1998 Jul;4(7):801-15. PubMed PMID: 9671053; PubMed Central PMCID: PMC1369660.
- Zhou H, Huang C, Chen H, Wang D, Landel CP, Xia PY, Bowser R, Liu YJ, Xia XG. Transgenic rat model of neurodegeneration caused by mutation in the TDP gene. PLoS Genet. 2010 Mar 26;6(3):e1000887. doi: 10.1371/journal.pgen.1000887. PubMed PMID: 20361056; PubMed Central PMCID: PMC2845661.
- Zhu H, Zhou HL, Hasman RA, Lou H. Hu proteins regulate polyadenylation by blocking sites containing U-rich sequences. J Biol Chem. 2007 Jan 26;282(4):2203-10. Epub 2006 Nov 26. PubMed PMID: 17127772.
- Zünd D, Gruber AR, Zavolan M, Mühlemann O. Translation-dependent displacement of UPF1 from coding sequences causes its enrichment in 3' UTRs. Nat Struct Mol Biol. 2013 Aug;20(8):936-43. doi: 10.1038/nsmb.2635. Epub 2013 Jul 7. PubMed PMID: 23832275.

ACKNOWLEDGMENTS

This Ph.D. thesis represents the work of the last four years, during which I collaborated with several people. From them, I tried to learn as much as possible, and I would like to emphasize in this last chapter how important they have been for me.

I would like to thank my tutor Prof. Alessandro Quattrone for giving me the opportunity to work on this project, for encouraging my research, and for allowing me to grow as a scientist.

I am much obliged to the members of my thesis committee for their comments and questions which led me to widen my work and improve this manuscript.

My sincere thanks go to Dr. Daniele Peroni, who accepted to be my advisor. His guidance helped me in all the time of research. He taught me how to develop my scientific skills and critical thinking. I could not have imagined having a better mentor for my Ph.D. study. I have to say a big thank to Dr. Paola Zuccotti for her continuous support, patience and motivation and Dr. Toma Tebaldi for his incredible capabilities in data mining and color matching. We will always be a great team.

I would like to express my special thanks to Dr. Matthias Selbach who gave me access to his laboratory and powerful toys. Not everyone has the opportunity to work with machines of 700.000 €... a dream that came true. A special thank to Katrina Meyer and all the member of the Selbach's lab.

I would also like to thank Dr. Niels Gehring who provided me the opportunity to join his team. Without him and the precious support of Dr. Volker Bőhm, it would not be possible to answer several questions and solve the case of the mysterious band.

Also, I thank the LTG group for the stimulating discussions and for all the fun, food and coffee we have had in the last four years. A special thought to my young helpers, Federica and Elisabetta. I hope that the time we have spent together will remain as a good memory.

I can not forget to acknowledge the CIBIO people and the members of the facilities... The list would be too long to mention you all.

Last but not the least, I thank my family: my parents and my boyfriend Nicola for supporting me to follow my passions and achieve my goals.

I would also like to mention my volleyball team. Thank you for your friendship and sorry for all the times I came late because of an experiment or a meeting.

All of you helped me to deal with this very important part of my life.

Thank you again!